research report

# A Design Approach for Complex Stiffeners

**RESEARCH REPORT RP00-3**

**OCTOBER 2000**
**REVISION 2006**

Committee on Specifications
for the Design of Cold-Formed
Steel Structural Members

American Iron and Steel Institute

The material contained herein has been developed by researchers based on their research findings. The material has also been reviewed by the American Iron and Steel Institute Committee on Specifications for the Design of Cold-Formed Steel Structural Members. The Committee acknowledges and is grateful for the contributions of such researchers.

The material herein is for general information only. The information in it should not be used without first securing competent advice with respect to its suitability for any given application. The publication of the information is not intended as a representation or warranty on the part of the American Iron and Steel Institute, or of any other person named herein, that the information is suitable for any general or particular use or of freedom from infringement of any patent or patents. Anyone making use of the information assumes all liability arising from such use.

# A DESIGN APPROACH FOR COMPLEX STIFFENERS

FINAL REPORT

By

ANDREW T. SARAWIT
PROFESSOR TEOMAN PEKÖZ, PROJECT DIRECTOR

A PROJECT SPONSORED BY
THE AMERICAN IRON AND STEEL INSTITUTE

Date Submitted 18 October 2000

SCHOOL OF CIVIL AND ENVIRONMENTAL ENGINEERING
CORNELL UNIVERSITY
HOLLISTER HALL, ITHACA NY 14853-3501

**TABLE OF CONTENTS**

**LIST OF TABLES**

**LIST OF FIGURES**

# A Design Approach for Complex Stiffeners

## 1 Introduction

This report presents a design approach for laterally braced cold-formed steel flexural members with edge stiffened flanges other than simple lips. The objectives of the research are as follows:

- To study the feasibility of using the design method for flexural members given by Schafer (1997), Schafer and Peköz (1999) to design these complex stiffeners and then compare the results with the finite element method and AISI (1996). (Chapters 2-4)
- To use a computer program, CU-EWA, developed to perform parameter studies for cross section optimization. (Chapter 5-6)
- To conduct a preliminary study on a two-point bending experiment setup as preparation for future testing by doing a full finite element simulation of the experimental arrangement and by making comparisons with previous physical test results. (Chapter 7)
- To study an alternative approach for introducing the initial geometric imperfection by using the stochastic process to randomly generate signals for the imperfection geometric shape instead of introducing the initial geometric imperfection by superimposing the eigenmodes. (Chapter 8)

The following is a summary of the design procedures for flexural members given by Schafer (1997), Schafer and Peköz (1999). The design procedures are based on the need for the integration of the distortional mode into the design procedure. Two behavioral phenomena must be considered. First, the distortional mode has less post-buckling capacity than the local mode. Second, the distortional mode has the ability to control failure even when it occurs at a higher critical stress than the local mode. A design method incorporating these phenomena is needed to provide an integrated approach to strength prediction involving local and distortional buckling. For consistency with the existing cold-form steel design specifications an effective width approach was undertaken. Effective section properties are based on effective widths, $b$.

$$b = \rho w \tag{1}$$

where $w$ is the actual element width and post-buckling reduction factor, $\rho$, is

$$\rho = \left(1 - 0.22/\lambda\right)/\lambda \text{ for } \lambda > 0.673 \text{ otherwise } \rho = 1. \tag{2}$$

where

$$\lambda = \sqrt{f_y / f_{cr}} \tag{3}$$

In order to properly integrate distortional buckling, reduced post-buckling capacity in the distortional mode and the ability of the distortional mode to control the failure mechanism even when at a higher buckling stress than the local mode must be incorporated. Therefore, the critical buckling stress of the element was defined by comparing the local buckling stress and distortional buckling stress to determine the governing mode as follows:

$$\left(f_{cr}\right) = \min\left[\left(f_{cr}\right)_{local}, R_d\left(f_{cr}\right)_{dist.}\right] \tag{4}$$

$$R_d = \min\left(1, \frac{1.17}{\lambda_d + 1} + 0.3\right) \text{ where } \lambda_d = \sqrt{f_y / \left(f_{cr}\right)_{dist.}} \tag{5}$$

$R_d$ reflects the reduced strength in mechanisms associated with distortional failures. For $R_d < 1$ this method provides an additional reduction on the post-buckling capacity. Further, the method allows the distortional mode to control situations where the distortional buckling stress is greater than the local buckling stress. Thus, $R_d$ provides a framework for solving the problem of predicting the failure mode and reducing the post-buckling capacity in the distortional mode. Schafer (1997), Schafer and Peköz (1999) developed the expression for $R_d$ based on post-buckling capacity as shown in Figure 1.2, 1.3 and from the experimental results of Hancock et al. (1994). With $f_{cr}$ of the element known the effective width of each element may readily be determined and the effective section properties generated.

To investigate the post-buckling behavior and develop the expression for $R_d$ the authors analyzed an isolated flange-stiffener model as shown in Figure 1.1 rather then using the full section. Two types of imperfections, local and distortional mode, are superposed to give the initial geometric imperfections. The magnitude of the imperfection is selected based on the statistical summary provided in Schafer (1997), Schafer and Peköz (1999). Then the ultimate strength of these isolated flanges is found for different

magnitudes of imperfection. Two maximum imperfection magnitudes, one at 25% and the other at 75% probability of exceedance, are used. The percent differences in the strength are used to measure the imperfection sensitivity.

$$\frac{(f_u)_{75\%imp.} - (f_u)_{25\%imp.}}{\frac{1}{2}\left((f_u)_{75\%imp.} + (f_u)_{25\%imp.}\right)} \times 100\% \qquad (6)$$

The error bars in Figure 1.2 show the range of strengths predicted for imperfections varying over the central 50% portion of expected imperfection magnitudes. The greater the error bars, the greater the imperfection sensitivity. A contour plot of this imperfection sensitivity statistic is shown in Figure 1.3. Stocky members tending to failure in the distortional mode have the highest sensitivity.

The design approach given by Schafer (1997), Schafer and Peköz (1999) was developed based on simple lips edge stiffeners. Therefore, before adopting this approach for other types of stiffeners verification on the reduction factor for distortional stress, $R_d$ is needed. This is done by creating a post-buckling capacity graph and imperfection sensitivity contour plot on the types of stiffeners in interest for comparison with the original Figure 1.2 and 1.3. In this research 4 types of complex stiffeners shown in Figure 2.1 are studied.

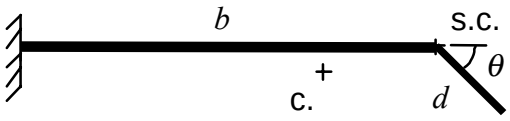


Figure 1.1 Isolated Flange-Stiffener Model

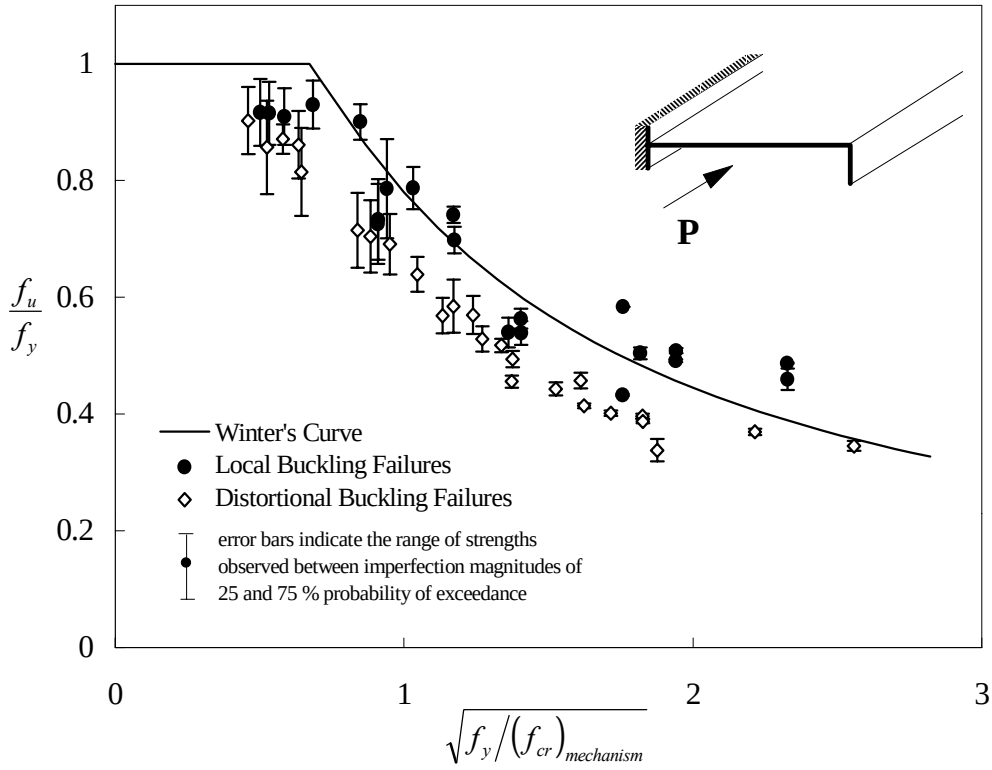


Figure 1.2 Post-Buckling Capacity of Edge Stiffened Flanges

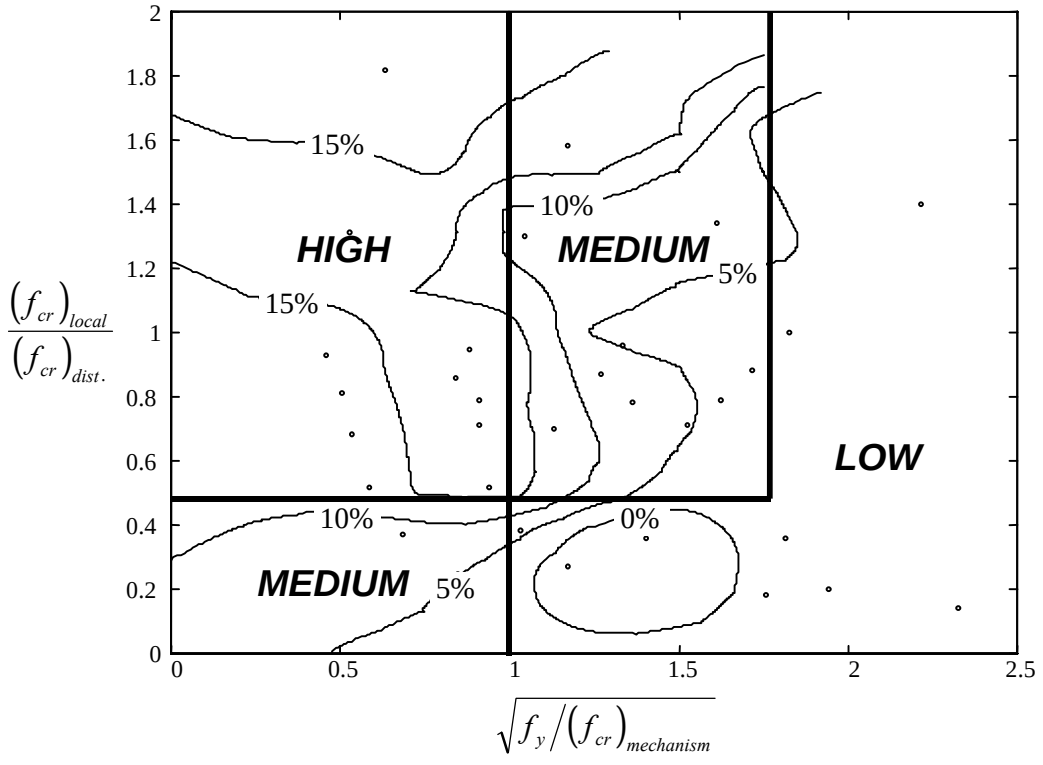


Figure 1.3 Imperfection Sensitivity of Edge Stiffened Flanges

## 2 Design Approach for Complex Stiffeners

Similar to the design approach given by Schafer (1997), Schafer and Peköz (1999) to account for the distortional buckling an evaluation of the reduction factor for distortional stress, $R_d$ based on experimental and FEM studies must be considered. FEM studies were carried out for 4 types of complex stiffeners shown in Figure 2.1.

### 2.1 Finite Element Study

In order to study the post-buckling behavior of complex stiffened elements nonlinear FEM analyses are performed using ABAQUS. To study only the complex stiffened element behavior an idealization of the boundary conditions at the web/flange junction are made by restraining all degrees of freedom except for the translation along the length. Roller supports are used at both ends. To avoid localized failure at the ends, the uniform load has been distributed to the first row of elements. Boundary conditions are shown in Figure 2.2. The material model used is elastic-plastic with strain hardening and $f_y$ = 347 MPa. Residual stress is also included with a 30% yield stress throughout the thickness in the longitudinal direction. The residual stresses are assumed tension on the outside and compression in the inside of the section.

Initial geometric imperfection is introduced by superimposing the eigenmodes for the local and distortional buckling shown in Figure 2.3. The magnitude of the imperfection is selected based on the statistical summary provided in Schafer (1997), Schafer and Peköz (1999). Four types of complex stiffeners shown in Figure 2.1 have been studied. The length of the model is selected by using the length that would give the least buckling strength in the distortional mode, which is obtained, by using the Finite Strip Method CUFSM. Table 2.1 summarizes the geometry of the members. An imperfection sensitivity study has been performed for each type of stiffener. Figure 2.4, 2.6, 2.8, 2.10 and contour plot in Figure 2.5, 2.7, 2.9, 2.11 show the results. For each type of stiffener a total of 42 models were investigated.

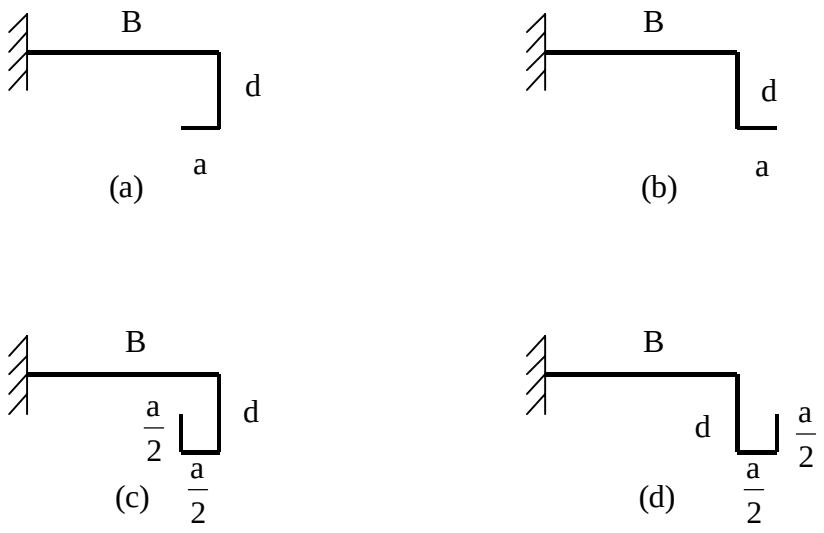


Figure 2.1 Isolated Flange-Complex Stiffener Model (a) Inside Angled Stiffener (b) Outside Angled Stiffener (c) Inside Hooked Stiffener (d) Outside Hooked Stiffener

Table 2.1 Geometry of Members *

| B | d | a |
|---|---|---|
| 25 | 6.25 | 0,3.125,6.25 |
| | 12.5 | 0,6.25,12.5 |
| 50 | 6.25 | 0,3.125,6.25 |
| | 12.5 | 0,6.25,12.5 |
| | 25 | 0,12.5,25 |
| 75 | 6.25 | 0,3.125,6.25 |
| | 12.5 | 0,6.25,12.5 |
| | 25 | 0,12.5,25 |
| | 37.5 | 0,18.75,37.5 |
| 100 | 6.25 | 0,3.125,6.25 |
| | 12.5 | 0,6.25,12.5 |
| | 25 | 0,12.5,25 |
| | 37.5 | 0,18.75,37.5 |
| | 50 | 0,25,50 |

* Thickness = 1 mm in all cases

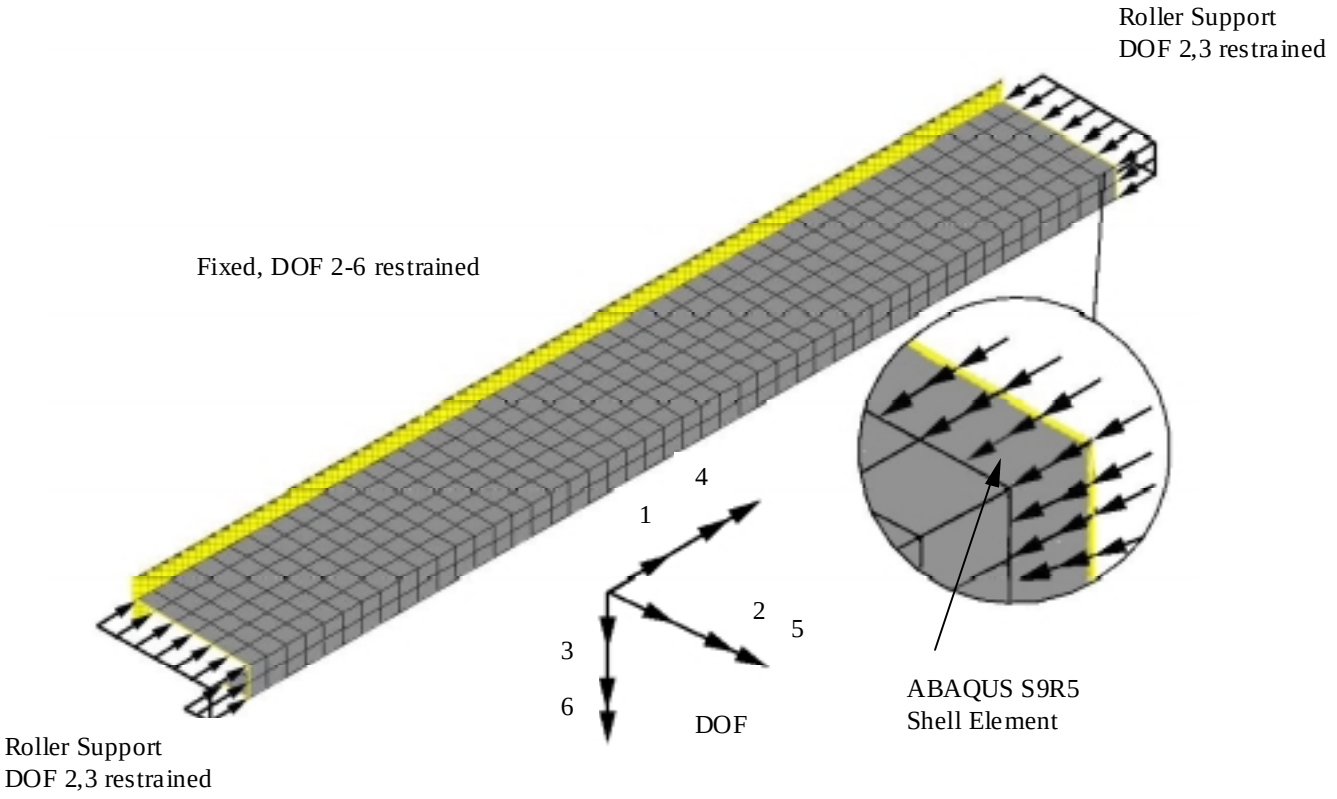


Figure 2.2 Boundary and Loading Condition

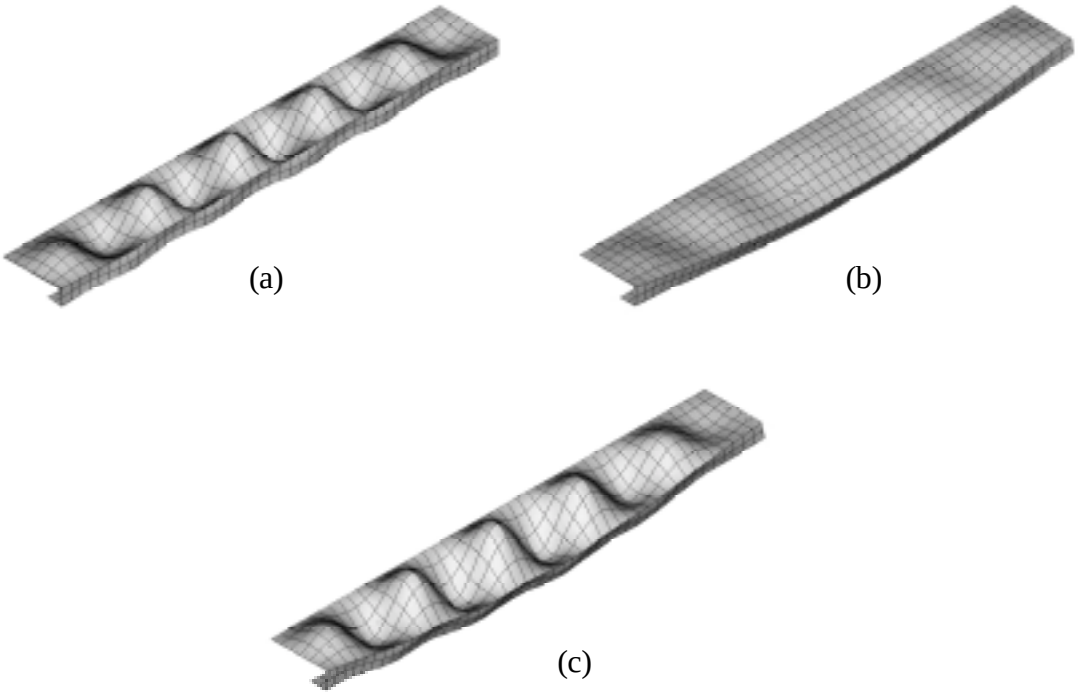


Figure 2.3 (a) Local Buckling (b) Distortional Buckling (c) Geometric Imperfection

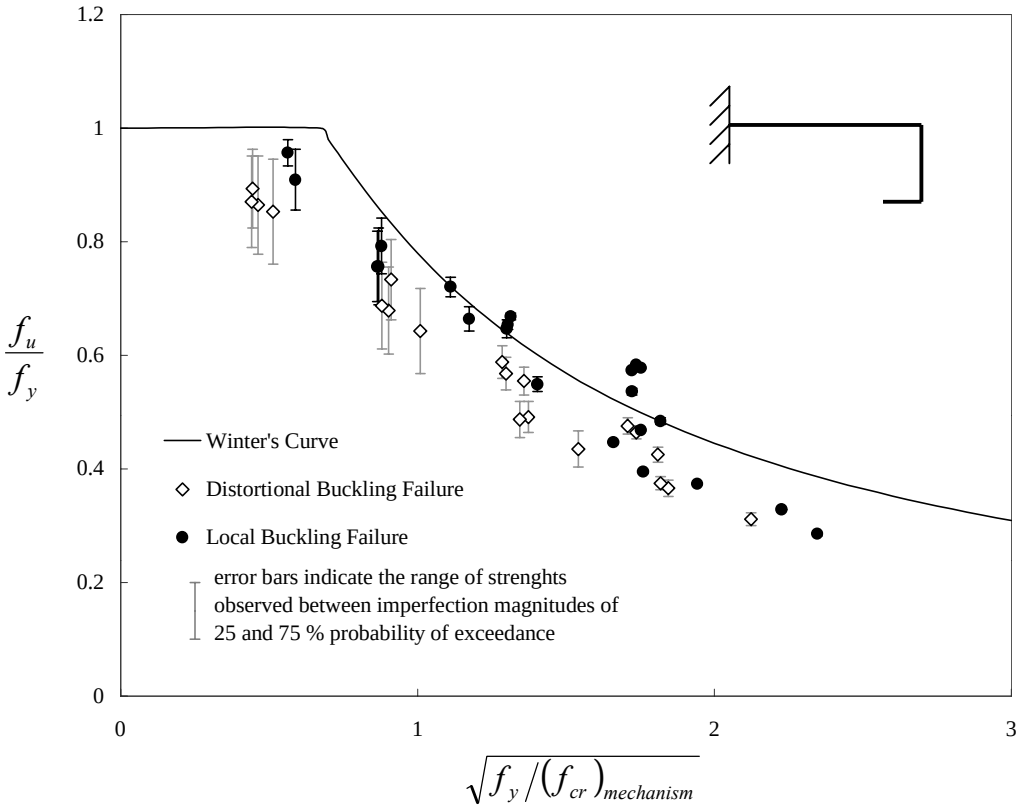


Figure 2.4 Post-Buckling Capacity of Inside Angled Stiffener

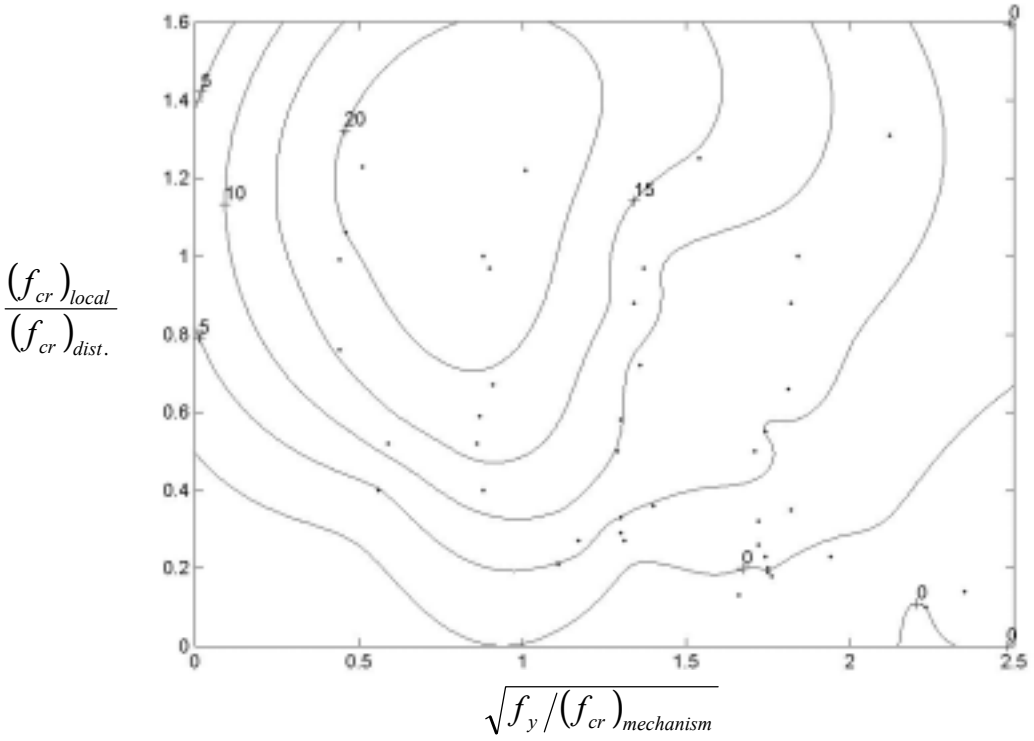


Figure 2.5 Imperfection Sensitivity of Inside Angled Stiffener

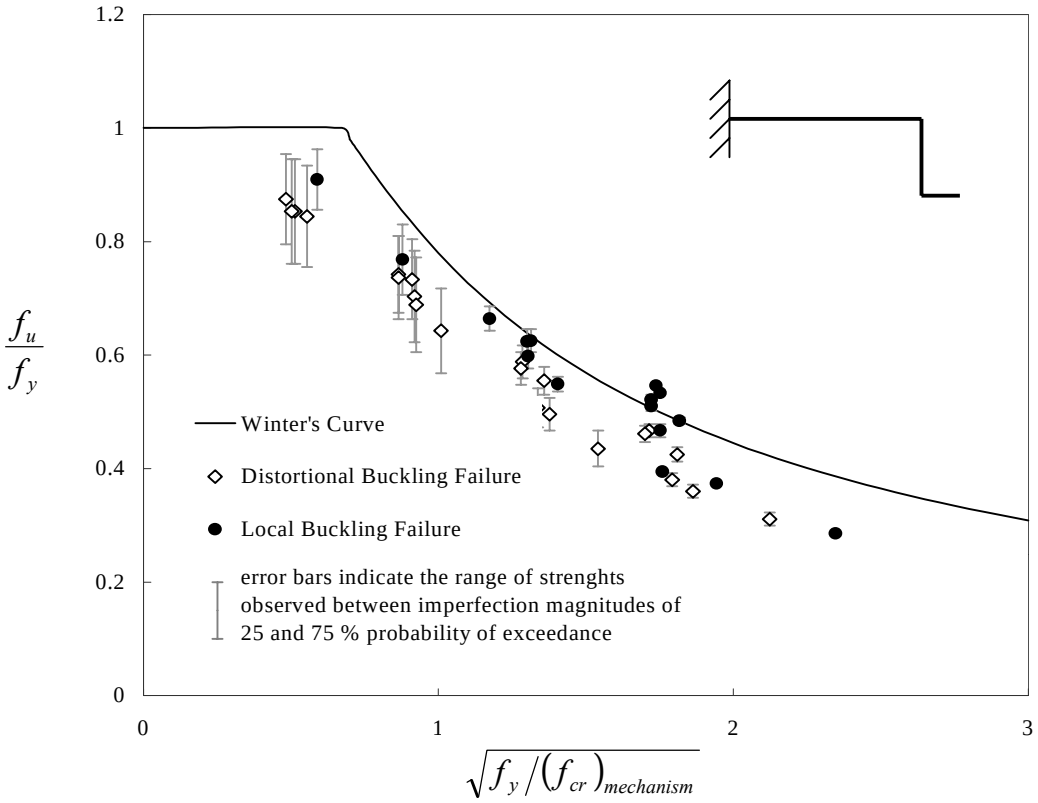


Figure 2.6 Post-Buckling Capacity of Outside Angled Stiffener

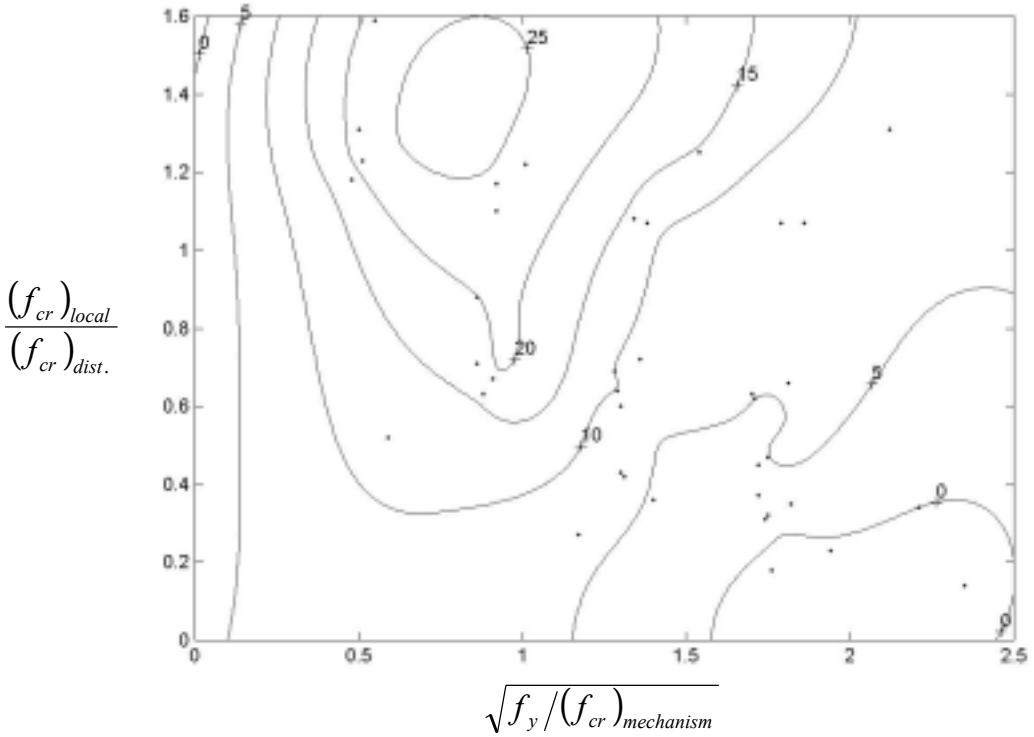


Figure 2.7 Imperfection Sensitivity of Outside Angled Stiffener

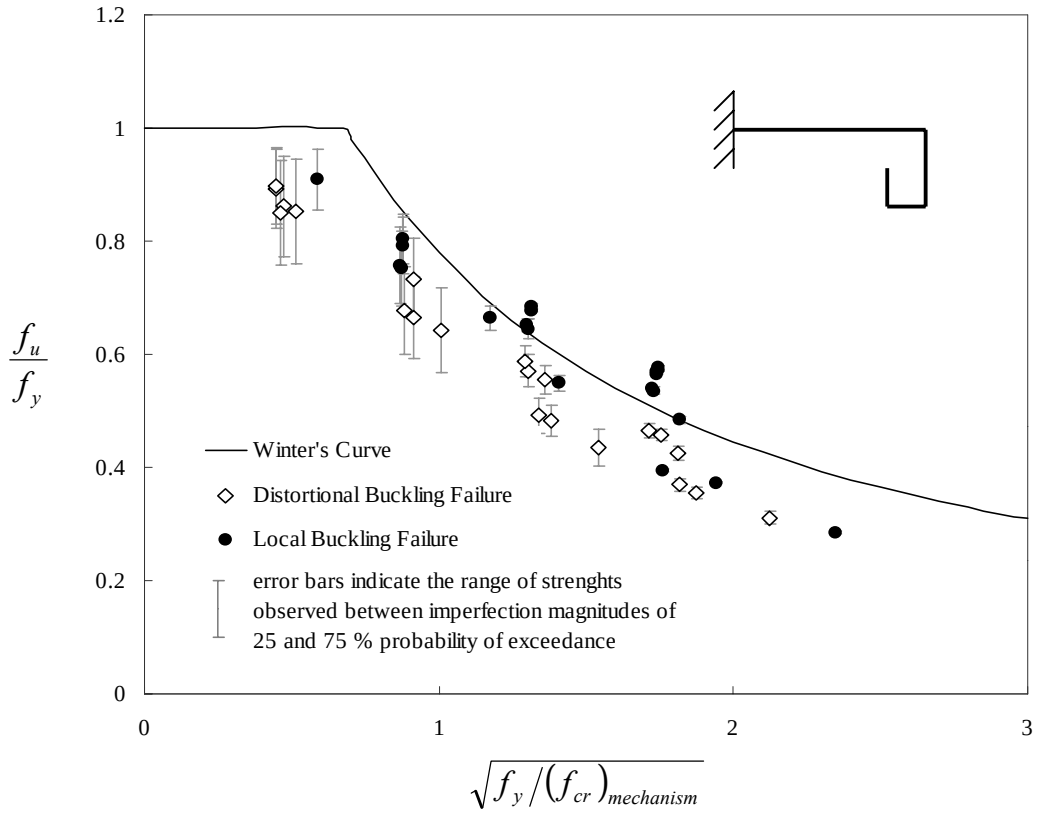


Figure 2.8 Post-Buckling Capacity of Inside Hooked Stiffener

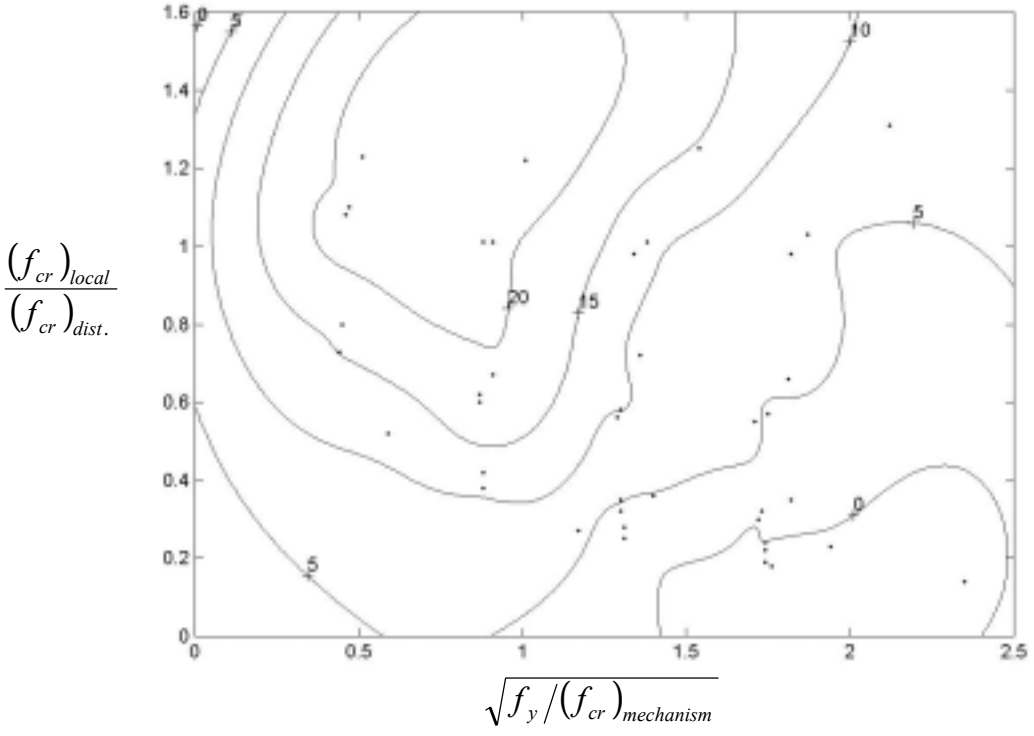


Figure 2.9 Imperfection Sensitivity of Inside Hooked Stiffener

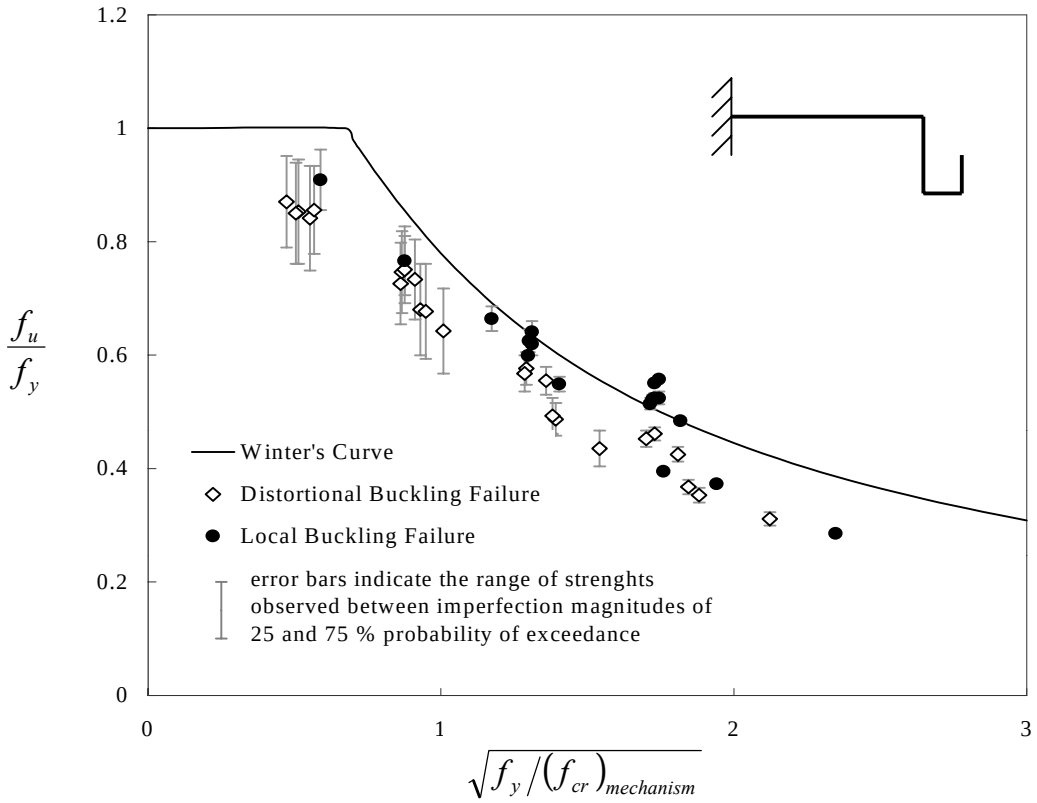


Figure 2.10 Post-Buckling Capacity of Outside Hooked Stiffener

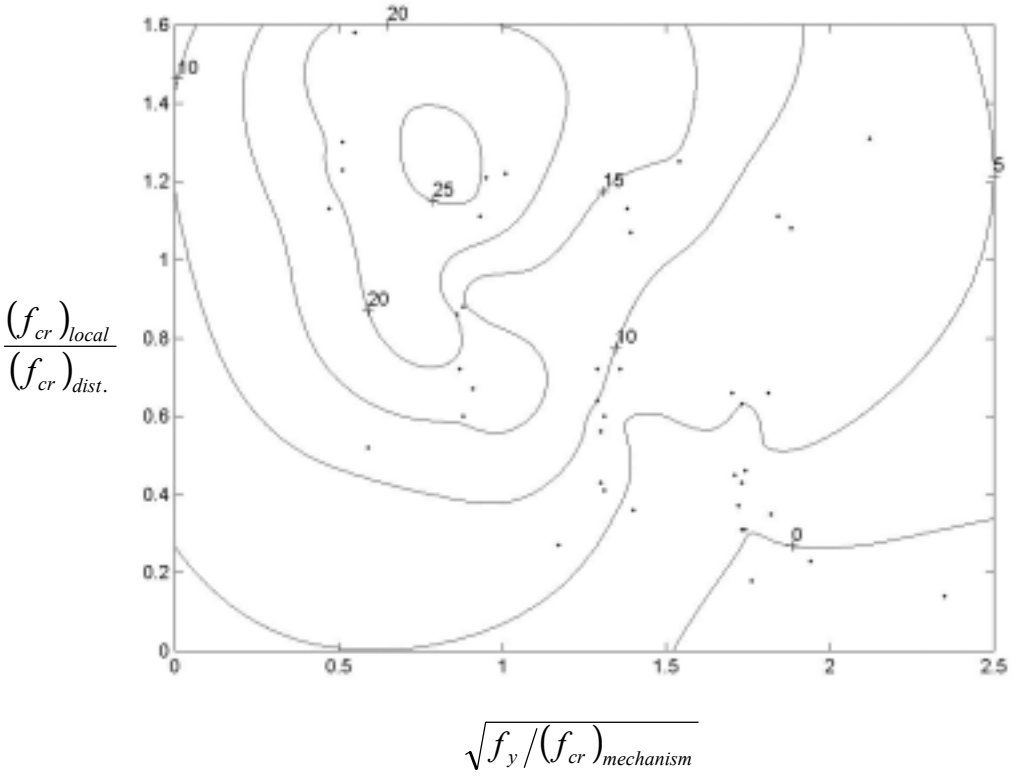


Figure 2.11 Imperfection Sensitivity of Outside Hooked Stiffener

### 2.2 Conclusion and Verification of the Proposed Design Approach

It can be seen that the imperfection sensitivity contour plots are similar to those obtained by edge stiffened flanges. Therefore, the reduction factor for distortional stress, $R_d$ is expected to be similar to Schafer (1997), Schafer and Peköz (1999).

## 3 Parametric Studies on Laterally Braced Flexural Members with Complex Stiffeners

Two Z-section parameter studies are carried out for different types of stiffeners to compare the moment capacity determined by FEM, AISI (1996) approach and the proposed design approach for flexural members given by Schafer (1997), Schafer and Peköz (1999). First parameter study consists of different Z-section geometries with all cross sections having the same thickness while the second parameter study uses one standard Z-section but varies thickness. The cross sections selected for both these parameter studies are intend to cover a wide range of slendernesses and maintain the cross section area between each types of stiffeners to compare the efficiency.

### 3.1 Z-Section Parameter Study for Constant Thickness

The parameter study is done by changing different widths of the web, flange and stiffeners for five types of stiffeners simple lip, inside angled, outside angled, inside hooked, and outside hooked stiffeners. All cross sections have the same thickness. Figure 3.1 and Table 3.1 summarize the geometry of the members. Local and distortional buckling stresses obtained by finite strip method are used for the proposed design approach for flexural members given by Schafer (1997), Schafer and Peköz (1999). Results for each type of stiffeners for this parameter study are shown in Table 3.2, 3.3, 3.4, 3.5, and 3.6. Table 3.7, 3.8, 3.9,3.10 and Figure 3.3, 3.4, 3.5 summarize the results for different approaches.

### 3.2 Finite Element Modeling Assumptions

The web/flange junction is restrained only for the translation degree of freedom perpendicular to the length to brace the member laterally. Roller supports are used at both ends. To avoid localized failure at the ends, the constant moment modeled by nodal loads is distributed to the first row of elements. Boundary and loading conditions are shown in Figure 3.2 (a). The material model used is elastic-plastic with strain hardening and $f_y$ = 345 MPa. Residual stress throughout the thickness in the longitudinal direction is assumed to be 30% of the yield stress in the flange and 40% of the yield stress in the web. The residual stresses are also assumed to be tension on the outside and compression in the inside of the section.

Initial geometric imperfections are introduced by superimposing the eigenmodes for the local and distortional buckling shown in Figure 3.2. Three different imperfection magnitudes 100% (no imperfections), 75% and 25% probability of exceedance based on the statistical summary provided in Schafer (1997), Schafer and Peköz (1999) are used for each model. The length of the model is selected by using three half-wave lengths of the distortional mode that gives the least buckling strength. The wavelengths are obtained using the Finite Strip Method.

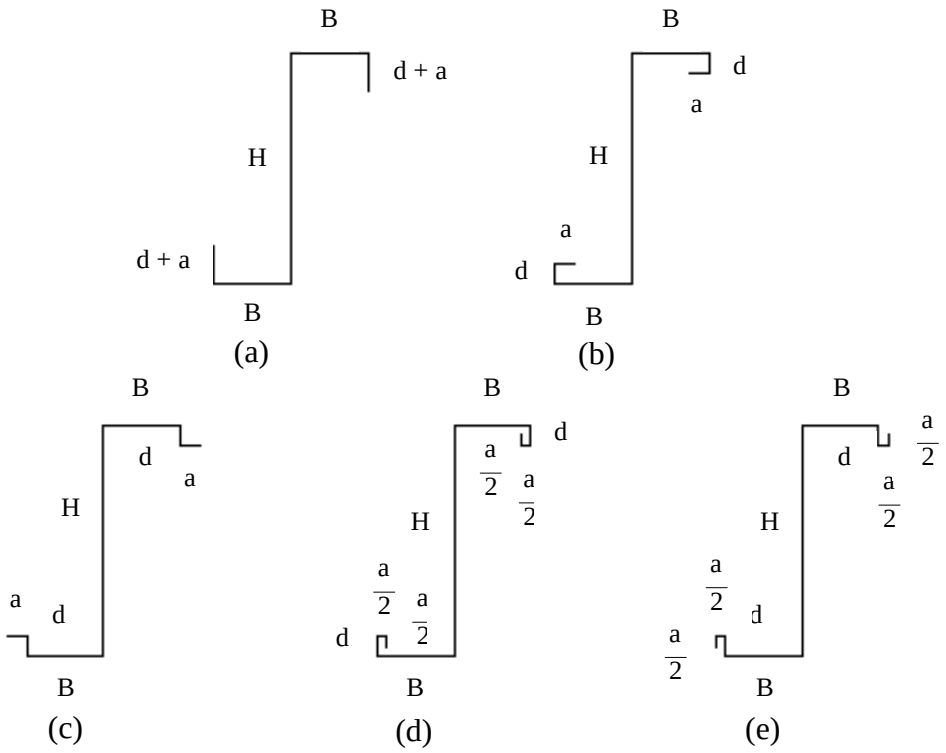


Figure 3.1 Z-section with (a) Simple Lip Stiffener (b) Inside Angled Stiffener (c) Outside Angled Stiffener (d) Inside Hooked Stiffener (e) Outside Hooked Stiffener

Table 3.1 Summary of Models Geometry *

| Model | Dimensions | | | | | | | | |
|---|---|---|---|---|---|---|---|---|---|
| | | | | | Length, L (mm) | | | | |
| | H (mm) | B (mm) | d (mm) | a (mm) | Simple Lip | Inside Angled | Outside Angled | Inside Hooked | Outside Hooked |
| 1 | 50 | 25 | 6.25 | 3.125 | 630 | 600 | 570 | 600 | 570 |
| 2 | 50 | 25 | 6.25 | 6.25 | 780 | 690 | 570 | 630 | 570 |
| 3 | 100 | 25 | 6.25 | 3.125 | 720 | 690 | 660 | 660 | 630 |
| 4 | 100 | 25 | 6.25 | 6.25 | 900 | 780 | 660 | 720 | 660 |
| 5 | 100 | 50 | 6.25 | 3.125 | 1170 | 1080 | 1050 | 1050 | 1050 |
| 6 | 100 | 50 | 6.25 | 6.25 | 1410 | 1200 | 1110 | 1140 | 1080 |
| 7 | 100 | 50 | 12.5 | 6.25 | 1830 | 1740 | 1620 | 1680 | 1620 |
| 8 | 100 | 50 | 12.5 | 12.5 | 2190 | 1950 | 1650 | 1830 | 1650 |
| 9 | 150 | 25 | 6.25 | 3.125 | 720 | 660 | 660 | 660 | 630 |
| 10 | 150 | 25 | 6.25 | 6.25 | 930 | 780 | 690 | 750 | 690 |
| 11 | 150 | 50 | 6.25 | 3.125 | 1230 | 1170 | 1140 | 1140 | 1110 |
| 12 | 150 | 50 | 6.25 | 6.25 | 1500 | 1290 | 1200 | 1230 | 1170 |
| 13 | 150 | 50 | 12.5 | 6.25 | 1980 | 1860 | 1770 | 1800 | 1740 |
| 14 | 150 | 50 | 12.5 | 12.5 | 2370 | 2100 | 1800 | 1980 | 1770 |

* Thickness = 1 mm in all cases

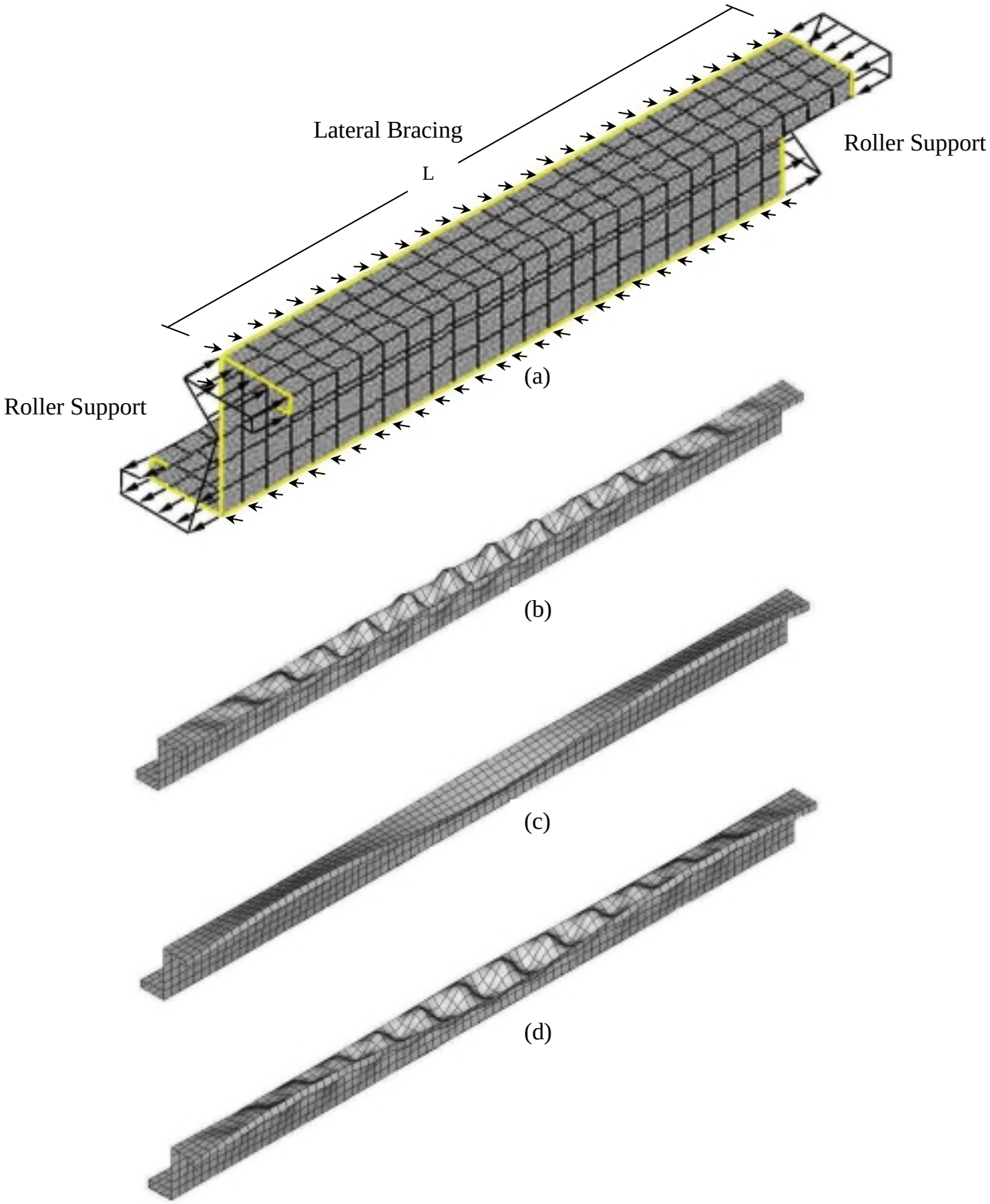


Figure 3.2 (a) Boundary and Loading Condition (b) Local Buckling (c) Distortional Buckling (d) Initial Geometric Imperfection

Table 3.2 Moment Capacity for Z-section with Simple Lip Stiffener

| Model | Finite Strip Analysis | | | | | FEM | | AISI | PRO | $M_{PRO}/M_{AISI}$ | $M_{FEM}/M_{AISI}$ | $M_{FEM}/M_{PRO}$ |
|---|---|---|---|---|---|---|---|---|---|---|---|---|
| | (fcr)d (MPa) | Rd | Rd(fcr)d (MPa) | (fcr)l (MPa) | fcr (MPa) | fu100 fu75 fu25 | Mu100 Mu75 Mu25 | $M_{AISI}$ (N-m) | $M_{PRO}$ (N-m) | | imp 100% imp 75% imp 25% | imp 100% imp 75% imp 25% |
| 1 | 942 | 1 | 942 | 1346 | 942 | 376 | 745 | 670 | 670 | 1.00 | 1.11 | 1.11 |
| | | | | | | 362 | 718 | | | | 1.07 | 1.07 |
| | | | | | | 309 | 613 | | | | 0.92 | 0.92 |
| 2 | 1132 | 1 | 1132 | 1263 | 1132 | 380 | 771 | 682 | 687 | 1.01 | 1.13 | 1.12 |
| | | | | | | 373 | 757 | | | | 1.11 | 1.10 |
| | | | | | | 340 | 691 | | | | 1.01 | 1.01 |
| 3 | 583 | 0.961 | 560 | 573 | 560 | 373 | 1840 | 1687 | 1574 | 0.93 | 1.09 | 1.17 |
| | | | | | | 337 | 1665 | | | | 0.99 | 1.06 |
| | | | | | | 314 | 1551 | | | | 0.92 | 0.99 |
| 4 | 659 | 0.979 | 645 | 573 | 573 | 380 | 1947 | 1734 | 1645 | 0.95 | 1.12 | 1.18 |
| | | | | | | 355 | 1823 | | | | 1.05 | 1.11 |
| | | | | | | 322 | 1650 | | | | 0.95 | 1.00 |
| 5 | 245 | 0.835 | 205 | 345 | 205 | 265 | 1969 | 1945 | 1740 | 0.89 | 1.01 | 1.13 |
| | | | | | | 226 | 1684 | | | | 0.87 | 0.97 |
| | | | | | | 222 | 1650 | | | | 0.85 | 0.95 |
| 6 | 317 | 0.873 | 277 | 348 | 277 | 309 | 2356 | 2185 | 1976 | 0.90 | 1.08 | 1.19 |
| | | | | | | 285 | 2174 | | | | 1.00 | 1.10 |
| | | | | | | 242 | 1845 | | | | 0.84 | 0.93 |
| 7 | 445 | 0.922 | 410 | 342 | 342 | 314 | 2489 | 2190 | 2201 | 1.01 | 1.14 | 1.13 |
| | | | | | | 289 | 2292 | | | | 1.05 | 1.04 |
| | | | | | | 252 | 1994 | | | | 0.91 | 0.91 |
| 8 | 542 | 0.951 | 515 | 317 | 317 | 307 | 2492 | 2120 | 2226 | 1.05 | 1.18 | 1.12 |
| | | | | | | 299 | 2430 | | | | 1.15 | 1.09 |
| | | | | | | 276 | 2243 | | | | 1.06 | 1.01 |
| 9 | 331 | 0.879 | 291 | 266 | 266 | 324 | 2828 | 2879 | 2282 | 0.79 | 0.98 | 1.24 |
| | | | | | | 311 | 2719 | | | | 0.94 | 1.19 |
| | | | | | | 291 | 2544 | | | | 0.88 | 1.12 |
| 10 | 380 | 0.899 | 341 | 266 | 266 | 330 | 2998 | 2950 | 2372 | 0.80 | 1.02 | 1.26 |
| | | | | | | 321 | 2916 | | | | 0.99 | 1.23 |
| | | | | | | 308 | 2794 | | | | 0.95 | 1.18 |
| 11 | 204 | 0.808 | 165 | 238 | 165 | 252 | 3149 | 3010 | 2742 | 0.91 | 1.05 | 1.15 |
| | | | | | | 221 | 2766 | | | | 0.92 | 1.01 |
| | | | | | | 218 | 2719 | | | | 0.90 | 0.99 |
| 12 | 255 | 0.841 | 215 | 238 | 215 | 252 | 3227 | 3468 | 3081 | 0.89 | 0.93 | 1.05 |
| | | | | | | 246 | 3160 | | | | 0.91 | 1.03 |
| | | | | | | 219 | 2815 | | | | 0.81 | 0.91 |
| 13 | 342 | 0.884 | 302 | 238 | 238 | 293 | 3930 | 3465 | 3345 | 0.97 | 1.13 | 1.17 |
| | | | | | | 278 | 3736 | | | | 1.08 | 1.12 |
| | | | | | | 250 | 3356 | | | | 0.97 | 1.00 |
| 14 | 400 | 0.907 | 363 | 235 | 235 | 278 | 3857 | 3321 | 3466 | 1.04 | 1.16 | 1.11 |
| | | | | | | 271 | 3766 | | | | 1.13 | 1.09 |
| | | | | | | 253 | 3508 | | | | 1.06 | 1.01 |
| | | | | | | | | | mean | 0.94 | 1.08 | 1.15 |
| | | | | | | | | | mean | | 1.02 | 1.09 |
| | | | | | | | | | mean | | 0.93 | 0.99 |

(fcr)d – Distortional Buckling critical stress
Rd – Reduction factor for Distortional Buckling critical stress
(fcr)l – Local Buckling critical stress
fcr – Controlling critical stress
fu100, fu75, fu25 – Ultimate stress for imperfection magnitudes 100%, 75% and 25% probability of exceedance
Mu100, Mu75, Mu25 – Ultimate moment for imperfection magnitudes 100%, 75% and 25% probability of exceedance
$M_{FEM}$, $M_{AISI}$, $M_{PRO}$ – Nominal Moment from FEM, AISI and proposed design approach for flexural members

Table 3.3 Moment Capacity for Z-section with Inside Angled Stiffener

| Model | Finite Strip Analysis | | | | | FEM | | AISI | PRO | $M_{PRO}/M_{AISI}$ | $M_{FEM}/M_{AISI}$ | $M_{FEM}/M_{PRO}$ |
|---|---|---|---|---|---|---|---|---|---|---|---|---|
| | (fcr)d (MPa) | Rd | Rd(fcr)d (MPa) | (fcr)l (MPa) | fcr (MPa) | fu<br>fu25<br>fu75 | Mu<br>Mu25<br>Mu75 | $M_{AISI}$ (N-m) | $M_{PRO}$ (N-m) | | imp 100%<br>imp 75%<br>imp 25% | imp 100%<br>imp 75%<br>imp 25% |
| 1 | 869 | 1.000 | 869 | 1418 | 869 | 373 | 744 | 675 | 675 | 1.00 | 1.10 | 1.10 |
| | | | | | | 355 | 709 | | | | 1.05 | 1.05 |
| | | | | | | 299 | 596 | | | | 0.88 | 0.88 |
| 2 | 980 | 1.000 | 980 | 1504 | 980 | 373 | 776 | 705 | 705 | 1.00 | 1.10 | 1.10 |
| | | | | | | 362 | 755 | | | | 1.07 | 1.07 |
| | | | | | | 305 | 635 | | | | 0.90 | 0.90 |
| 3 | 549 | 0.953 | 522 | 566 | 522 | 362 | 1795 | 1693 | 1554 | 0.92 | 1.06 | 1.16 |
| | | | | | | 332 | 1647 | | | | 0.97 | 1.06 |
| | | | | | | 306 | 1517 | | | | 0.90 | 0.98 |
| 4 | 600 | 0.966 | 580 | 569 | 569 | 369 | 1918 | 1775 | 1666 | 0.94 | 1.08 | 1.15 |
| | | | | | | 337 | 1753 | | | | 0.99 | 1.05 |
| | | | | | | 300 | 1558 | | | | 0.88 | 0.94 |
| 5 | 221 | 0.820 | 181 | 342 | 181 | 264 | 1968 | 2027 | 1678 | 0.83 | 0.97 | 1.17 |
| | | | | | | 209 | 1556 | | | | 0.77 | 0.93 |
| | | | | | | 206 | 1536 | | | | 0.76 | 0.92 |
| 6 | 245 | 0.835 | 205 | 355 | 205 | 274 | 2105 | 2131 | 1805 | 0.85 | 0.99 | 1.17 |
| | | | | | | 238 | 1832 | | | | 0.86 | 1.02 |
| | | | | | | 204 | 1569 | | | | 0.74 | 0.87 |
| 7 | 407 | 0.909 | 370 | 386 | 370 | 315 | 2517 | 2372 | 2263 | 0.95 | 1.06 | 1.11 |
| | | | | | | 296 | 2360 | | | | 0.99 | 1.04 |
| | | | | | | 251 | 2002 | | | | 0.84 | 0.88 |
| 8 | 466 | 0.929 | 433 | 390 | 390 | 308 | 2570 | 2490 | 2407 | 0.97 | 1.03 | 1.07 |
| | | | | | | 296 | 2470 | | | | 0.99 | 1.03 |
| | | | | | | 247 | 2059 | | | | 0.83 | 0.86 |
| 9 | 311 | 0.870 | 270 | 262 | 262 | 320 | 2800 | 2885 | 2283 | 0.79 | 0.97 | 1.23 |
| | | | | | | 296 | 2595 | | | | 0.90 | 1.14 |
| | | | | | | 275 | 2404 | | | | 0.83 | 1.05 |
| 10 | 345 | 0.885 | 305 | 262 | 262 | 325 | 2977 | 3020 | 2384 | 0.79 | 0.99 | 1.25 |
| | | | | | | 312 | 2850 | | | | 0.94 | 1.20 |
| | | | | | | 294 | 2693 | | | | 0.89 | 1.13 |
| 11 | 183 | 0.793 | 145 | 235 | 145 | 252 | 3145 | 3184 | 2638 | 0.83 | 0.99 | 1.19 |
| | | | | | | 217 | 2709 | | | | 0.85 | 1.03 |
| | | | | | | 215 | 2688 | | | | 0.84 | 1.02 |
| 12 | 200 | 0.806 | 161 | 238 | 161 | 236 | 3044 | 3365 | 2819 | 0.84 | 0.90 | 1.08 |
| | | | | | | 207 | 2666 | | | | 0.79 | 0.95 |
| | | | | | | 190 | 2452 | | | | 0.73 | 0.87 |
| 13 | 317 | 0.873 | 277 | 245 | 245 | 301 | 4056 | 3842 | 3386 | 0.88 | 1.06 | 1.20 |
| | | | | | | 286 | 3856 | | | | 1.00 | 1.14 |
| | | | | | | 261 | 3521 | | | | 0.92 | 1.04 |
| 14 | 359 | 0.891 | 320 | 248 | 248 | 302 | 4261 | 4052 | 3569 | 0.88 | 1.05 | 1.19 |
| | | | | | | 292 | 4130 | | | | 1.02 | 1.16 |
| | | | | | | 262 | 3696 | | | | 0.91 | 1.04 |
| | | | | | | | | | mean | 0.89 | 1.03 | 1.15 |
| | | | | | | | | | mean | | 0.94 | 1.06 |
| | | | | | | | | | mean | | 0.85 | 0.95 |

Table 3.4 Moment Capacity for Z-section with Outside Angled Stiffener

| Model | Finite Strip Analysis | | | | | FEM | | AISI | PRO | $M_{PRO}/M_{AISI}$ | $M_{FEM}/M_{AISI}$ | $M_{FEM}/M_{PRO}$ |
|---|---|---|---|---|---|---|---|---|---|---|---|---|
| | (fcr)d (MPa) | Rd | Rd(fcr)d (MPa) | (fcr)l (MPa) | fcr (MPa) | fu100 Mu100<br>fu75 Mu75<br>fu25 Mu25 | | $M_{AISI}$ (N-m) | $M_{PRO}$ (N-m) | | imp 100%<br>imp 75%<br>imp 25% | imp 100%<br>imp 75%<br>imp 25% |
| 1 | 749 | 0.997 | 746 | 1521 | 746 | 369 | 737 | 675 | 673 | 1.00 | 1.09 | 1.09 |
| | | | | | | 352 | 702 | | | | 1.04 | 1.04 |
| | | | | | | 298 | 594 | | | | 0.88 | 0.88 |
| 2 | 645 | 0.976 | 630 | 1542 | 630 | 369 | 769 | 705 | 678 | 0.96 | 1.09 | 1.13 |
| | | | | | | 355 | 740 | | | | 1.05 | 1.09 |
| | | | | | | 314 | 654 | | | | 0.93 | 0.96 |
| 3 | 486 | 0.935 | 455 | 573 | 455 | 362 | 1795 | 1693 | 1499 | 0.89 | 1.06 | 1.20 |
| | | | | | | 345 | 1708 | | | | 1.01 | 1.14 |
| | | | | | | 309 | 1532 | | | | 0.90 | 1.02 |
| 4 | 428 | 0.916 | 392 | 580 | 392 | 366 | 1900 | 1775 | 1510 | 0.85 | 1.07 | 1.26 |
| | | | | | | 339 | 1764 | | | | 0.99 | 1.17 |
| | | | | | | 305 | 1583 | | | | 0.89 | 1.05 |
| 5 | 207 | 0.811 | 168 | 400 | 168 | 267 | 1991 | 2027 | 1635 | 0.81 | 0.98 | 1.22 |
| | | | | | | 258 | 1922 | | | | 0.95 | 1.18 |
| | | | | | | 229 | 1708 | | | | 0.84 | 1.04 |
| 6 | 204 | 0.808 | 165 | 393 | 165 | 275 | 2113 | 2131 | 1675 | 0.79 | 0.99 | 1.26 |
| | | | | | | 262 | 2015 | | | | 0.95 | 1.20 |
| | | | | | | 232 | 1784 | | | | 0.84 | 1.07 |
| 7 | 348 | 0.887 | 309 | 393 | 309 | 318 | 2536 | 2372 | 2145 | 0.90 | 1.07 | 1.18 |
| | | | | | | 297 | 2371 | | | | 1.00 | 1.11 |
| | | | | | | 252 | 2008 | | | | 0.85 | 0.94 |
| 8 | 297 | 0.863 | 256 | 393 | 256 | 317 | 2639 | 2490 | 2116 | 0.85 | 1.06 | 1.25 |
| | | | | | | 292 | 2435 | | | | 0.98 | 1.15 |
| | | | | | | 247 | 2056 | | | | 0.83 | 0.97 |
| 9 | 286 | 0.858 | 246 | 266 | 246 | 317 | 2779 | 2885 | 2239 | 0.78 | 0.96 | 1.24 |
| | | | | | | 297 | 2604 | | | | 0.90 | 1.16 |
| | | | | | | 284 | 2486 | | | | 0.86 | 1.11 |
| 10 | 269 | 0.849 | 228 | 266 | 228 | 318 | 2913 | 3020 | 2285 | 0.76 | 0.96 | 1.27 |
| | | | | | | 295 | 2702 | | | | 0.89 | 1.18 |
| | | | | | | 278 | 2544 | | | | 0.84 | 1.11 |
| 11 | 173 | 0.785 | 135 | 242 | 135 | 252 | 3154 | 3184 | 2576 | 0.81 | 0.99 | 1.22 |
| | | | | | | 249 | 3115 | | | | 0.98 | 1.21 |
| | | | | | | 236 | 2947 | | | | 0.93 | 1.14 |
| 12 | 169 | 0.782 | 132 | 245 | 132 | 252 | 3244 | 3365 | 2631 | 0.78 | 0.96 | 1.23 |
| | | | | | | 190 | 2448 | | | | 0.73 | 0.93 |
| | | | | | | 172 | 2216 | | | | 0.66 | 0.84 |
| 13 | 273 | 0.851 | 232 | 248 | 232 | 299 | 4032 | 3842 | 3327 | 0.87 | 1.05 | 1.21 |
| | | | | | | 280 | 3777 | | | | 0.98 | 1.14 |
| | | | | | | 265 | 3567 | | | | 0.93 | 1.07 |
| 14 | 235 | 0.829 | 194 | 248 | 194 | 294 | 4159 | 4052 | 3292 | 0.81 | 1.03 | 1.26 |
| | | | | | | 280 | 3964 | | | | 0.98 | 1.20 |
| | | | | | | 254 | 3588 | | | | 0.89 | 1.09 |
| | | | | | | | | | mean | 0.85 | 1.03 | 1.22 |
| | | | | | | | | | mean | | 0.96 | 1.14 |
| | | | | | | | | | mean | | 0.86 | 1.02 |

Table 3.5 Moment Capacity for Z-section with Inside Hooked Stiffener

| Model | Finite Strip Analysis | | | | | FEM | | AISI | PRO | $M_{PRO}/M_{AISI}$ | $M_{FEM}/M_{AISI}$ | $M_{FEM}/M_{PRO}$ |
|---|---|---|---|---|---|---|---|---|---|---|---|---|
| | (fcr)d (MPa) | Rd | Rd(fcr)d (MPa) | (fcr)l (MPa) | fcr (MPa) | fu100 fu75 fu25 | Mu100 Mu75 Mu25 | $M_{AISI}$ (N-m) | $M_{PRO}$ (N-m) | | imp 100% imp 75% imp 25% | imp 100% imp 75% imp 25% |
| 1 | 825 | 1 | 825 | 1397 | 825 | 369 | 738 | 676 | 676 | 1.00 | 1.09 | 1.09 |
| | | | | | | 355 | 710 | | | | 1.05 | 1.05 |
| | | | | | | 298 | 596 | | | | 0.88 | 0.88 |
| 2 | 866 | 1 | 866 | 1487 | 866 | 373 | 782 | 710 | 710 | 1.00 | 1.10 | 1.10 |
| | | | | | | 355 | 746 | | | | 1.05 | 1.05 |
| | | | | | | 300 | 630 | | | | 0.89 | 0.89 |
| 3 | 528 | 0.947 | 500 | 566 | 500 | 362 | 1797 | 1694 | 1539 | 0.91 | 1.06 | 1.17 |
| | | | | | | 326 | 1616 | | | | 0.95 | 1.05 |
| | | | | | | 303 | 1503 | | | | 0.89 | 0.98 |
| 4 | 545 | 0.952 | 519 | 569 | 519 | 366 | 1906 | 1781 | 1634 | 0.92 | 1.07 | 1.17 |
| | | | | | | 335 | 1744 | | | | 0.98 | 1.07 |
| | | | | | | 304 | 1584 | | | | 0.89 | 0.97 |
| 5 | 210 | 0.813 | 171 | 683 | 171 | 263 | 1964 | 2019 | 1656 | 0.82 | 0.97 | 1.19 |
| | | | | | | 203 | 1513 | | | | 0.75 | 0.91 |
| | | | | | | 198 | 1480 | | | | 0.73 | 0.89 |
| 6 | 224 | 0.822 | 184 | 359 | 184 | 257 | 1982 | 2121 | 1754 | 0.83 | 0.93 | 1.13 |
| | | | | | | 221 | 1703 | | | | 0.80 | 0.97 |
| | | | | | | 208 | 1602 | | | | 0.76 | 0.91 |
| 7 | 386 | 0.902 | 348 | 380 | 348 | 325 | 2602 | 2377 | 2229 | 0.94 | 1.09 | 1.17 |
| | | | | | | 295 | 2362 | | | | 0.99 | 1.06 |
| | | | | | | 257 | 2058 | | | | 0.87 | 0.92 |
| 8 | 407 | 0.909 | 370 | 386 | 370 | 325 | 2728 | 2514 | 2389 | 0.95 | 1.09 | 1.14 |
| | | | | | | 292 | 2453 | | | | 0.98 | 1.03 |
| | | | | | | 252 | 2114 | | | | 0.84 | 0.88 |
| 9 | 304 | 0.866 | 263 | 273 | 263 | 319 | 2799 | 2886 | 2296 | 0.80 | 0.97 | 1.22 |
| | | | | | | 299 | 2623 | | | | 0.91 | 1.14 |
| | | | | | | 279 | 2442 | | | | 0.85 | 1.06 |
| 10 | 321 | 0.874 | 281 | 273 | 273 | 325 | 2976 | 3027 | 2425 | 0.80 | 0.98 | 1.23 |
| | | | | | | 313 | 2869 | | | | 0.95 | 1.18 |
| | | | | | | 297 | 2726 | | | | 0.90 | 1.12 |
| 11 | 176 | 0.787 | 139 | 235 | 139 | 247 | 3090 | 3166 | 2615 | 0.83 | 0.98 | 1.18 |
| | | | | | | 191 | 2387 | | | | 0.75 | 0.91 |
| | | | | | | 189 | 2369 | | | | 0.75 | 0.91 |
| 12 | 183 | 0.793 | 145 | 238 | 145 | 248 | 3204 | 3343 | 2737 | 0.82 | 0.96 | 1.17 |
| | | | | | | 195 | 2522 | | | | 0.75 | 0.92 |
| | | | | | | 184 | 2371 | | | | 0.71 | 0.87 |
| 13 | 304 | 0.866 | 263 | 242 | 242 | 299 | 4042 | 3847 | 3384 | 0.88 | 1.05 | 1.19 |
| | | | | | | 293 | 3949 | | | | 1.03 | 1.17 |
| | | | | | | 266 | 3586 | | | | 0.93 | 1.06 |
| 14 | 317 | 0.873 | 277 | 248 | 248 | 298 | 4227 | 4095 | 3592 | 0.88 | 1.03 | 1.18 |
| | | | | | | 294 | 4178 | | | | 1.02 | 1.16 |
| | | | | | | 261 | 3708 | | | | 0.91 | 1.03 |
| | | | | | | | | | mean | 0.88 | 1.03 | 1.17 |
| | | | | | | | | | mean | | 0.93 | 1.05 |
| | | | | | | | | | mean | | 0.84 | 0.96 |

Table 3.6 Moment Capacity for Z-section with Outside Hooked Stiffener

| Model | Finite Strip Analysis | | | | | FEM | | AISI | PRO | $M_{PRO}/M_{AISI}$ | $M_{FEM}/M_{AISI}$ | $M_{FEM}/M_{PRO}$ |
|---|---|---|---|---|---|---|---|---|---|---|---|---|
| | (fcr)d (MPa) | Rd | Rd(fcr)d (MPa) | (fcr)l (MPa) | fcr (MPa) | fu100<br>fu75<br>fu25 | Mu100<br>Mu75<br>Mu25 | $M_{AISI}$ (N-m) | $M_{PRO}$ (N-m) | | imp 100%<br>imp 75%<br>imp 25% | imp 100%<br>imp 75%<br>imp 25% |
| 1 | 735 | 0.994 | 731 | 1490 | 731 | 369 | 738 | 676 | 671 | 0.99 | 1.09 | 1.10 |
| | | | | | | 355 | 710 | | | | 1.05 | 1.06 |
| | | | | | | 319 | 637 | | | | 0.94 | 0.95 |
| 2 | 642 | 0.975 | 626 | 1532 | 626 | 366 | 768 | 710 | 683 | 0.96 | 1.08 | 1.12 |
| | | | | | | 345 | 724 | | | | 1.02 | 1.06 |
| | | | | | | 294 | 617 | | | | 0.87 | 0.90 |
| 3 | 480 | 0.933 | 447 | 573 | 447 | 359 | 1780 | 1694 | 1496 | 0.88 | 1.05 | 1.19 |
| | | | | | | 331 | 1643 | | | | 0.97 | 1.10 |
| | | | | | | 307 | 1523 | | | | 0.90 | 1.02 |
| 4 | 428 | 0.916 | 392 | 576 | 392 | 362 | 1888 | 1781 | 1518 | 0.85 | 1.06 | 1.24 |
| | | | | | | 321 | 1674 | | | | 0.94 | 1.10 |
| | | | | | | 295 | 1536 | | | | 0.86 | 1.01 |
| 5 | 200 | 0.806 | 161 | 359 | 161 | 266 | 1982 | 2019 | 1623 | 0.80 | 0.98 | 1.22 |
| | | | | | | 201 | 1498 | | | | 0.74 | 0.92 |
| | | | | | | 199 | 1488 | | | | 0.74 | 0.92 |
| 6 | 193 | 0.801 | 155 | 386 | 155 | 271 | 2089 | 2121 | 1652 | 0.78 | 0.98 | 1.26 |
| | | | | | | 223 | 1722 | | | | 0.81 | 1.04 |
| | | | | | | 216 | 1668 | | | | 0.79 | 1.01 |
| 7 | 342 | 0.884 | 302 | 386 | 302 | 317 | 2535 | 2377 | 2137 | 0.90 | 1.07 | 1.19 |
| | | | | | | 296 | 2364 | | | | 0.99 | 1.11 |
| | | | | | | 250 | 2003 | | | | 0.84 | 0.94 |
| 8 | 297 | 0.863 | 256 | 393 | 256 | 323 | 2711 | 2514 | 2134 | 0.85 | 1.08 | 1.27 |
| | | | | | | 290 | 2433 | | | | 0.97 | 1.14 |
| | | | | | | 248 | 2080 | | | | 0.83 | 0.97 |
| 9 | 283 | 0.856 | 242 | 262 | 242 | 321 | 2814 | 2886 | 2241 | 0.78 | 0.97 | 1.26 |
| | | | | | | 302 | 2644 | | | | 0.92 | 1.18 |
| | | | | | | 284 | 2487 | | | | 0.86 | 1.11 |
| 10 | 269 | 0.849 | 228 | 266 | 228 | 316 | 2894 | 3027 | 2300 | 0.76 | 0.96 | 1.26 |
| | | | | | | 298 | 2736 | | | | 0.90 | 1.19 |
| | | | | | | 282 | 2581 | | | | 0.85 | 1.12 |
| 11 | 169 | 0.782 | 132 | 238 | 132 | 246 | 3082 | 3166 | 2573 | 0.81 | 0.97 | 1.20 |
| | | | | | | 194 | 2430 | | | | 0.77 | 0.94 |
| | | | | | | 189 | 2361 | | | | 0.75 | 0.92 |
| 12 | 162 | 0.776 | 126 | 242 | 126 | 247 | 3191 | 3343 | 2607 | 0.78 | 0.95 | 1.22 |
| | | | | | | 179 | 2308 | | | | 0.69 | 0.89 |
| | | | | | | 174 | 2251 | | | | 0.67 | 0.86 |
| 13 | 269 | 0.849 | 228 | 245 | 228 | 298 | 4023 | 3847 | 3323 | 0.86 | 1.05 | 1.21 |
| | | | | | | 292 | 3939 | | | | 1.02 | 1.19 |
| | | | | | | 262 | 3539 | | | | 0.92 | 1.06 |
| 14 | 235 | 0.829 | 194 | 248 | 194 | 294 | 4169 | 4095 | 3315 | 0.81 | 1.02 | 1.26 |
| | | | | | | 285 | 4041 | | | | 0.99 | 1.22 |
| | | | | | | 250 | 3547 | | | | 0.87 | 1.07 |
| | | | | | | | | | mean | 0.84 | 1.02 | 1.21 |
| | | | | | | | | | mean | | 0.91 | 1.08 |
| | | | | | | | | | mean | | 0.83 | 0.99 |

Table 3.7 Finite Element Results for Imperfection Magnitude 100% Probability of Exceedance

| Model | Simple Lip $M_{SL}/M_{MAX}$ | Inside Angled $M_{IA}/M_{MAX}$ | Outside Angled $M_{OA}/M_{MAX}$ | Inside Hooked $M_{IH}/M_{MAX}$ | Outside Hooked $M_{OH}/M_{MAX}$ | $M_{MAX}$ (N-m) |
|---|---|---|---|---|---|---|
| 1 | 1 | 0.998 | 0.989 | 0.990 | 0.990 | 745 |
| 2 | 0.986 | 0.993 | 0.984 | 1 | 0.981 | 782 |
| 3 | 1 | 0.976 | 0.976 | 0.976 | 0.967 | 1840 |
| 4 | 1 | 0.985 | 0.976 | 0.979 | 0.970 | 1947 |
| 5 | 0.989 | 0.988 | 1 | 0.986 | 0.995 | 1991 |
| 6 | 1 | 0.894 | 0.897 | 0.841 | 0.887 | 2356 |
| 7 | 0.957 | 0.967 | 0.975 | 1 | 0.975 | 2602 |
| 8 | 0.913 | 0.942 | 0.967 | 1 | 0.994 | 2728 |
| 9 | 1 | 0.990 | 0.983 | 0.990 | 0.995 | 2828 |
| 10 | 1 | 0.993 | 0.972 | 0.993 | 0.965 | 2998 |
| 11 | 0.999 | 0.997 | 1 | 0.980 | 0.977 | 3154 |
| 12 | 0.995 | 0.938 | 1 | 0.988 | 0.984 | 3244 |
| 13 | 0.969 | 1 | 0.994 | 0.997 | 0.992 | 4056 |
| 14 | 0.905 | 1 | 0.976 | 0.992 | 0.978 | 4261 |

$M_{SL}$, $M_{IA}$, $M_{OA}$, $M_{IH}$, $M_{OH}$ – Z-section moment capacity for Simple Lip, Inside Angled, Outside Angled, Inside Hooked and Outside Hooked stiffeners

$M_{MAX}$ – Maximum moment capacity between $M_{SL}$, $M_{IA}$, $M_{OA}$, $M_{IH}$, $M_{OH}$

Table 3.8 Finite Element Results for Imperfection Magnitude 75% Probability of Exceedance

| Model | Simple Lip $M_{SL}/M_{MAX}$ | Inside Angled $M_{IA}/M_{MAX}$ | Outside Angled $M_{OA}/M_{MAX}$ | Inside Hooked $M_{IH}/M_{MAX}$ | Outside Hooked $M_{OH}/M_{MAX}$ | $M_{MAX}$ (N-m) |
|---|---|---|---|---|---|---|
| 1 | 1 | 0.988 | 0.978 | 0.990 | 0.990 | 718 |
| 2 | 1 | 0.997 | 0.978 | 0.985 | 0.957 | 757 |
| 3 | 0.975 | 0.964 | 1 | 0.946 | 0.962 | 1708 |
| 4 | 1 | 0.962 | 0.967 | 0.957 | 0.918 | 1823 |
| 5 | 0.876 | 0.810 | 1 | 0.788 | 0.780 | 1922 |
| 6 | 1 | 0.842 | 0.927 | 0.783 | 0.792 | 2174 |
| 7 | 0.967 | 0.995 | 1 | 0.996 | 0.997 | 2371 |
| 8 | 0.984 | 1 | 0.986 | 0.993 | 0.985 | 2470 |
| 9 | 1 | 0.954 | 0.958 | 0.965 | 0.973 | 2719 |
| 10 | 1 | 0.977 | 0.926 | 0.984 | 0.938 | 2916 |
| 11 | 0.888 | 0.870 | 1 | 0.766 | 0.780 | 3115 |
| 12 | 1 | 0.843 | 0.774 | 0.798 | 0.730 | 3160 |
| 13 | 0.946 | 0.976 | 0.956 | 1 | 0.998 | 3949 |
| 14 | 0.901 | 0.988 | 0.949 | 1 | 0.967 | 4178 |

Table 3.9 Finite Element Results for Imperfection Magnitude 25% Probability of Exceedance

| Model | Simple Lip $M_{SL}/M_{MAX}$ | Inside Angled $M_{IA}/M_{MAX}$ | Outside Angled $M_{OA}/M_{MAX}$ | Inside Hooked $M_{IH}/M_{MAX}$ | Outside Hooked $M_{OH}/M_{MAX}$ | $M_{MAX}$ (N-m) |
|---|---|---|---|---|---|---|
| 1 | 0.962 | 0.936 | 0.932 | 0.935 | 1 | 637 |
| 2 | 1 | 0.920 | 0.947 | 0.912 | 0.893 | 691 |
| 3 | 1 | 0.978 | 0.988 | 0.969 | 0.982 | 1551 |
| 4 | 1 | 0.944 | 0.959 | 0.960 | 0.931 | 1650 |
| 5 | 0.966 | 0.899 | 1 | 0.866 | 0.871 | 1708 |
| 6 | 1 | 0.850 | 0.967 | 0.868 | 0.904 | 1845 |
| 7 | 0.969 | 0.973 | 0.975 | 1 | 0.973 | 2058 |
| 8 | 1 | 0.918 | 0.917 | 0.943 | 0.927 | 2243 |
| 9 | 1 | 0.945 | 0.977 | 0.960 | 0.978 | 2544 |
| 10 | 1 | 0.964 | 0.910 | 0.976 | 0.924 | 2794 |
| 11 | 0.923 | 0.912 | 1 | 0.804 | 0.801 | 2947 |
| 12 | 1 | 0.871 | 0.787 | 0.842 | 0.799 | 2815 |
| 13 | 0.936 | 0.982 | 0.995 | 1 | 0.987 | 3586 |
| 14 | 0.946 | 0.997 | 0.968 | 1 | 0.956 | 3708 |

Table 3.10 AISI and Proposed Design Approach for Flexural Members

| Model | AISI Method | | | | Proposed Design Approach for Flexural Members Method | | | | | |
|---|---|---|---|---|---|---|---|---|---|---|
| | Simple Lip $M_{SL}/M_{MAX}$ | Inside, Outside Angled $M_{IOA}/M_{MAX}$ | Inside, Outside Hooked $M_{IOH}/M_{MAX}$ | $M_{MAX}$ (N-m) | Simple Lip $M_{SL}/M_{MAX}$ | Inside Angled $M_{IA}/M_{MAX}$ | Outside Angled $M_{OA}/M_{MAX}$ | Inside Hooked $M_{IH}/M_{MAX}$ | Outside Hooked $M_{OH}/M_{MAX}$ | $M_{MAX}$ (N-m) |
| 1 | 0.991 | 0.998 | 1 | 676 | 0.991 | 0.998 | 0.996 | 1 | 0.993 | 676 |
| 2 | 0.960 | 0.993 | 1 | 710 | 0.968 | 0.993 | 0.956 | 1 | 0.962 | 710 |
| 3 | 0.996 | 0.999 | 1 | 1694 | 1 | 0.987 | 0.952 | 0.978 | 0.950 | 1574 |
| 4 | 0.974 | 0.997 | 1 | 1781 | 0.988 | 1 | 0.907 | 0.981 | 0.911 | 1666 |
| 5 | 0.959 | 1 | 0.996 | 2027 | 1 | 0.964 | 0.939 | 0.951 | 0.932 | 1740 |
| 6 | 1 | 0.975 | 0.971 | 2185 | 1 | 0.913 | 0.848 | 0.888 | 0.836 | 1976 |
| 7 | 0.921 | 0.998 | 1 | 2377 | 0.973 | 1 | 0.948 | 0.985 | 0.944 | 2263 |
| 8 | 0.843 | 0.991 | 1 | 2514 | 0.925 | 1 | 0.879 | 0.993 | 0.886 | 2407 |
| 9 | 0.997 | 0.999 | 1 | 2886 | 0.994 | 0.994 | 0.975 | 1 | 0.976 | 2296 |
| 10 | 0.975 | 0.998 | 1 | 3027 | 0.978 | 0.983 | 0.942 | 1 | 0.949 | 2425 |
| 11 | 0.946 | 1 | 0.994 | 3184 | 1 | 0.962 | 0.939 | 0.954 | 0.938 | 2742 |
| 12 | 1 | 0.970 | 0.964 | 3468 | 1 | 0.915 | 0.854 | 0.888 | 0.846 | 3081 |
| 13 | 0.901 | 0.999 | 1 | 3847 | 0.988 | 1 | 0.982 | 0.999 | 0.981 | 3386 |
| 14 | 0.811 | 0.990 | 1 | 4095 | 0.965 | 0.994 | 0.916 | 1 | 0.923 | 3592 |

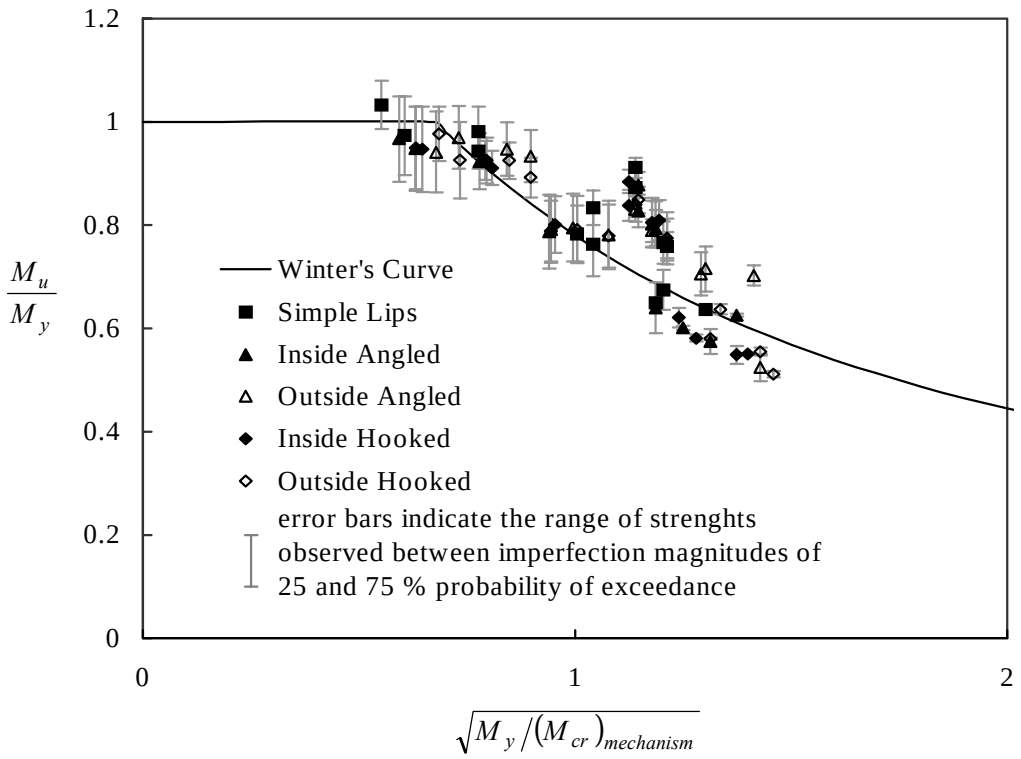


Figure 3.3 Post-Buckling Capacity by Finite Element Method

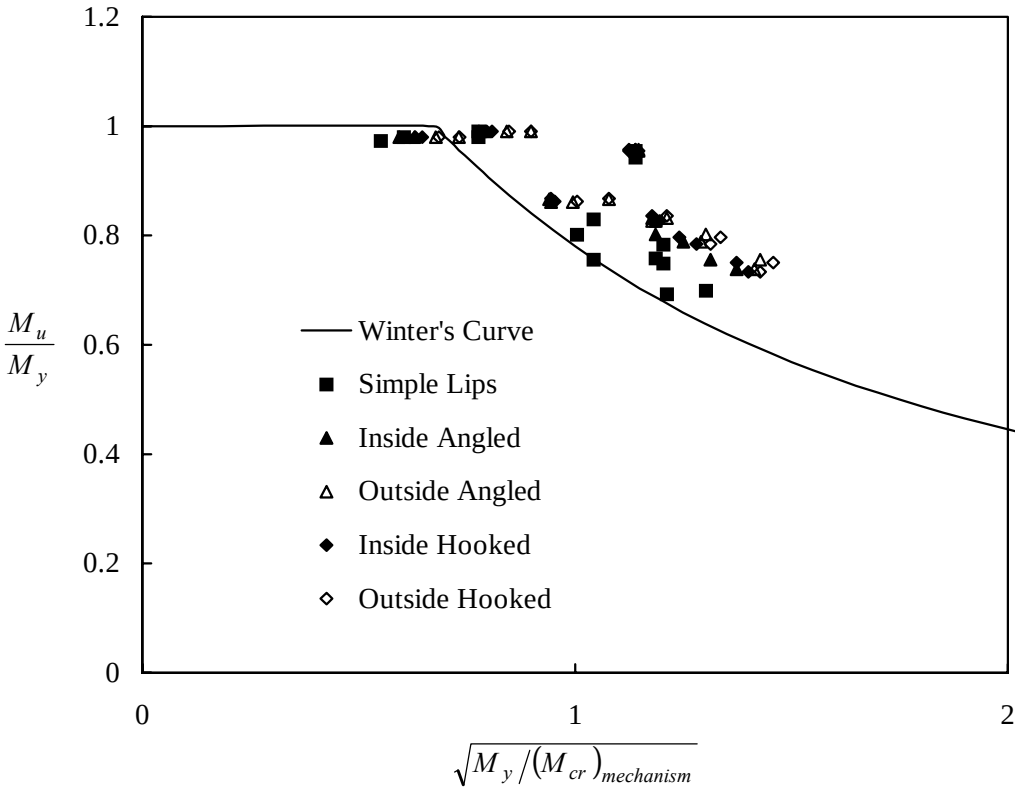


Figure 3.4 Post-Buckling Capacity by AISI Method

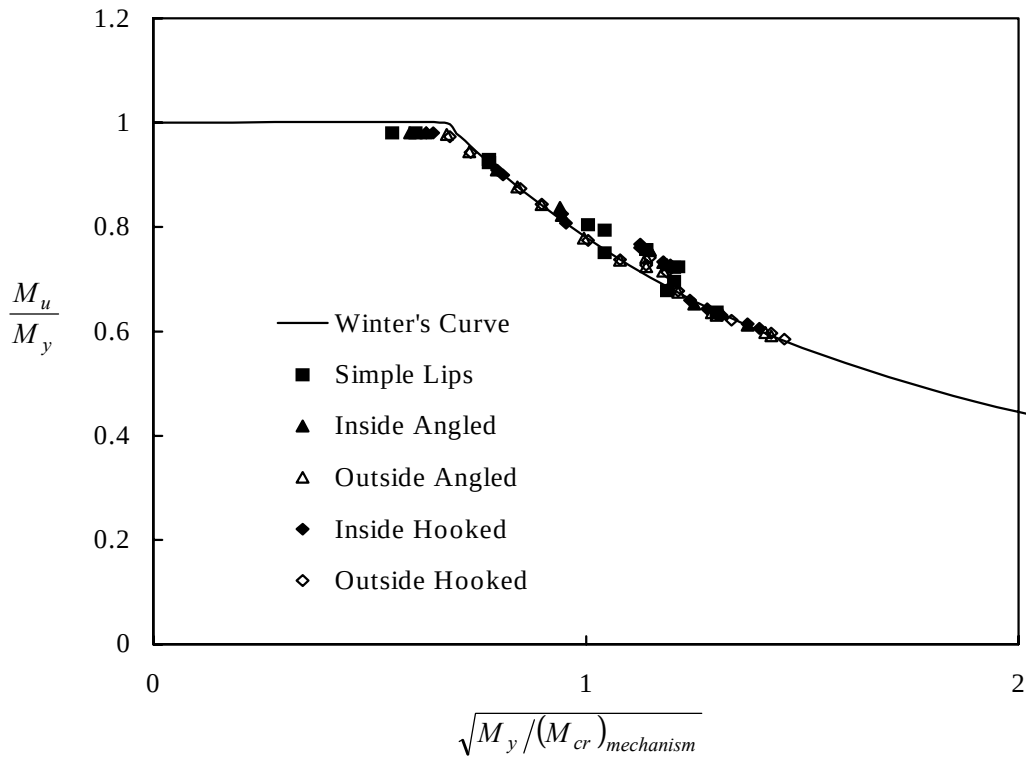


Figure 3.5 Post-Buckling Capacity by Proposed Design Approach for Flexural Members

### 3.3 Z-Section Parameter Study for Various Thickness

This second parameter study was carried out by modifying the stiffeners of a standard cross section 12ZS3.25, which has a sloping lip stiffener. The sloping lip stiffener was modified into simple lip, outside angled and inside angled stiffeners. Cross-section area for each type of stiffeners is maintained to compare the efficiency. This was done for different thickness. The finite element assumptions are the same as in the first parameter study except for the yield stress and the lateral bracing conditions. This study uses a 55 ksi yield stress and instead of fully bracing along the length as in the first parameter study, only four brace points are used. Brace points one at each end and additional ones at one-third of the length, which is the same length as the half-wave lengths of the distortional mode that gives the least buckling strength. Figure 3.7 shows the second parameter study boundary and loading conditions. For this cross section and bracing length, full formation of the distortional mode is still possible without causing a lateral-torsional failure. Figure 3.6 and Table 3.11 summarize the geometry of the members. Results for each type of stiffeners for this parameter study are shown in Table 3.12. Table 3.13, 3.14, 3.15, 3.16 and Figure 3.8, 3.9, 3.10 summarizes the results for different approaches.

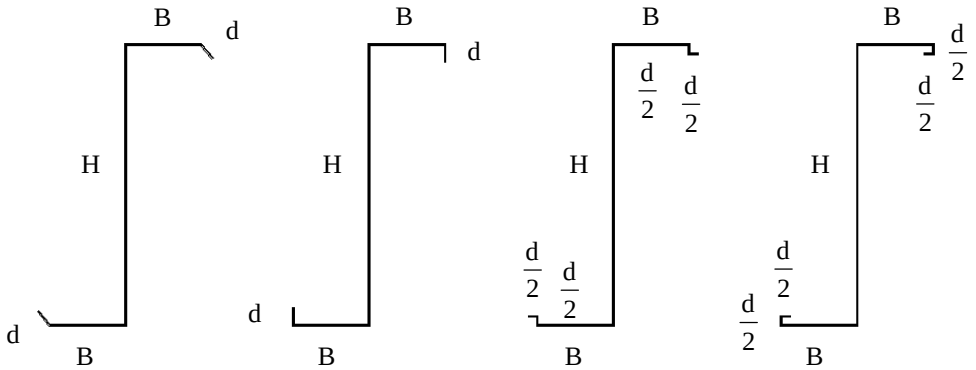


Figure 3.6 Z-section 12ZS3.25 with (a) Sloping Lip Stiffener 50 degree respect to the flange (b) Simple Lip Stiffener (c) Outside Angled Stiffener (d) Inside Angled Stiffener

Table 3.11 Summary of Models Geometry

| Model | Dimensions | | | | | | | |
|---|---|---|---|---|---|---|---|---|
| | | | | | Length, L (in.) | | | |
| | H (in.) | B (in.) | d (in.) | t (in.) | Sloping Lip | Simple Lip | Inside Angled | Outside Angled |
| 1 | 12 | 3.25 | 0.75 | 0.135 | 54 | 60 | 51 | 51 |
| 2 | 12 | 3.25 | 0.75 | 0.105 | 63 | 69 | 57 | 60 |
| 3 | 12 | 3.25 | 0.75 | 0.090 | 69 | 75 | 63 | 75 |
| 4 | 12 | 3.25 | 0.75 | 0.075 | 75 | 84 | 69 | 72 |
| 5 | 12 | 3.25 | 0.75 | 0.060 | 84 | 96 | 78 | 81 |

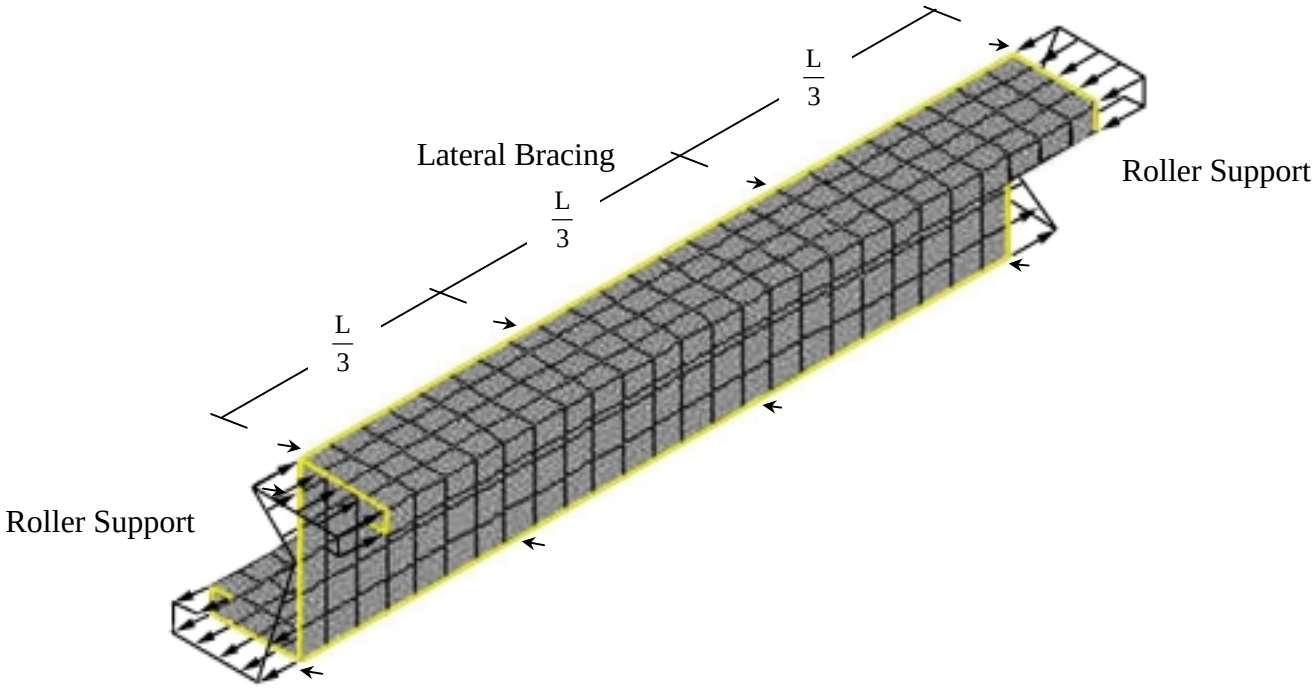


Figure 3.7 Boundary and Loading Condition

Table 3.12 Moment Capacity for Z-section 12ZS3.25 with Sloping Lip, Simple Lip, Outside Angled, Inside Angled Stiffeners

| Model | | Finite Strip Analysis | | | | | FEM | | AISI | PRO | $M_{PRO}/M_{AISI}$ | $M_{FEM}/M_{AISI}$ | $M_{FEM}/M_{PRO}$ |
|---|---|---|---|---|---|---|---|---|---|---|---|---|---|
| | | (fcr)d (ksi) | Rd | Rd(fcr)d (ksi) | (fcr)l (ksi) | fcr (ksi) | fu100<br>fu75<br>fu25 | Mu100<br>Mu75<br>Mu25 | $M_{AISI}$ (kip-in.) | $M_{PRO}$ (kip-in.) | | imp 100%<br>imp 75%<br>imp 25% | imp 100%<br>imp 75%<br>imp 25% |
| Sloping Lip Stiffener | 1 | 56 | 0.888 | 50 | 77 | 50 | 51 | 468 | 463 | 397 | 0.86 | 1.01 | 1.18 |
| | | | | | | | 48 | 436 | | | | 0.94 | 1.10 |
| | | | | | | | 41 | 378 | | | | 0.82 | 0.95 |
| | 2 | 40 | 0.838 | 33 | 59 | 33 | 45 | 322 | 327 | 275 | 0.84 | 0.98 | 1.17 |
| | | | | | | | 36 | 262 | | | | 0.80 | 0.95 |
| | | | | | | | 37 | 267 | | | | 0.82 | 0.97 |
| | 3 | 33 | 0.809 | 26 | 46 | 26 | 41 | 253 | 263 | 219 | 0.83 | 0.96 | 1.15 |
| | | | | | | | 31 | 194 | | | | 0.74 | 0.89 |
| | | | | | | | 30 | 185 | | | | 0.70 | 0.84 |
| | 4 | 26 | 0.776 | 20 | 32 | 20 | 36 | 188 | 192 | 167 | 0.87 | 0.98 | 1.13 |
| | | | | | | | 27 | 141 | | | | 0.73 | 0.84 |
| | | | | | | | 26 | 135 | | | | 0.70 | 0.81 |
| | 5 | 20 | 0.738 | 15 | 21 | 15 | 28 | 118 | 134 | 119 | 0.89 | 0.88 | 0.99 |
| | | | | | | | 23 | 94 | | | | 0.71 | 0.79 |
| | | | | | | | 22 | 91 | | | | 0.68 | 0.76 |
| Simple Lip Stiffener | 1 | 71 | 0.922 | 65 | 102 | 65 | 54 | 488 | 473 | 426 | 0.90 | 1.03 | 1.14 |
| | | | | | | | 48 | 433 | | | | 0.92 | 1.02 |
| | | | | | | | 45 | 411 | | | | 0.87 | 0.96 |
| | 2 | 51 | 0.875 | 45 | 63 | 45 | 48 | 338 | 339 | 302 | 0.89 | 1.00 | 1.12 |
| | | | | | | | 40 | 283 | | | | 0.83 | 0.94 |
| | | | | | | | 37 | 264 | | | | 0.78 | 0.88 |
| | 3 | 43 | 0.847 | 36 | 46 | 36 | 44 | 268 | 276 | 242 | 0.88 | 0.97 | 1.11 |
| | | | | | | | 36 | 221 | | | | 0.80 | 0.91 |
| | | | | | | | 35 | 214 | | | | 0.78 | 0.88 |
| | 4 | 34 | 0.816 | 28 | 32 | 28 | 35 | 180 | 204 | 186 | 0.91 | 0.88 | 0.96 |
| | | | | | | | 33 | 170 | | | | 0.83 | 0.91 |
| | | | | | | | 34 | 174 | | | | 0.86 | 0.94 |
| | 5 | 26 | 0.779 | 21 | 21 | 21 | 29 | 120 | 145 | 135 | 0.93 | 0.83 | 0.89 |
| | | | | | | | 29 | 122 | | | | 0.84 | 0.90 |
| | | | | | | | 28 | 118 | | | | 0.81 | 0.87 |
| Outside Angled Stiffener | 1 | 54 | 0.881 | 47 | 69 | 47 | 50 | 454 | 480 | 393 | 0.82 | 0.95 | 1.16 |
| | | | | | | | 46 | 420 | | | | 0.88 | 1.07 |
| | | | | | | | 41 | 376 | | | | 0.78 | 0.96 |
| | 2 | 38 | 0.830 | 31 | 54 | 31 | 43 | 305 | 345 | 271 | 0.79 | 0.89 | 1.13 |
| | | | | | | | 36 | 257 | | | | 0.74 | 0.95 |
| | | | | | | | 37 | 264 | | | | 0.77 | 0.97 |
| | 3 | 31 | 0.800 | 24 | 46 | 24 | 39 | 239 | 286 | 215 | 0.75 | 0.84 | 1.11 |
| | | | | | | | 31 | 192 | | | | 0.67 | 0.89 |
| | | | | | | | 31 | 188 | | | | 0.66 | 0.87 |
| | 4 | 24 | 0.766 | 19 | 32 | 19 | 34 | 176 | 208 | 163 | 0.78 | 0.84 | 1.08 |
| | | | | | | | 27 | 141 | | | | 0.67 | 0.86 |
| | | | | | | | 26 | 135 | | | | 0.65 | 0.82 |
| | 5 | 18 | 0.728 | 13 | 21 | 13 | 27 | 114 | 144 | 116 | 0.81 | 0.79 | 0.98 |
| | | | | | | | 23 | 97 | | | | 0.68 | 0.84 |
| | | | | | | | 23 | 95 | | | | 0.66 | 0.81 |

| | | | | | | | | | | | | | |
|---|---|---|---|---|---|---|---|---|---|---|---|---|---|
| Inside Angled Stiffener | 1 | 59 | 0.896 | 53 | 77 | 53 | 51 | 466 | 480 | 406 | 0.85 | 0.97 | 1.15 |
| | | | | | | | 46 | 420 | | | | 0.88 | 1.04 |
| | | | | | | | 41 | 368 | | | | 0.77 | 0.91 |
| | 2 | 42 | 0.846 | 36 | 58 | 36 | 45 | 318 | 345 | 283 | 0.82 | 0.92 | 1.13 |
| | | | | | | | 38 | 269 | | | | 0.78 | 0.95 |
| | | | | | | | 38 | 270 | | | | 0.78 | 0.96 |
| | 3 | 34 | 0.817 | 28 | 45 | 28 | 41 | 255 | 286 | 244 | 0.85 | 0.89 | 1.04 |
| | | | | | | | 35 | 213 | | | | 0.74 | 0.87 |
| | | | | | | | 34 | 207 | | | | 0.72 | 0.85 |
| | 4 | 27 | 0.784 | 22 | 31 | 22 | 35 | 182 | 208 | 172 | 0.83 | 0.87 | 1.06 |
| | | | | | | | 29 | 149 | | | | 0.72 | 0.87 |
| | | | | | | | 28 | 145 | | | | 0.70 | 0.84 |
| | 5 | 21 | 0.746 | 16 | 20 | 16 | 28 | 117 | 144 | 123 | 0.85 | 0.82 | 0.95 |
| | | | | | | | 27 | 112 | | | | 0.78 | 0.91 |
| | | | | | | | 24 | 100 | | | | 0.69 | 0.81 |
| | | | | | | | | | | mean | 0.85 | 0.93 | 1.09 |
| | | | | | | | | | | mean | | 0.79 | 0.93 |
| | | | | | | | | | | mean | | 0.76 | 0.89 |

Table 3.13 Finite Element Results for Imperfection Magnitude 100% Probability of Exceedance

| Model | Sloping Lip $M_{SLL}/M_{MAX}$ | Simple Lip $M_{SL}/M_{MAX}$ | Outside Angled $M_{IA}/M_{MAX}$ | Inside Angled $M_{OA}/M_{MAX}$ | $M_{MAX}$ (kip-in.) |
|---|---|---|---|---|---|
| 1 | 0.960 | 1 | 0.930 | 0.955 | 488 |
| 2 | 0.950 | 1 | 0.902 | 0.941 | 338 |
| 3 | 0.941 | 1 | 0.892 | 0.949 | 268 |
| 4 | 1 | 0.954 | 0.935 | 0.970 | 188 |
| 5 | 0.983 | 1 | 0.946 | 0.977 | 120 |

$M_{SLL}$, $M_{SL}$, $M_{IA}$, $M_{OA}$ – Z-section moment capacity for Sloping Lip, Simple Lip, Inside Angled, Outside Angled stiffeners

$M_{MAX}$ – Maximum moment capacity between $M_{SLL}$, $M_{SL}$, $M_{IA}$, $M_{OA}$

Table 3.14 Finite Element Results for Imperfection Magnitude 75% Probability of Exceedance

| Model | Sloping Lip $M_{SLL}/M_{MAX}$ | Simple Lip $M_{SL}/M_{MAX}$ | Outside Angled $M_{IA}/M_{MAX}$ | Inside Angled $M_{OA}/M_{MAX}$ | $M_{MAX}$ (kip-in.) |
|---|---|---|---|---|---|
| 1 | 1 | 0.995 | 0.965 | 0.965 | 436 |
| 2 | 0.925 | 1 | 0.908 | 0.952 | 283 |
| 3 | 0.878 | 1 | 0.867 | 0.962 | 221 |
| 4 | 0.828 | 1 | 0.828 | 0.880 | 170 |
| 5 | 0.774 | 1 | 0.801 | 0.919 | 122 |

Table 3.15 Finite Element Results for Imperfection Magnitude 25% Probability of Exceedance

| Model | Sloping Lip $M_{SLL}/M_{MAX}$ | Simple Lip $M_{SL}/M_{MAX}$ | Outside Angled $M_{IA}/M_{MAX}$ | Inside Angled $M_{OA}/M_{MAX}$ | $M_{MAX}$ (kip-in.) |
|---|---|---|---|---|---|
| 1 | 0.920 | 1 | 0.915 | 0.895 | 411 |
| 2 | 0.987 | 0.976 | 0.975 | 1 | 270 |
| 3 | 0.864 | 1 | 0.878 | 0.965 | 214 |
| 4 | 0.772 | 1 | 0.772 | 0.831 | 174 |
| 5 | 0.770 | 1 | 0.805 | 0.850 | 118 |

Table 3.16 AISI and Proposed Design Approach for Flexural Members

| Model | AISI Method | | | | Proposed Design Approach for Flexural Members Method | | | | |
|---|---|---|---|---|---|---|---|---|---|
| | Sloping Lip $M_{SLL}/M_{MAX}$ | Simple Lip $M_{SL}/M_{MAX}$ | Outside, Inside Angled $M_{IOA}/M_{MAX}$ | $M_{MAX}$ (kip-in.) | Sloping Lip $M_{SLL}/M_{MAX}$ | Simple Lip $M_{SL}/M_{MAX}$ | Outside Angled $M_{IA}/M_{MAX}$ | Inside Angled $M_{OA}/M_{MAX}$ | $M_{MAX}$ (kip-in.) |
| 1 | 0.964 | 0.986 | 1 | 480 | 0.931 | 1 | 0.921 | 0.951 | 426 |
| 2 | 0.948 | 0.983 | 1 | 345 | 0.913 | 1 | 0.899 | 0.938 | 302 |
| 3 | 0.919 | 0.963 | 1 | 286 | 0.898 | 0.993 | 0.882 | 1 | 244 |
| 4 | 0.921 | 0.978 | 1 | 208 | 0.895 | 1 | 0.876 | 0.923 | 186 |
| 5 | 0.924 | 1 | 0.996 | 145 | 0.885 | 1 | 0.863 | 0.914 | 135 |

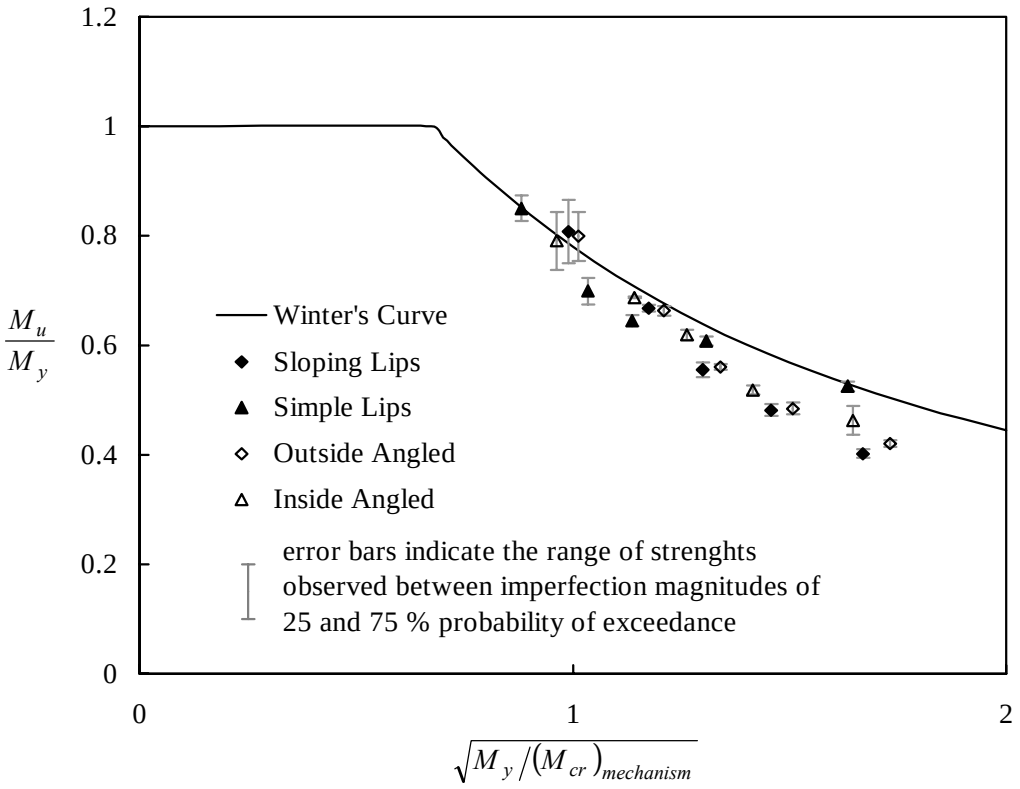


Figure 3.8 Post-Buckling Capacity by Finite Element Method

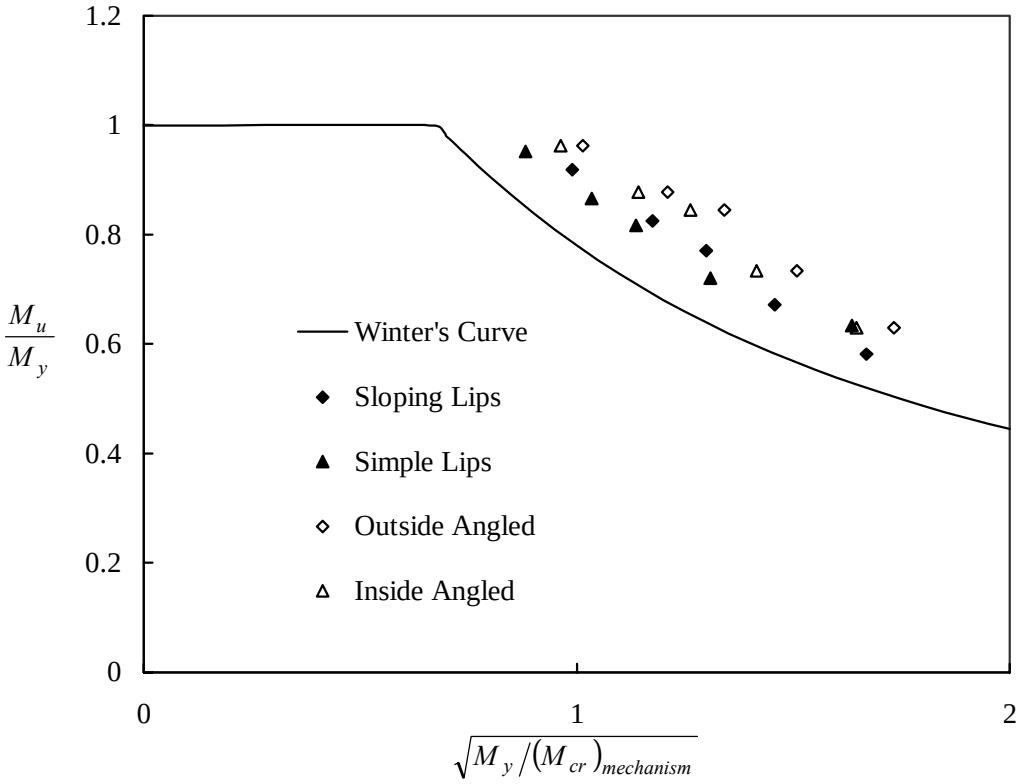


Figure 3.9 Post-Buckling Capacity by AISI Method

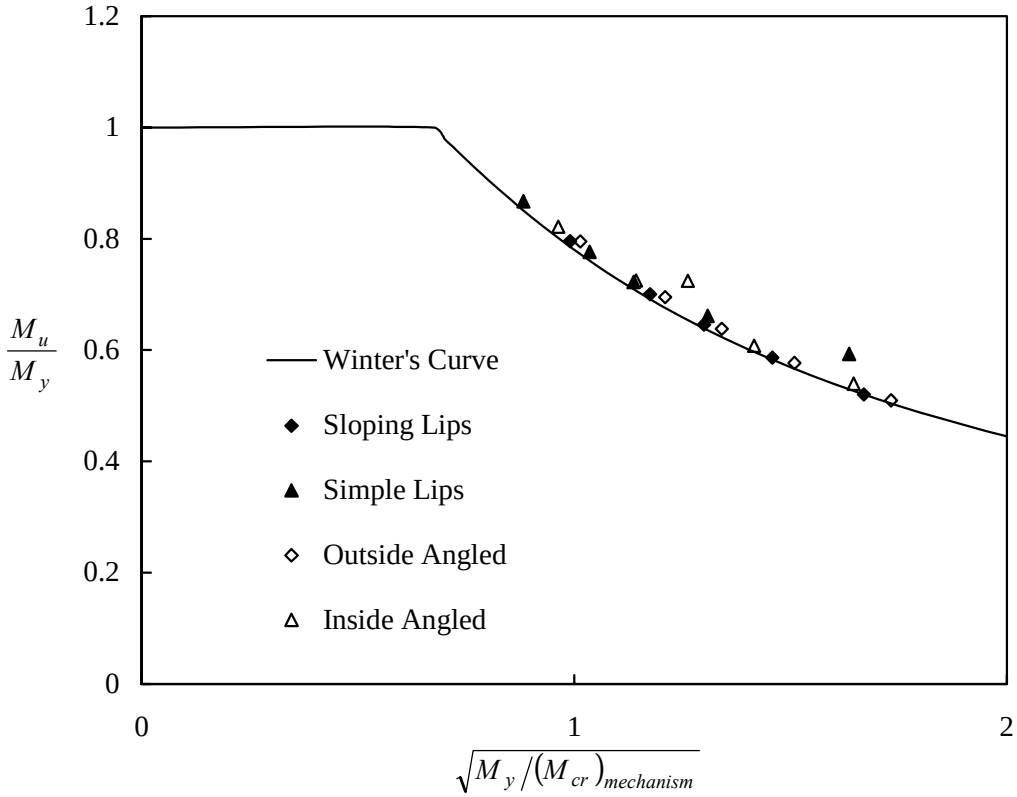


Figure 3.10 Post-Buckling Capacity by Proposed Design Approach for Flexural Members

### 3.4 Conclusions and Verification of the Proposed Design Approach

The first Z-section Parameter study of the simple lip, inside angled, outside angled, inside hooked and outside hooked stiffeners reveals that the AISI (1996) approach gives moment capacity closer to the perfect FEM model. While the proposed design approach for flexural members given by Schafer (1997), Schafer and Peköz (1999) gives a more conservative result closer to the imperfection magnitude of 25% probability of exceedance which these thin wall structure are likely to have. Almost all cases of the FEM analysis for the second parameter study suggest that for this 12ZS3.25 cross section the simple lip stiffeners give the highest moment capacity. While the AISI and the proposed design approach for flexural members given by Schafer (1997), Schafer and Peköz (1999) suggests outside angled and inside angled instead. There are no physical test results for these kinds of complex stiffeners. Some test results of members with cross sections such as in Figure 3.1 are desired to verify this approach.

# 4 Verification of the Reduction Factor for Distortional Buckling, $R_d$

Schafer (1997), Schafer and Peköz (1999) developed the expression for $R_d$ based on post-buckling capacity as shown in Figure 1.2, 1.3 and from the experimental results of Hancock et al. (1994). Based on the FEM results in the previous study section 3.1, two alternative $R_d$ expressions are developed here $(R_d)_a$ and $(R_d)_b$. The alternative expressions are then compared with the original $R_d$.

By combining the FEM results of different types of stiffeners from Figure 3.3 a regression line may be obtained as in Figure 4.1. A new expression for $(R_d)_a$ can be found by letting $R_d$ be a variable and recalculating back to find the best $(R_d)_a$ that fits the FEM regression line from the proposed design approach for flexural members given by Schafer (1997), Schafer and Peköz (1999). The result of this attempt is shown in Figure 4.2. As seen the data points do not all match the regression line due to the condition that $(R_d)_a$ is to be only equal to or less then one. These new $R_d$ values result from all models which are $(R_d)_a$ - *data* in Figure 4.3 are the data points of the new expression $(R_d)_a$. The same approach is also used to develop $(R_d)_b$ but instead of trying to match the FEM regression line as $(R_d)_a$ the expression for $(R_d)_b$ is found based on trying to match each model to its own FEM result. Results of this are shown in Figure 4.5 and 4.6.

The original $R_d$ is also plotted in Figure 4.3 and 4.6 to compare with $(R_d)_a$ and $(R_d)_b$. As seen $(R_d)_a$ is very close to $R_d$ but $(R_d)_b$ gives a larger reduction factor then $R_d$. Figures 4.4 and 4.7 show the results from using the two new expressions in the proposed design approach for flexural members given by Schafer (1997), Schafer and Peköz (1999). Comparing these figures with Figure 3.5 one can see that they do not differ much, thus verifying that the original $R_d$ used in the previous study is suitable for the overall cross sections in this study.

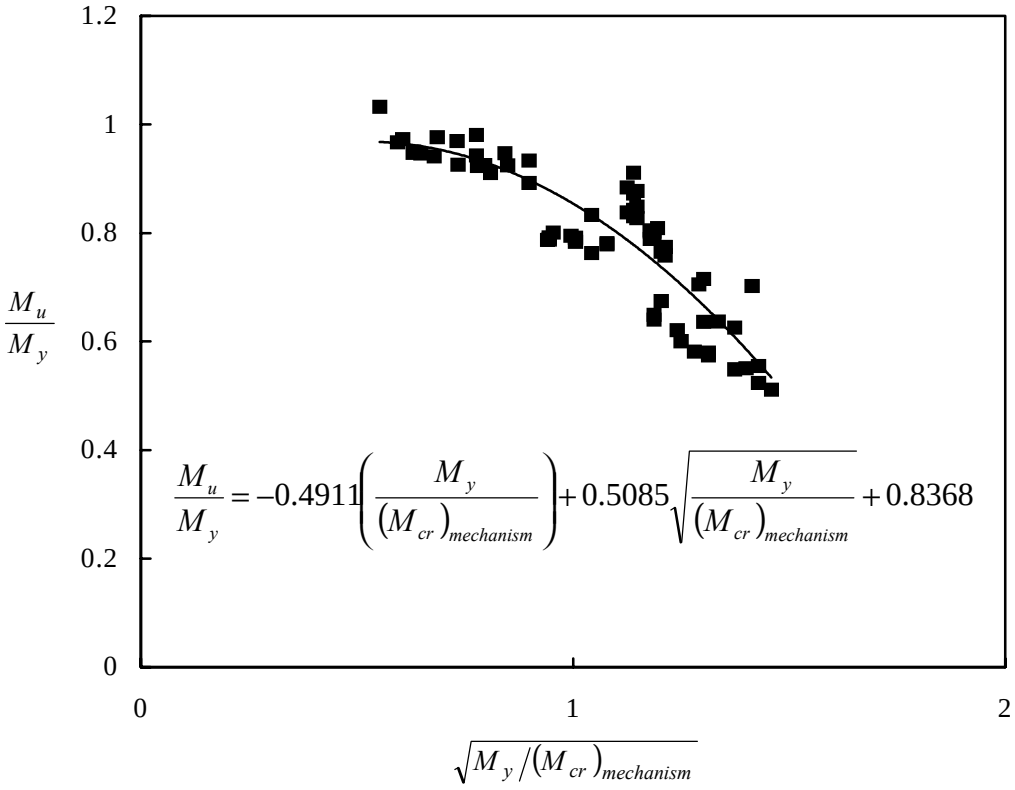


Figure 4.1 Post-Buckling Capacity by Finite Element Method (same as figure 3.3)

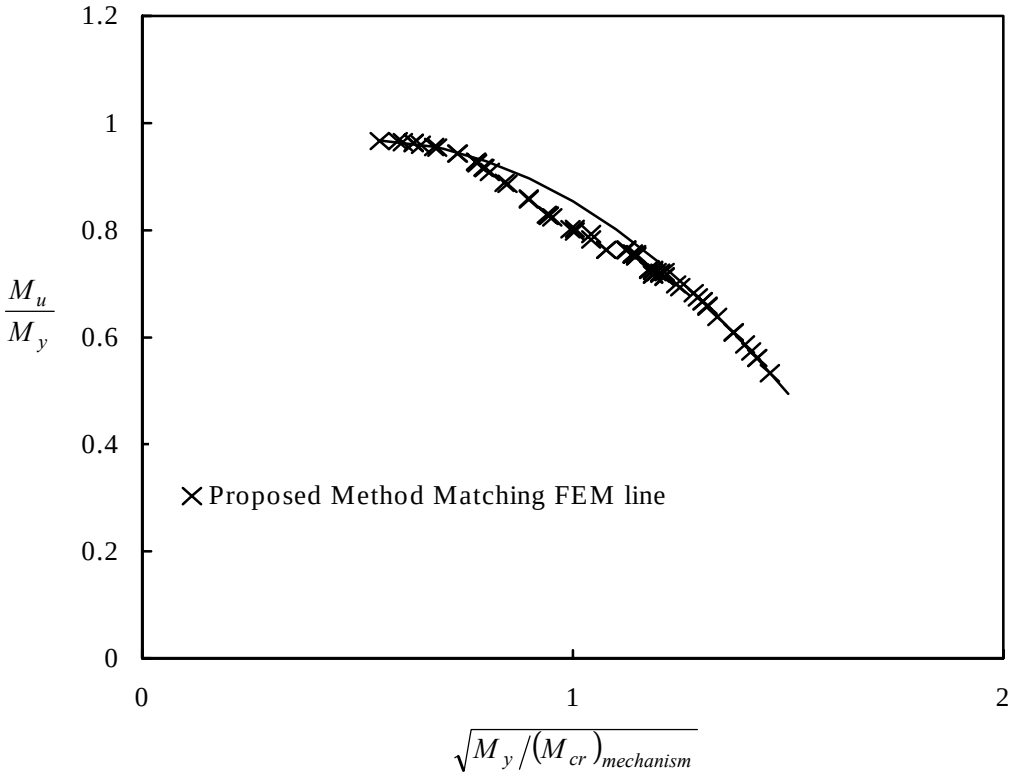


Figure 4.2 Post-Buckling Capacity by Proposed Method with $(R_d)_a$ - *data*

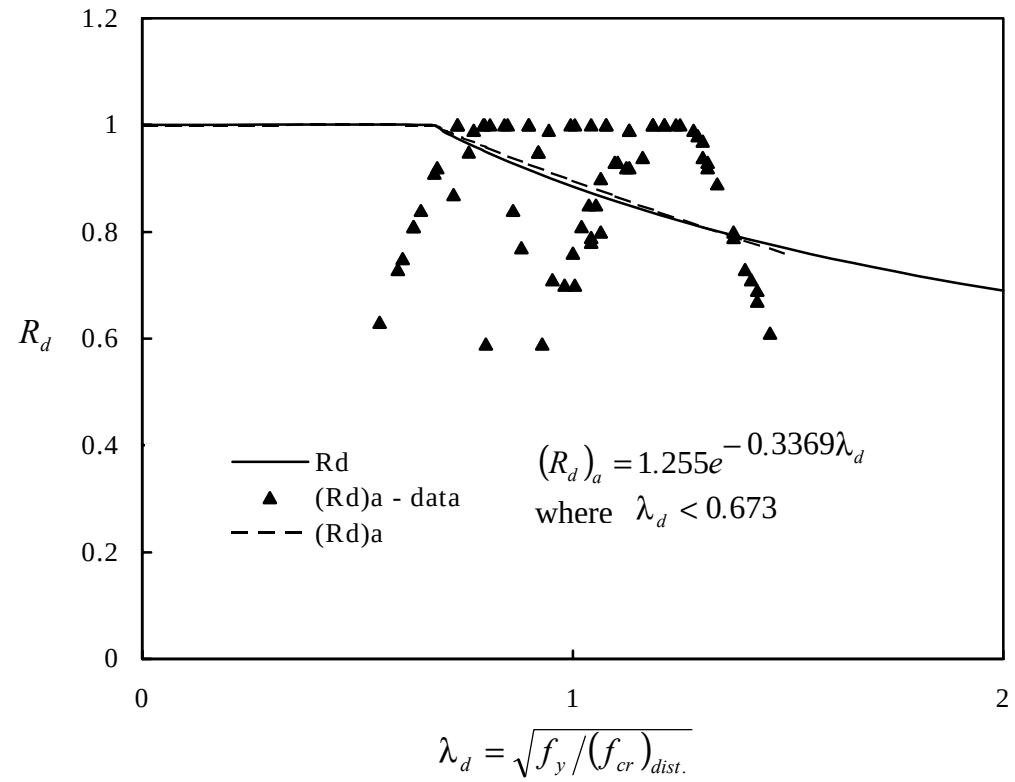


Figure 4.3 Reduction Factor for Distortional Buckling $R_d$ vs. $(R_d)_a$

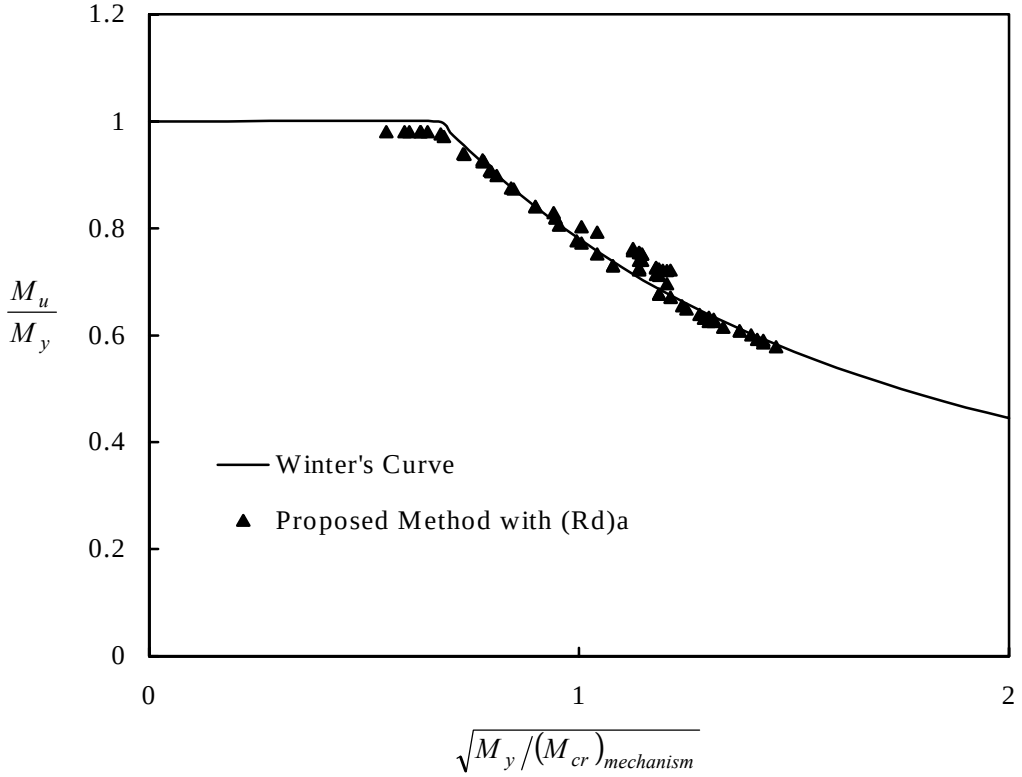


Figure 4.4 Post-Buckling Capacity by Proposed Method with $(R_d)_a$

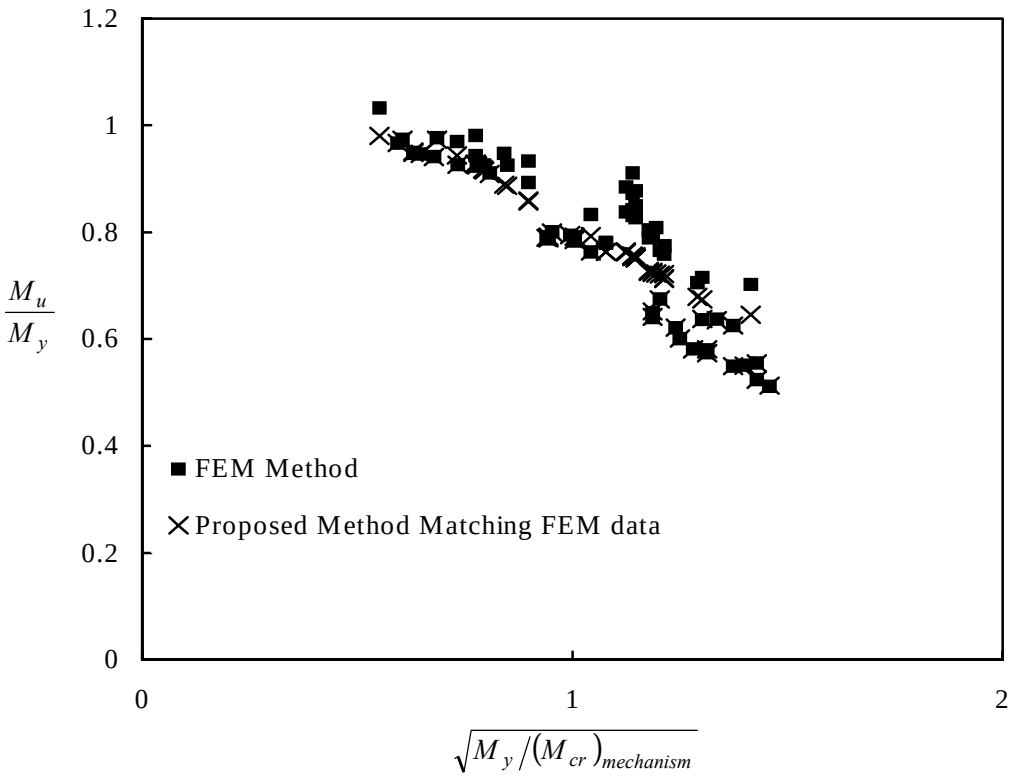


Figure 4.5 Post-Buckling Capacity by Proposed Method with $(R_d)_b$ - *data*

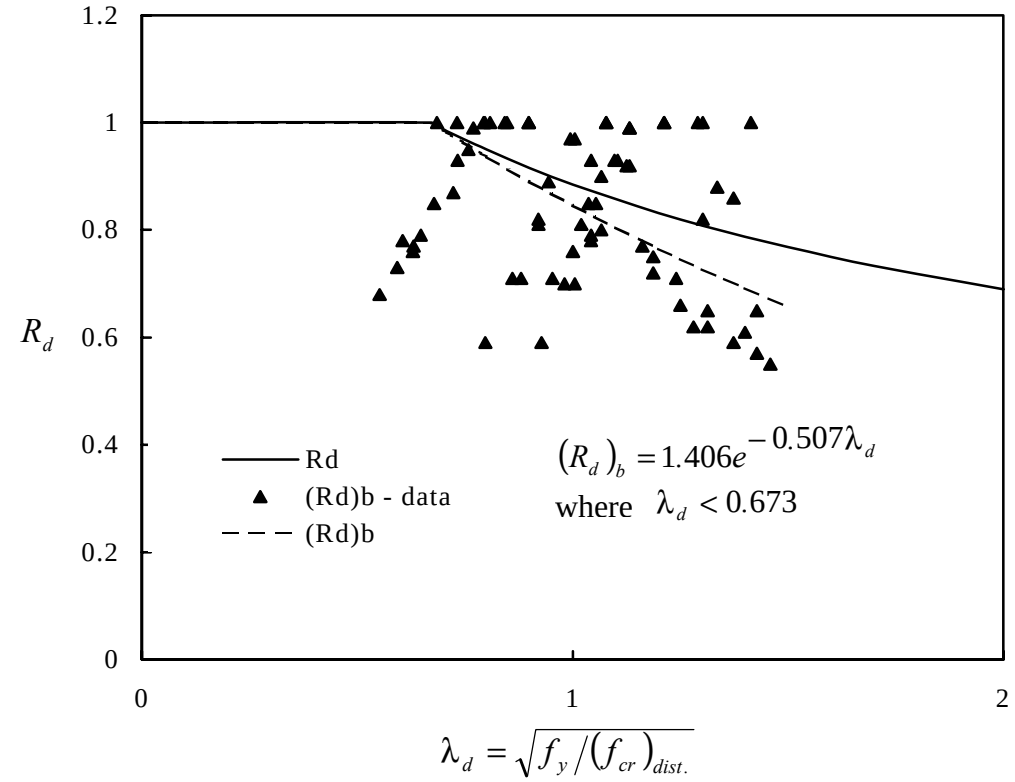


Figure 4.6 Reduction Factor for Distortional Buckling $R_d$ vs. $(R_d)_b$

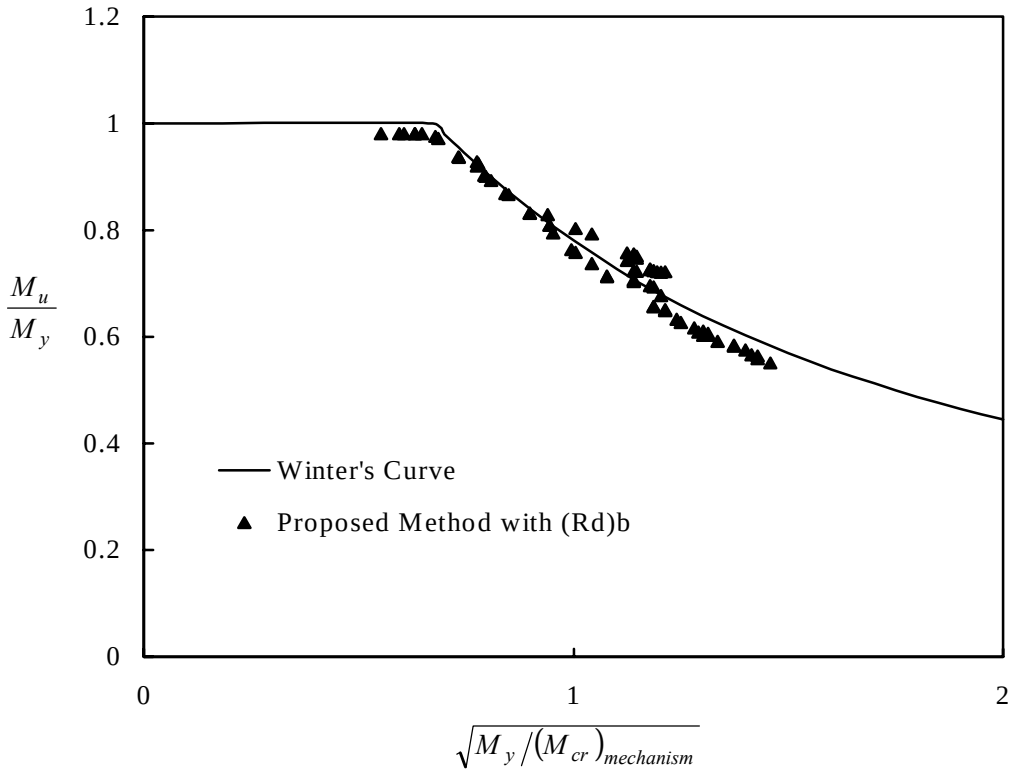


Figure 4.7 Post-Buckling Capacity by Proposed Method with $(R_d)_b$

## 5 Cross Section Optimization Study I

A computer program CU-EWA was developed to compute the nominal flexural strength, Mn, and the nominal axial strength, Pn, using two approaches. These approaches are the AISI (1996) method of initial yielding and the proposed design approach for flexural members given by Schafer (1997), Schafer and Peköz (1999). This program, CU-EWA, is used here to perform parameter studies on the cross section optimization. The nominal flexural strength divided by the cross section area is used here as the cross section efficiency index where three parameters are investigated independently: flange width, stiffener length and stiffener/flange ratio. For each parameter study four different types of stiffeners are considered to compare their advantages. Results from two approaches, the AISI (1996) initial yielding method and the proposed design approach for flexural members given by Schafer (1997), Schafer and Peköz (1999) are also compared. For the proposed method the local and distortional buckling stresses are required. Therefore, a finite strip analysis, CUFSM, was preformed for each cross section first. This parameter study was carried out for a standard cross section 12ZS3.25x090 with modified lips as in Figure 3.6.

### 5.1 Parameter Study I – Flanges Width Optimization

For the four types of stiffeners the flange width is varied to find the cross section that gives the highest efficiency index, Mn/A. Figure 5.1 shows how the geometry changes as the flange width increases and Figure 5.2 shows the results from this parameter study. The vertical line at flange width 3.25 in. is for the original cross section dimensions. Results from the proposed method in this parameter study suggest that by changing the stiffeners to simple lip and decreasing the flange width from the original values the cross section efficiency may be increased.

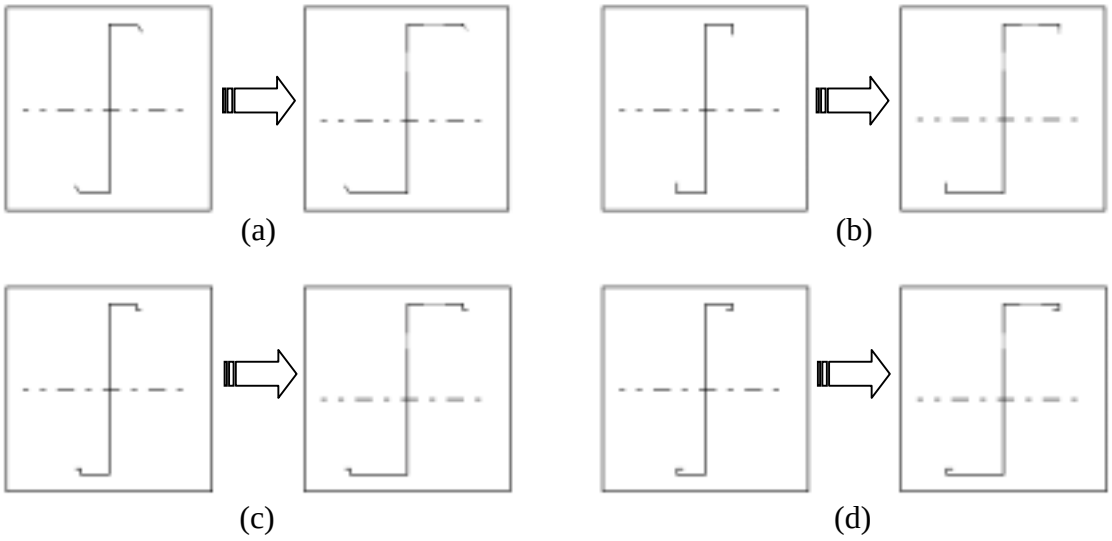


Figure 5.1 12ZS3.25x090 with (a) Sloping Lip Stiffener 50 degree respect to the flange (b) Simple Lip Stiffener (c) Outside Angled Stiffener (d) Inside Angled Stiffener

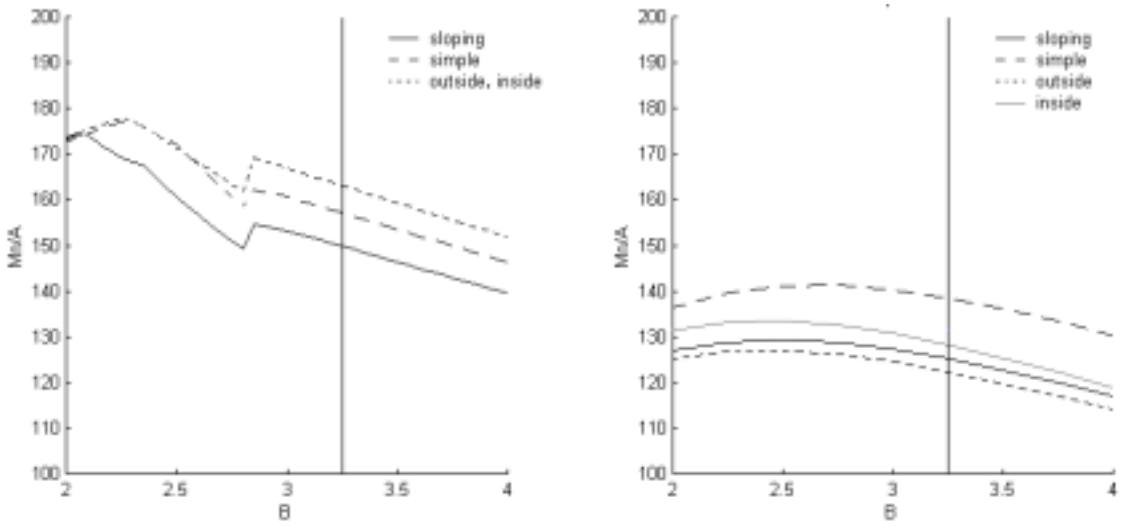


Figure 5.2 Flanges Width Optimization (a) AISI Method (b) Proposed Method

### 5.2 Parameter Study II – Stiffeners Length Optimization

Considering the stiffener length to be a varied variable and all others dimensions to be constant an optimum stiffener length may be found for different types of stiffeners. Figure 5.3 shows how the geometry changes as the stiffener length increases and Figure 5.4 shows the results from this parameter study. The vertical line at stiffener length 0.75 in. is the original cross section value. Results from the proposed method in this parameter study suggest that a simple lip with a length of 1 in. is the best section considering cross section efficiency.

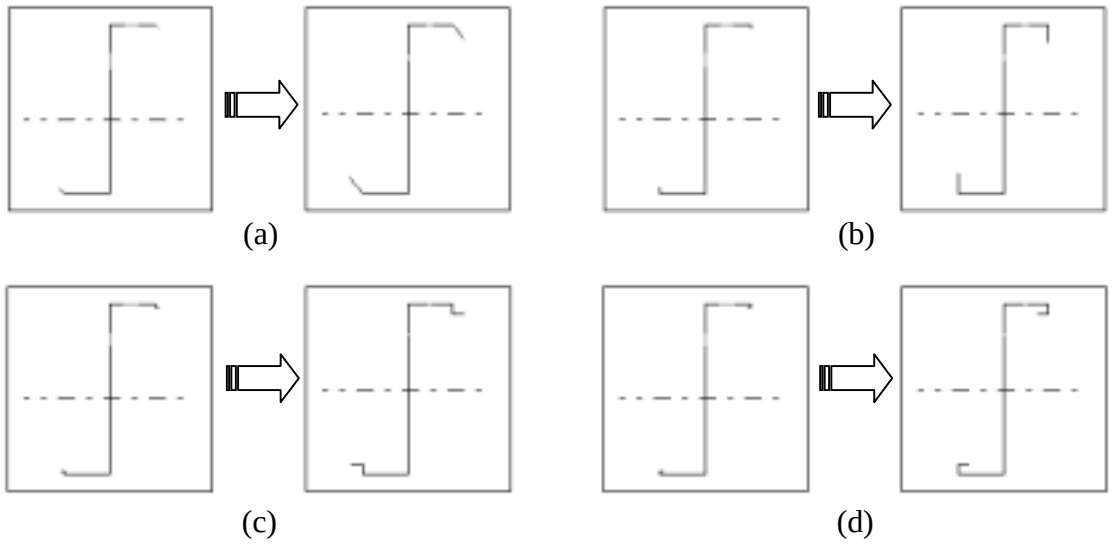


Figure 5.3 12ZS3.25x090 with (a) Sloping Lip Stiffener 50 degree respect to the flange (b) Simple Lip Stiffener (c) Outside Angled Stiffener (d) Inside Angled Stiffener

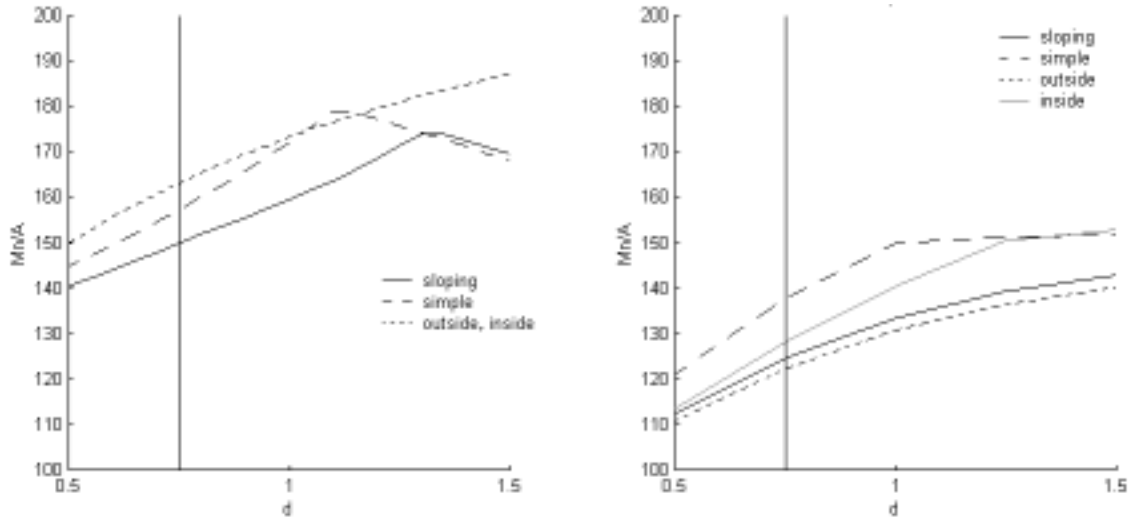


Figure 5.4 Stiffeners Length Optimization (a) AISI Method (b) Proposed Method

### 5.3 Parameter Study III – Stiffener/Flange Ratio Optimization

By changing both the stiffener and flange lengths but still maintaining the cross section area, the best stiffener/flange ratio may be found. Figure 5.5 shows how the geometry changes as the stiffener/flange ratio increases and Figure 5.6 shows the results from this parameter study. The first stiffener/flange ratio, 0.23, is the original cross section value. Results from the proposed method suggest that a simple lip with a stiffener/flange ratio of 0.33 is the best section considering efficiency.

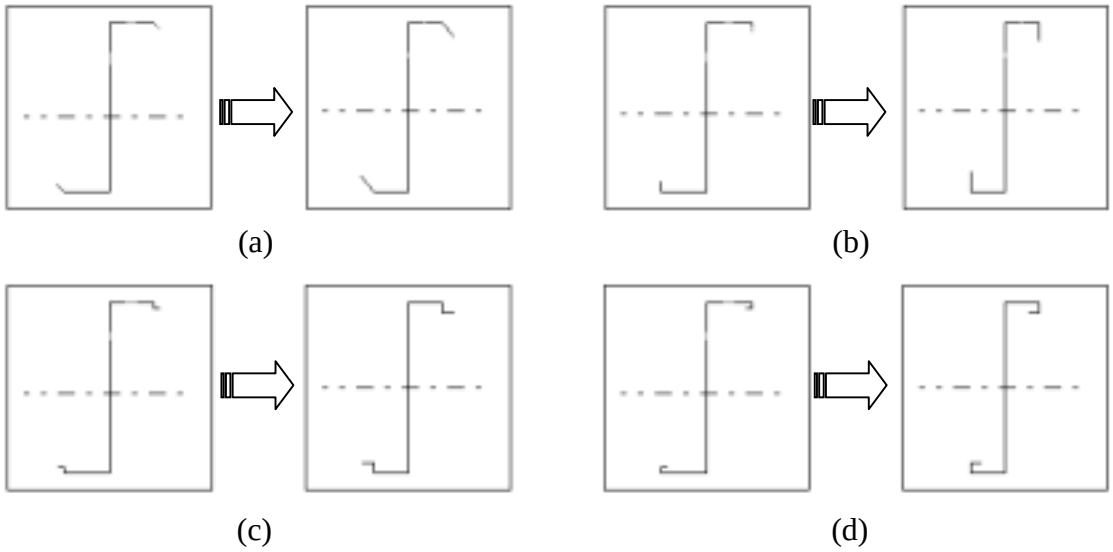


Figure 5.5 12ZS3.25x090 with (a) Sloping Lip Stiffener 50 degree respect to the flange (b) Simple Lip Stiffener (c) Outside Angled Stiffener (d) Inside Angled Stiffener

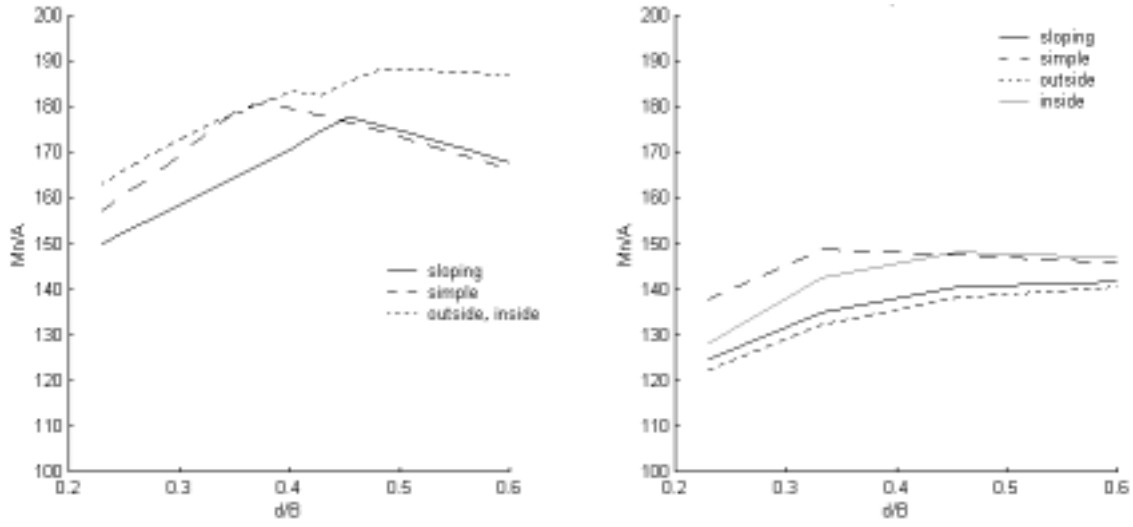


Figure 5.6 Stiffener/Flange Ratio Optimization (a) AISI Method (b) Proposed Method

# 6 Cross Section Optimization Study II

This second cross section optimization study was carried out by modifying the stiffeners of a standard cross section 9CS3x060, which has a simple lip stiffener. The simple lip stiffener was modified into different types of inside angled and outside angled stiffeners as shown in Figure 6.1. The nominal flexural strength divided by the cross section area is used here as the cross section efficiency index where the total length of the stiffener, $d$ is increased to find the optimal section. Three different approaches to calculate the section capacity, the FEM, AISI (1996) initial yielding method and the proposed design approach for flexural members given by Schafer (1997), Schafer and Peköz (1999) are compared. Results from these different approaches are shown in Figure 6.3, 6.4, 6.5, 6.6 and 6.7.

## 6.1 Finite Element Modeling Assumptions

In this study the length of the member is taken as the half-wave lengths of the distortional mode that gives the least buckling strength. Lateral bracings are only provided by roller supports at the ends. For this cross section and member length, full formation of the distortional mode is still possible without causing a lateral-torsional failure. To avoid localized failure at the ends, the constant moment modeled by nodal loads is distributed into the first two rows of elements. Boundary and loading conditions are shown in Figure 6.2. The material model used is elastic-plastic with strain hardening and $f_y$ = 65 ksi. Residual stress throughout the thickness in the longitudinal direction is assumed to be 25% of the yield stress in the flange, 40% of the yield stress in the web and 30% at of the yield stress in the corners. The residual stresses are also assumed to be tension on the outside and compression in the inside of the section. Initial geometric imperfections are introduced by superimposing the eigenmodes for the local and distortional buckling. The imperfection magnitude 50% probability of exceedance based on the statistical summary provided in Schafer (1997), Schafer and Peköz (1999) is used.

### 6.2 Conclusion

All three approaches agree well for the simple lip case that an optimized section may be obtained by increasing the stiffener length from the original given length of $d$ = 0.5 in. to about $d$ = 1 in. The current AISI (1996) method does not distinguish between the inside and outside angle stiffener. Results also show that this method is unconservative compared with the other two approaches. The overall trend of the results between the FEM and the proposed method shows agreement; that is, it is more efficient to have inside angled stiffeners then simple lip or outside angled stiffeners. A wider range of scattered data is obtained from thee FEM due to the initial geometric imperfection. A study on sections with higher material yield stress has also been considered. Results are similar to those obtained here where the inside angled stiffeners has slight advantage over the simple lip and outside angled stiffeners

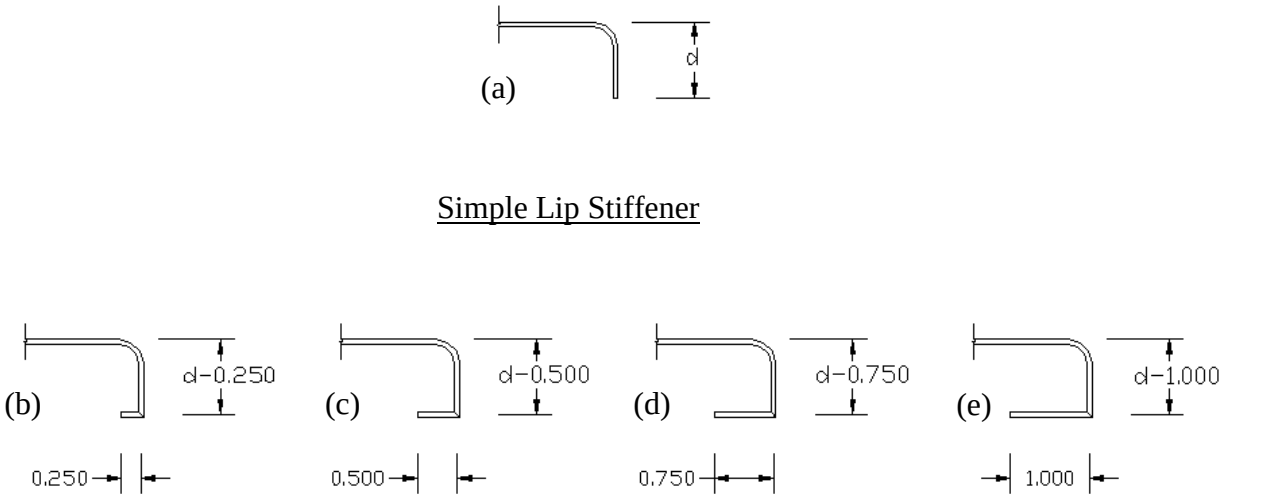


Figure 6.1 Various Types of Stiffener Under Consideration

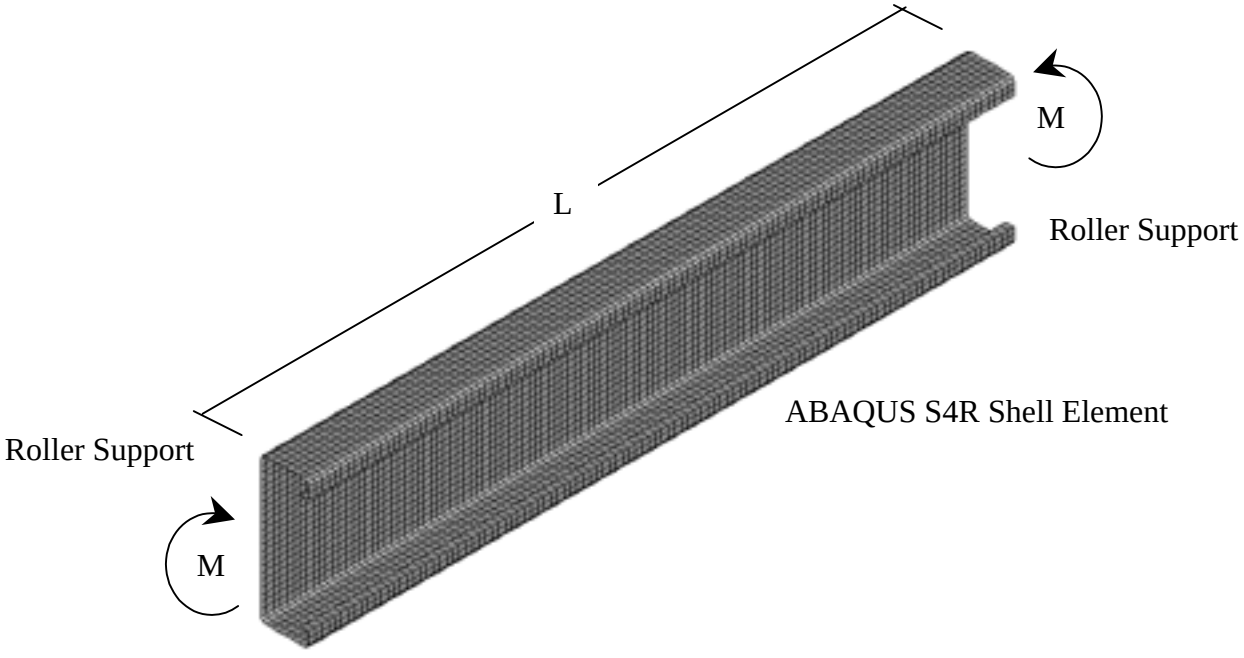


Figure 6.2 Boundary and Loading Condition

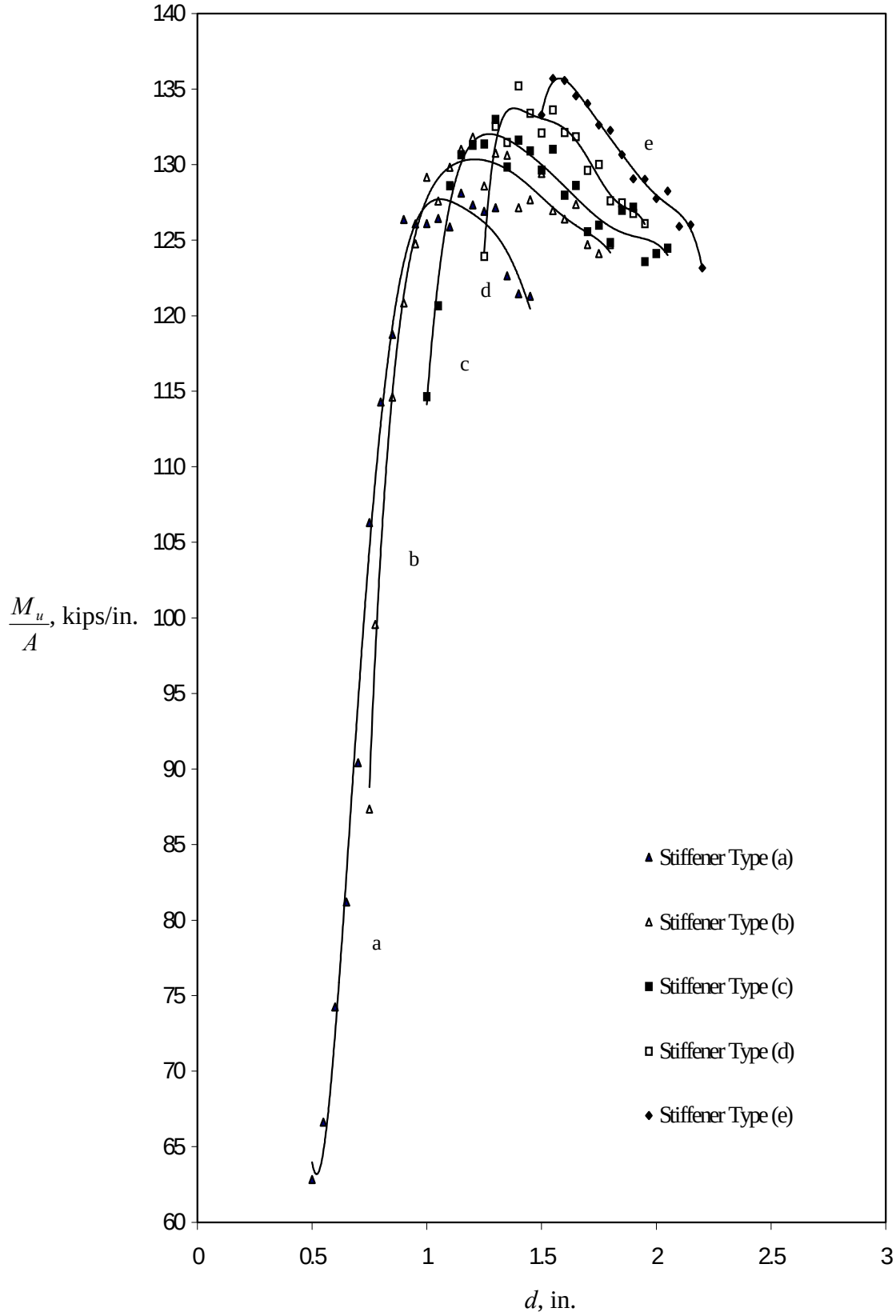


Figure 6.3 Inside Angled Optimization by Finite Element Method

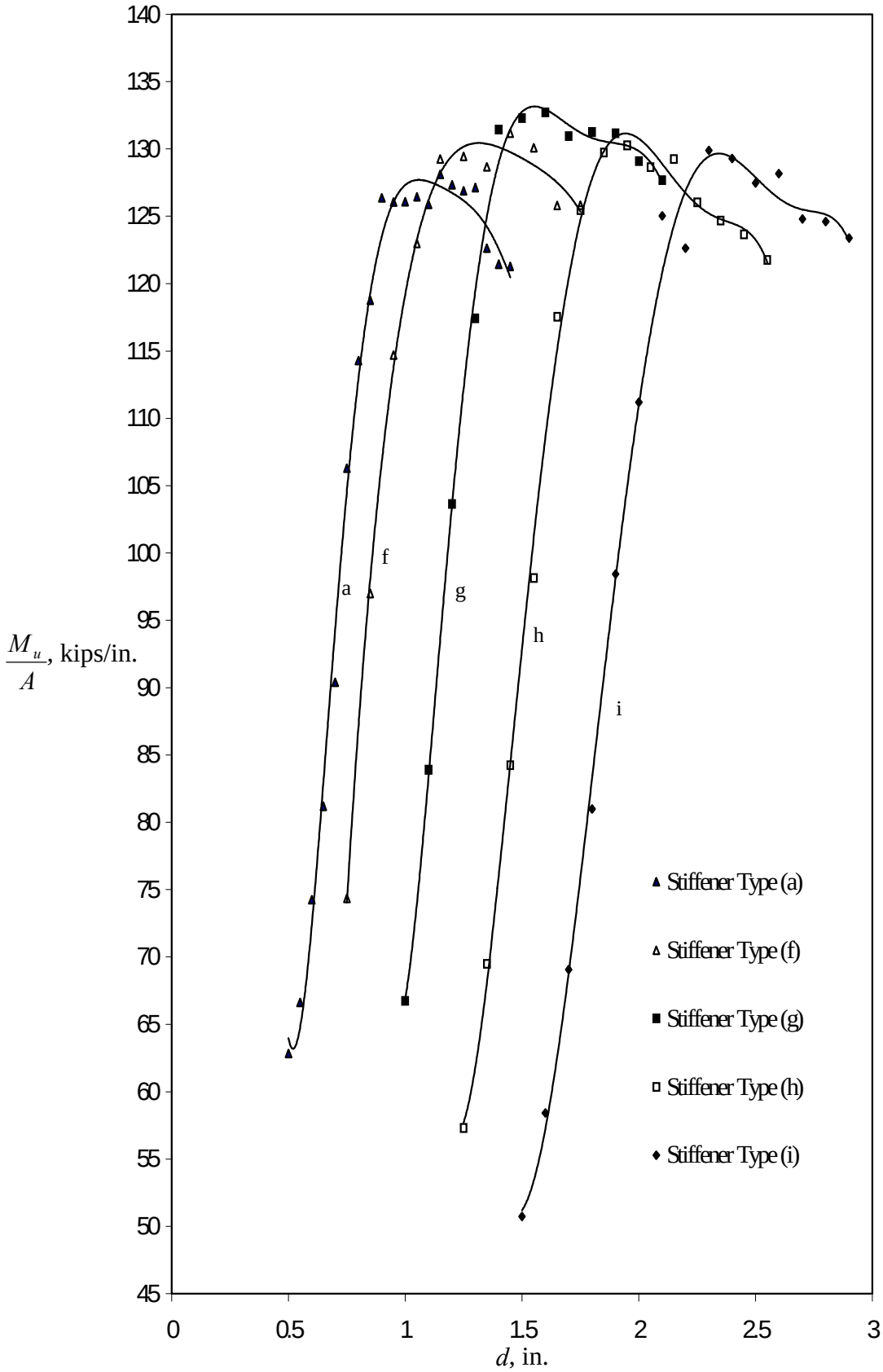


Figure 6.4 Outside Angled Optimization by Finite Element Method

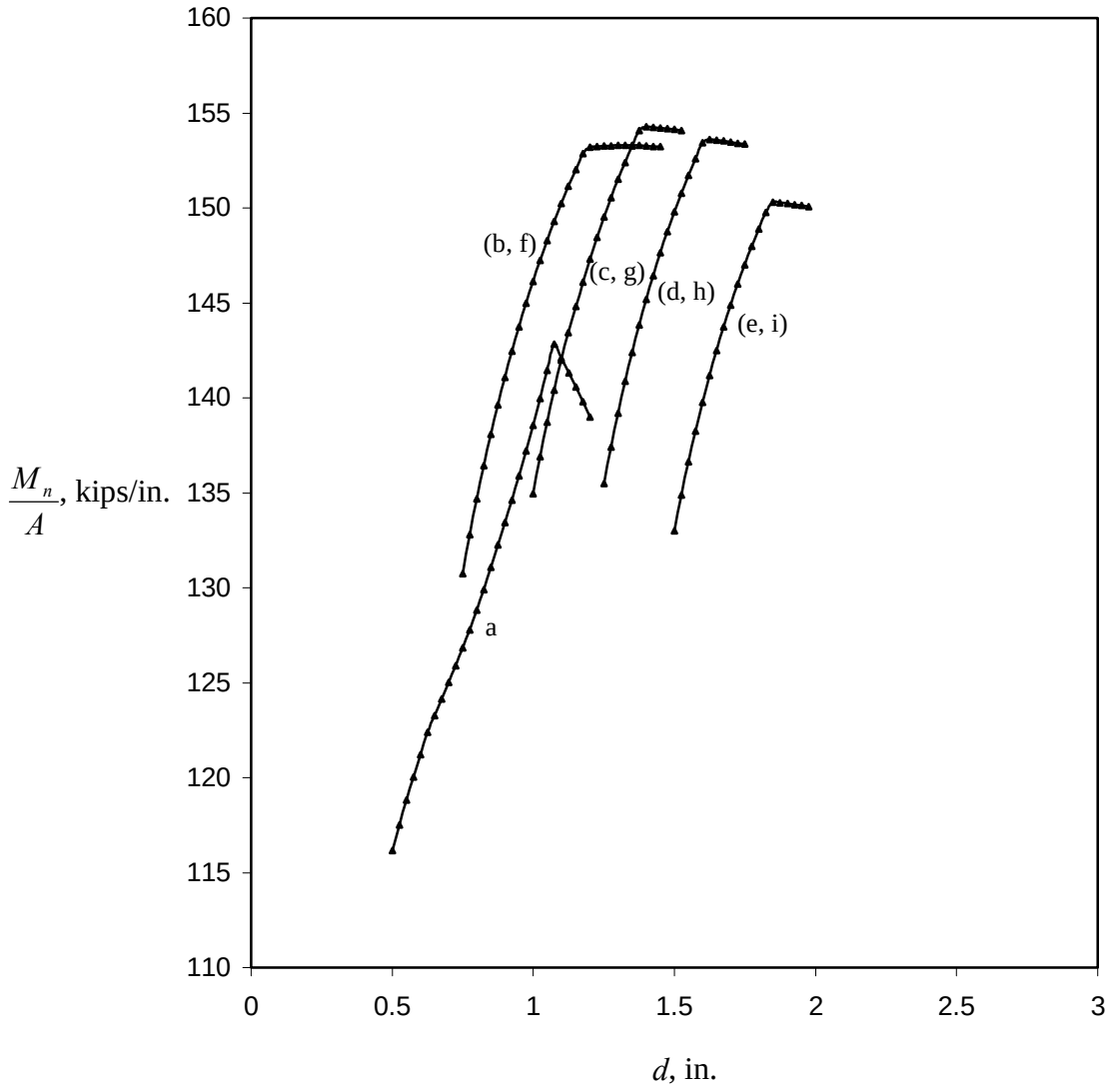


Figure 6.5 Inside and Outside Angled Optimization by AISI Method

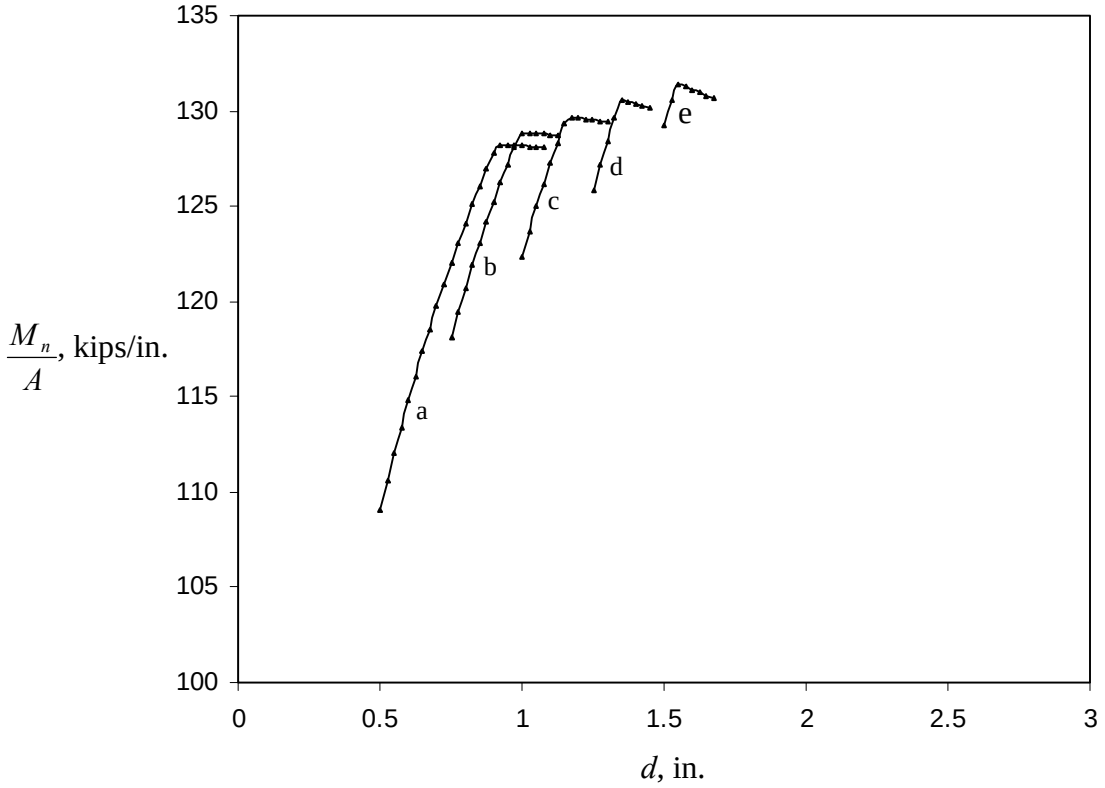


Figure 6.6 Inside Angled Optimization by Proposed Method

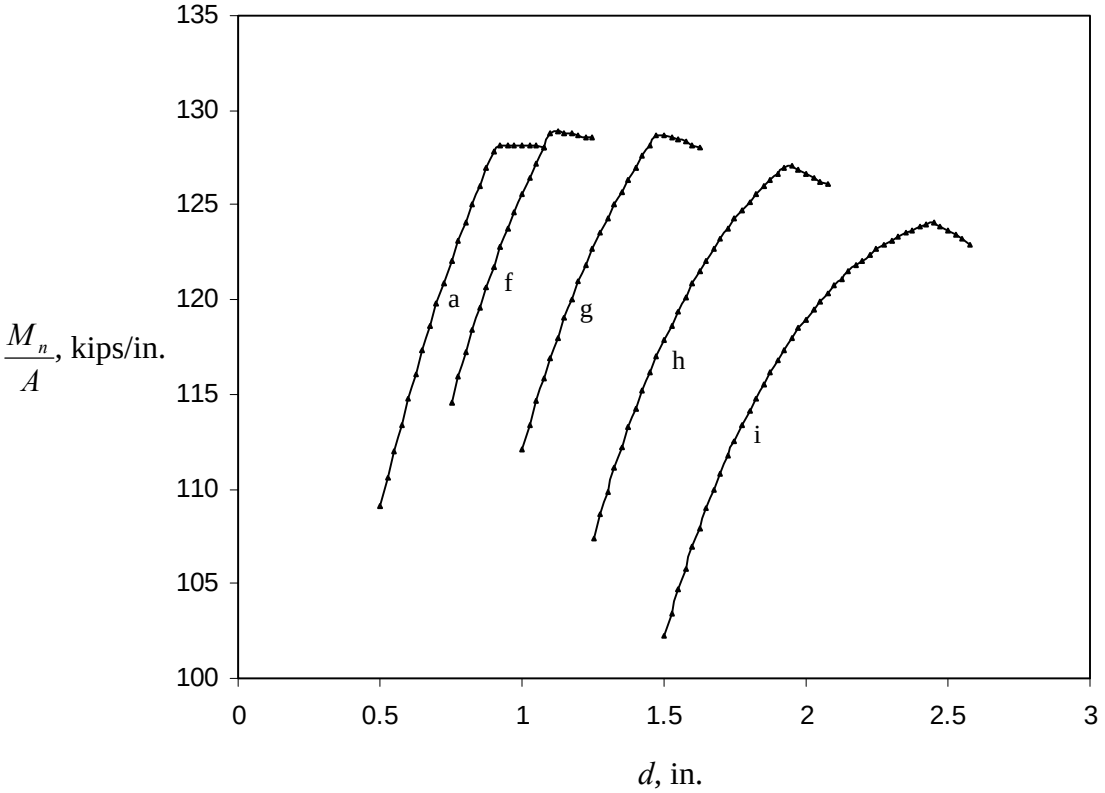


Figure 6.7 Outside Angled Optimization by Proposed Method

# 7 An Experimental Study

The two-point bending test shown in Figure 7.1 performed by Rinchen (1998) is studied here. A full finite element simulation of the experimental arrangement is carried out to compare with the physical test results.

## 7.1 Finite Element Simulation of Experimental Arrangement

The two-point bending experiment setup shown in Figure 7.1 is simulated by FEM. A pair of DHS200-1.8 sections is placed back-to-back with loading braces and end support plates, which were modeled with a much thicker shell element compared to the ones used for the DHS200-1.8 members and connected only at the bolts positions. Pins and rollers were used at the end supports and concentrated loads. Residual stresses are also introduced as in the previous study but no imperfections are incorporated in to the analysis due to lack of actual imperfection measurement at the preliminary studies. However, a first approximation can be obtained and results are expected to be reduced when there are some imperfections. Figure 7.2 and 7.3 shows the model of this simulation at the failure state.

## 7.2 Conclusion

As suggested by Rinchen (1998), due to the interaction of local buckling, distortional buckling and shear at the loading points, tests resulted in providing section strength for localized failure instead of providing the section strength for pure bending. FEM simulation of the experiment arrangement with no imperfections incorporated showed even lower moment capacity with the same local failure mode. Results are shown and compared in Figure 7.4. Modification in the experimental arrangement is needed and should be simulated by finite element before doing actual testing. Rinchen (1998) also suggested some changes in the experimental set up.

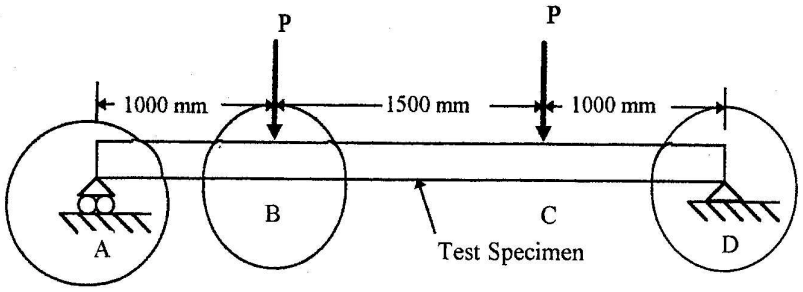


(a) General Arrangement

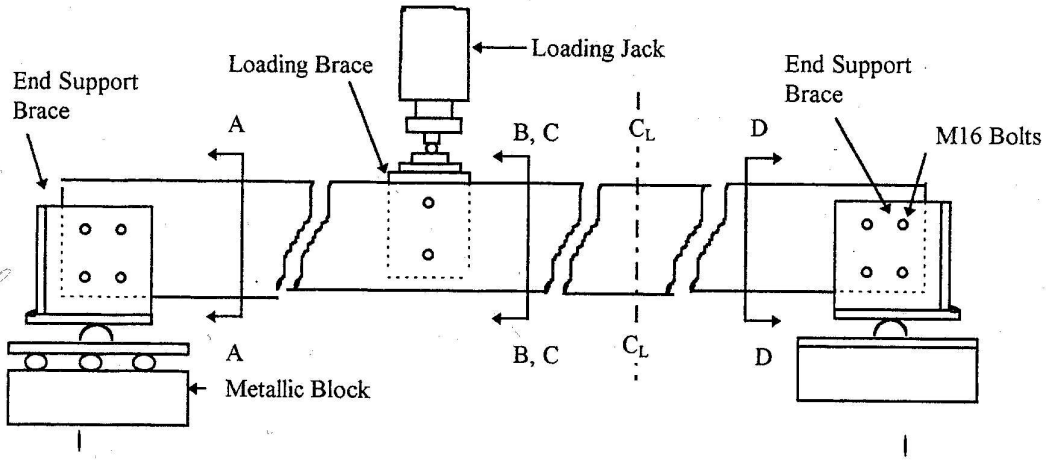


(b) Details of Experimental Arrangement in Elevation

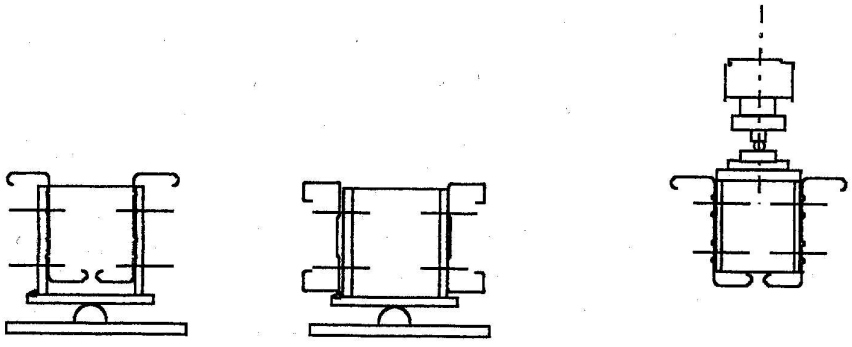


(c)Details of End Brace and Loading Brace

Figure 7.1 Details of Arrangement of Experiment, Rinchen (1998)

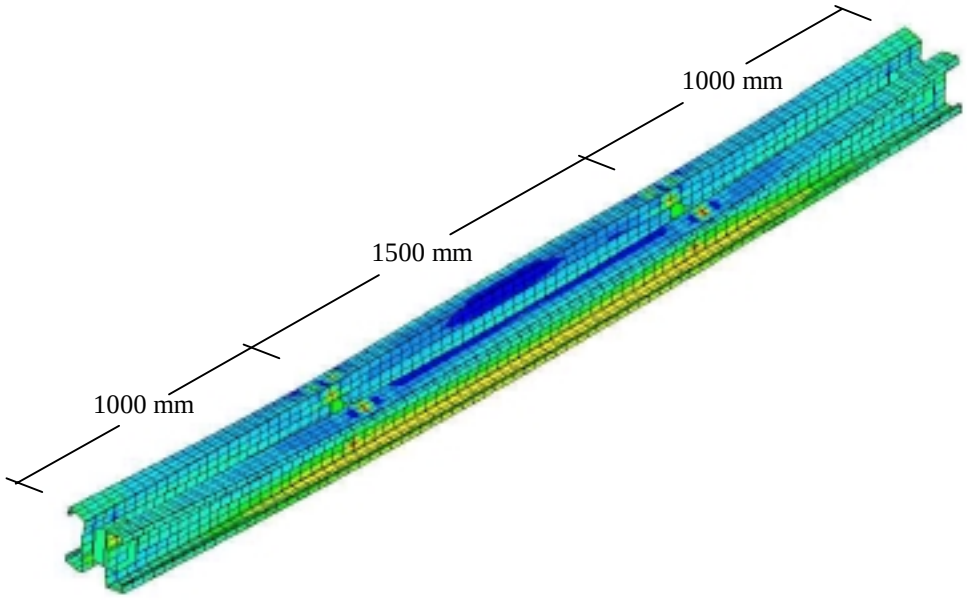


Figure 7.2 Simulation of Experimental Arrangement

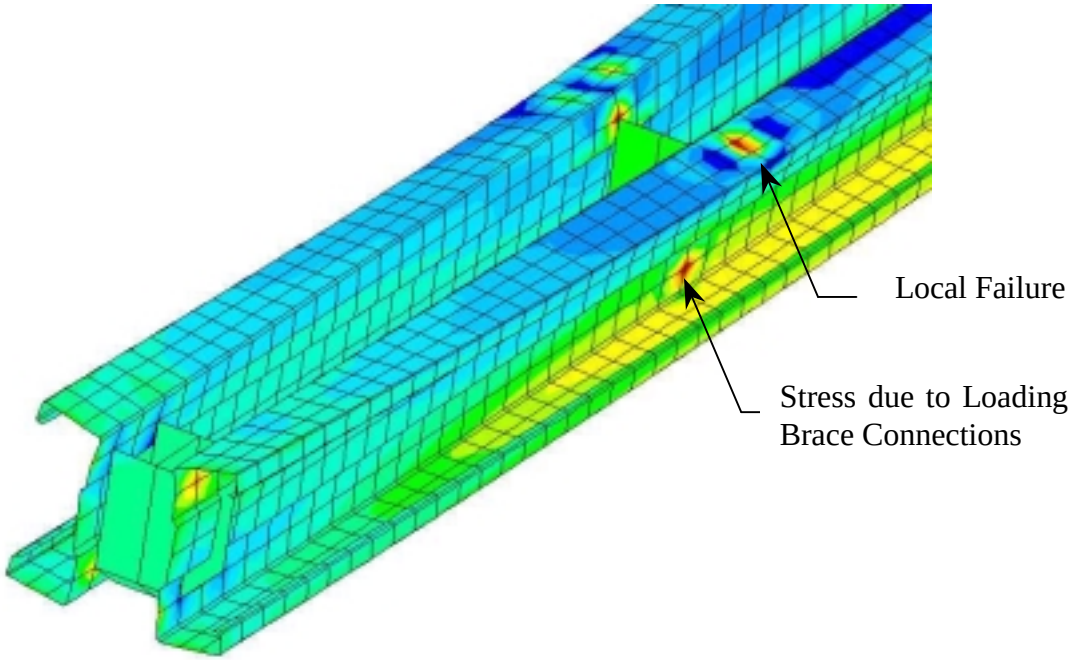


Figure 7.3 Failure Mode of DHS200-1.8 with Experimental Arrangement

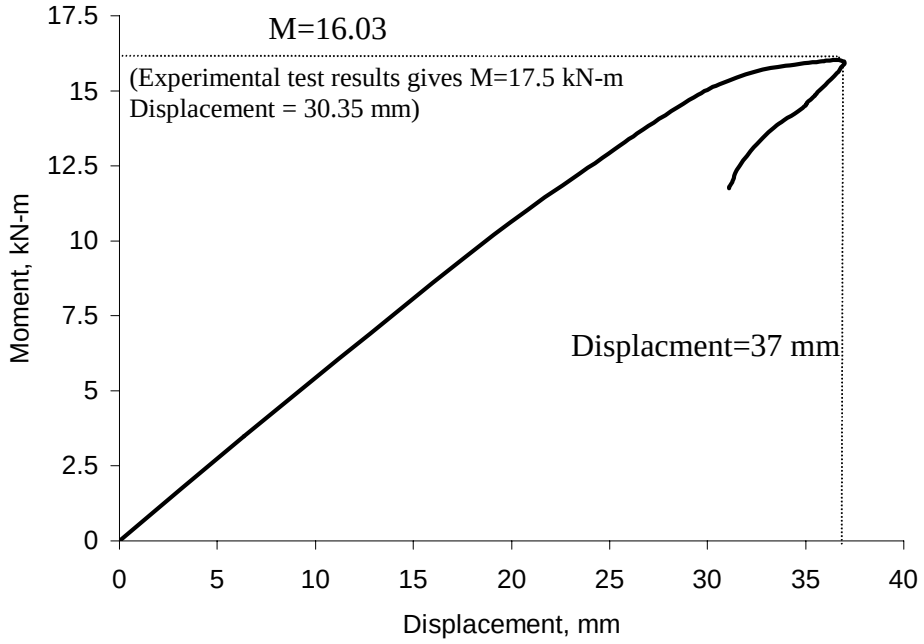


Figure 7.4 Finite Element Results for DHS200-1.8 with Experiment Arrangement

# 8 Initial Geometric Imperfection by Stochastic Process

The following is a joint study with Yongwook Kim in a structural reliability class. One of the most important factors that affect on the compressive strength in thin-walled sections such as cold-form steel is the geometric imperfection. In the previous study initial geometric imperfection was introduced by superimposing the eigenmodes for the local and distortional buckling. The magnitude of the imperfection was selected based on the statistical summary provided in Schafer (1997), Schafer and Peköz (1999). An alternative approach is studied here by using stochastic process to randomly generate signals for the imperfection geometric shape. From large numbers of the simulations, the relationships between ultimate compressive strength and standard deviation of the imperfection signal can be obtained. But because of lack of imperfection measurements there fore some assumptions had to be made first. The idea was to go threw the process and understand the approach.

## 8.1 Definitions and Assumptions

### 8.1.1 Definitions of the Section

Rather then using a full cross section an isolated flange-stiffener model in uniform compression is studied instead and a nonlinear FEM analyses are performed using ABAQUS. To study only the simple lip stiffened element an idealization of the boundary condition at the web/flange junction is made by restraining all degrees of freedom except for the translation along the length. Roller supports are used at both ends and to avoid localized failure at the ends the uniform load has been distributed to the first row of elements. The Geometry and boundary conditions are shown in Figure 8.1. The material model used is elastic-plastic with strain hardening and $f_y$ = 55 ksi. Residual stress is also included with a 30% yield stress throughout the thickness in the longitudinal direction. The residual stresses are assumed tension on the outside and compression in the inside of the section. The length of the model is selected by using the length that would give the least buckling strength in the distortional mode, which is obtained, by using the Finite Strip Method CUFSM.

### 8.1.2 Definitions of the Imperfection

Only one type of imperfection shown in Figure 8.1 (b) is considered. The web to flange junction is assumed to be perfectly straight while the web to stiffeners junction will have longitudinal imperfection. The longitudinal imperfection signal is assumed to be zero mean, real valued stationary Gaussian stochastic process for a certain standard deviation because the imperfection is deviation from the perfect plane. Imperfection between the web junction and stiffeners junction is assumed to be linear.

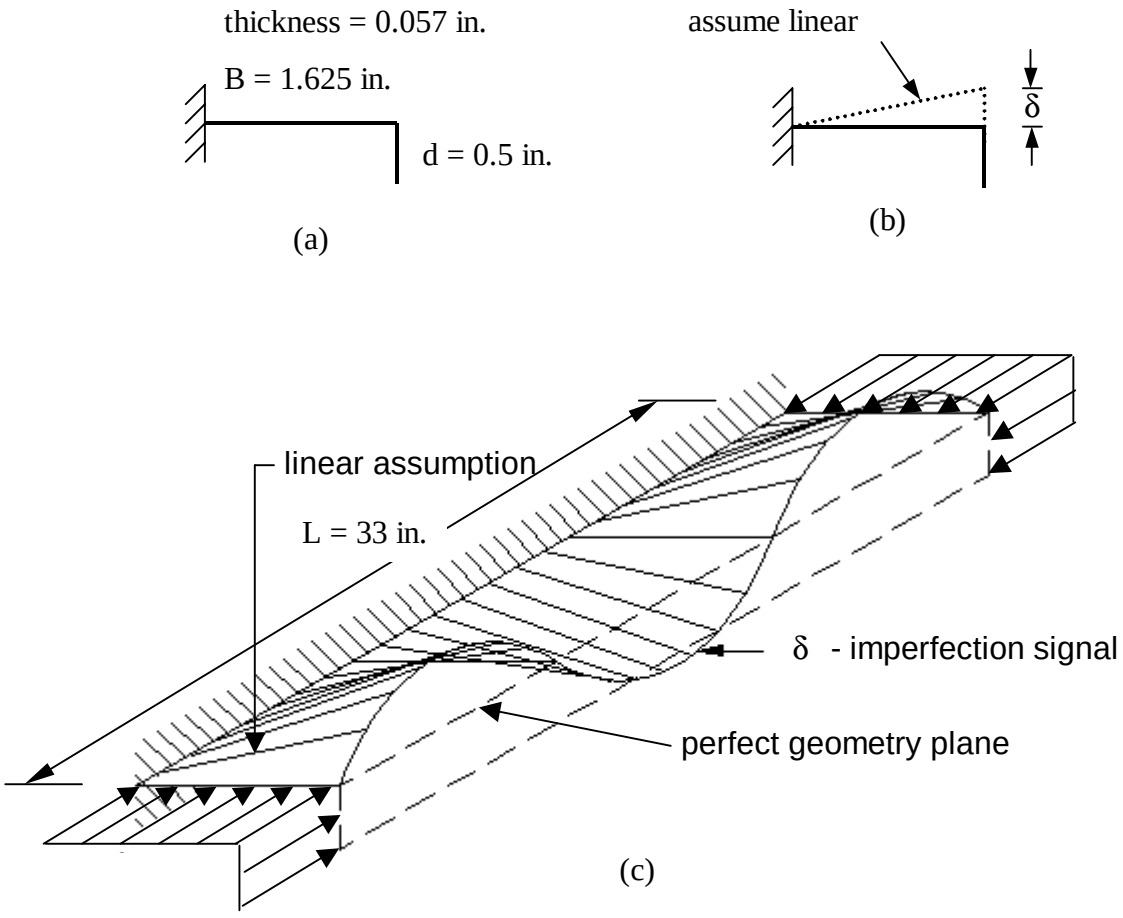


Figure 8.1 (a) Cross-section Geometry (b) Geometric Imperfection (c) Boundary Condition and Geometric Imperfection

## 8.2 Probabilistic Model for Uncertain Parameters

### 8.2.1 Imperfection is zero mean stationary Gaussian stochastic process:

A stochastic process is a function of two variables the parameter t and the probability parameter $\omega$. $X(t,\omega)$ , $t \in T$ , $\omega \in \Omega$ where parameter t usually refers to time but for geometric imperfection t will denote as location along the length of the member. If a manufacturer makes the members in a same process and condition, a set of imperfection data $X(\bullet,\omega)$ of the members can be called as sample, sample path or realization. In addition, $X(\bullet,\omega)$ can also be called as a stationary stochastic process, since due to uniformity of the manufacturing process, the distributions of $X$'s over the different members ($\omega$) for a fixed location 't' should be the identical regardless of its location ($t$). This is because if $X(t)$is finite dimensional distribution and it does not change at a time shift for $\forall n, \forall t_1, ...., \forall t_n$,

$$F(x_1,x_2,...,x_n ; t_1,t_2,...,t_n) = F(x_1,x_2,...,x_n ; t_1',t_2',...,t_n')$$

then $X(t)$ can be said to be stationary in the strict sense. That is, the distribution is only a function of time lag $(t_k - t_k'; k=1...n)$

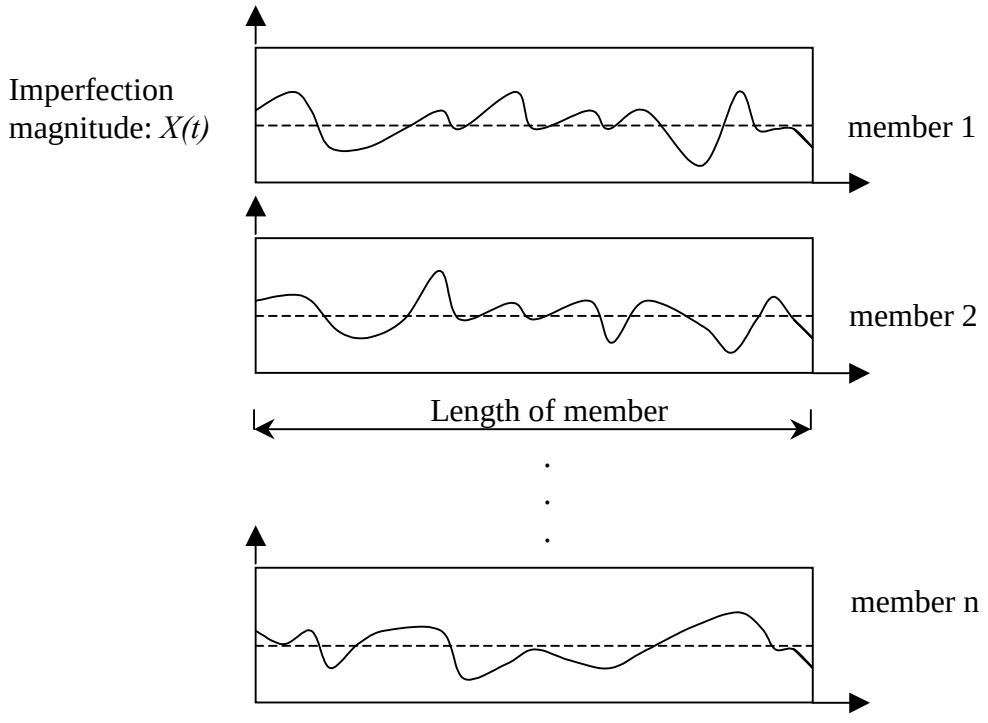


Figure 8.2 Imperfection Signal along the Length of the Member

### 8.2.2 Imperfection signal is assumed as:

$$\tilde{X}(t) = X_m(t) = \sum_{k=1}^{m} \sigma_k (V_k \cos(\omega_k t) + W_k \sin(\omega_k t))$$

If this process is zero mean, real valued, continuous, stationary Gaussian process then

$$X(t) = \int_0^{\infty} [\cos(\omega t) dU(\omega) + \sin(\omega t) dV(\omega)] \quad (*)$$

where $U(\omega)$ and $V(\omega)$ are real valued, zero mean, independent Gaussian process with properties $E\{dU^2(\omega)\}=E\{dV^2(\omega)\}=G(\omega)d\omega$. However, the measured imperfection data cannot be continuous, the equation (*) cannot be obtained. Instead, discrete approximation of this process is possible. If this process is assumed to be a discrete version $X(t)$ with one-sided truncated power. Then the stochastic process $X$(t) can be approximated as

$$\tilde{X}(t) = X_m(t) = \sum_{k=1}^{m} \sigma_k (V_k \cos(\omega_k t) + W_k \sin(\omega_k t))$$

where $V_k$ and $W_k$ are independent Gaussian random variables with zero means and unit variances.

spectral density, $\tilde{G}(\omega) = \begin{cases} G(\omega), & 0 \le \omega \le \tilde{\omega} \\ 0, & \omega > \tilde{\omega} \end{cases}$

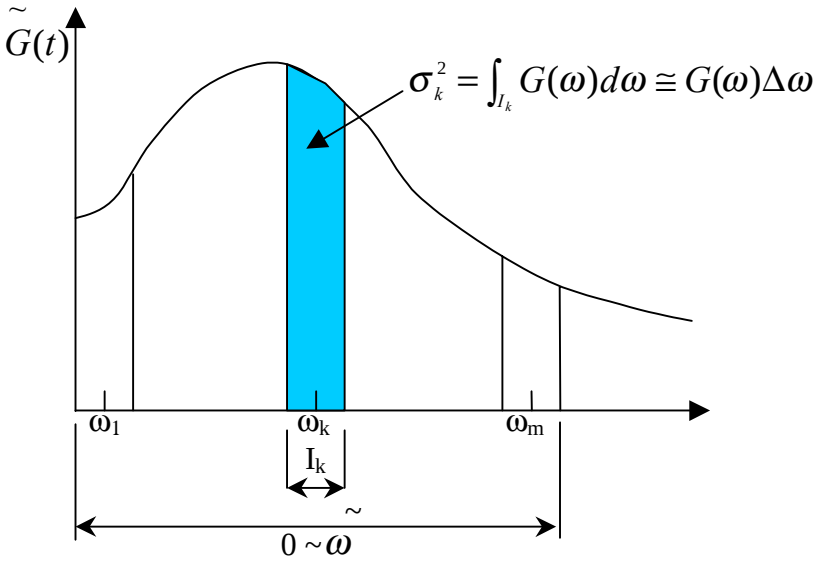


Figure 8.3 One-sided Power Spectral Density

### 8.2.3 Process is assumed as Band-Limited White Noise

If actual signals of imperfection from the measurement are available, the correlation function from the definition may be obtained. However, since the data is not available currently, the correlation function is assumed as Band-limited white noise, which is shown in Figure 8.4. $R(\tau) = G_o \sin(\omega_c \tau)/\tau$. where $\omega_c = 1.6$ is selected from the experimental result of Schafer (1997) from the Fourier Transform of some cold-form steel members, truncation ($\omega_c$) is decided at the 1.6 rad/in frequency. Standard deviation ($\sigma_{imp,i}$) of imperfection parameter is constant and decided from the assumptions that it varies from 0.25 to 2.0 (0.25, 0.50, 0.75, 1.00, 1.25, 1.50, 1.75 and 2.00). These numbers are normalized standard deviation by dividing actual standard deviation by thickness 0.057 in. Then square of one of the selected standard deviation ($\sigma_{imp,i}$) will be the total area of the one-sided spectral density. That is, $(\sigma_{imp,i})^2 = G_{o,i} \times \omega_c$ where, $i$=1~8. Then $G_o$ is obtained for each different $\sigma_{imp,i}$ and fixed $\omega_c$. In addition, $\sigma_k^2$ can be computed from $\sigma_k^2 = (\sigma_{imp,i})^2/5$. Finally, $V_k$,$W_k$ will be randomly generated.

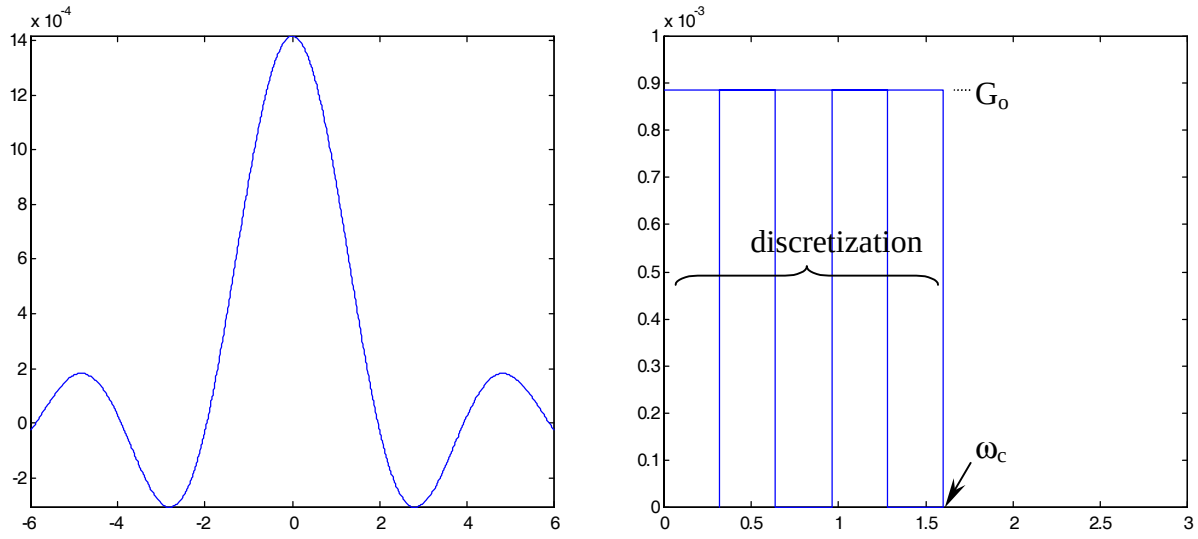


(a) (b)

Figure 8.4 Band-Limited White Noise: (a) Correlation Function
(b) One-sided Spectral Density, $G(\omega)$

### 8.2.4 Generation of Imperfection Signal

Total 30 numbers of signals were generated for each standard deviation. Figure 8.5 and 8.6 shows 1 and 10 numbers of signals generated when $\sigma_i$ =1.0 (=0.057 in.). For each standard deviation 30 numbers of signals were generated. Then with these, total 240 FEM analyses are implemented. Since 30 numbers of signals from one standard deviation are completely different, the ultimate capacities show scatter. For each scatter, histogram is made and relationships between ultimate compressive strength and standard deviation of the imperfection signal can be obtained. Results are shown in Figure 8.7 and 8.8.

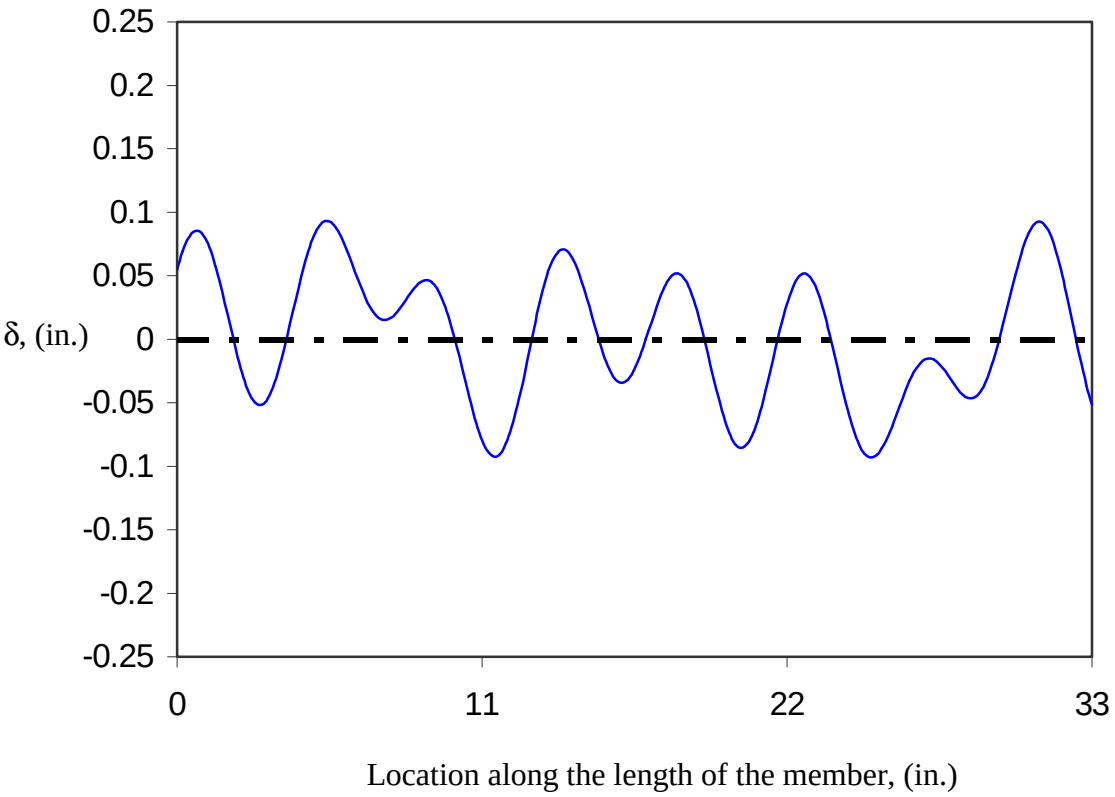


Figure 8.5 Zero mean, $\sigma_i$ =1.0 Stationary Guassian Stochastic Process: 1 Signal

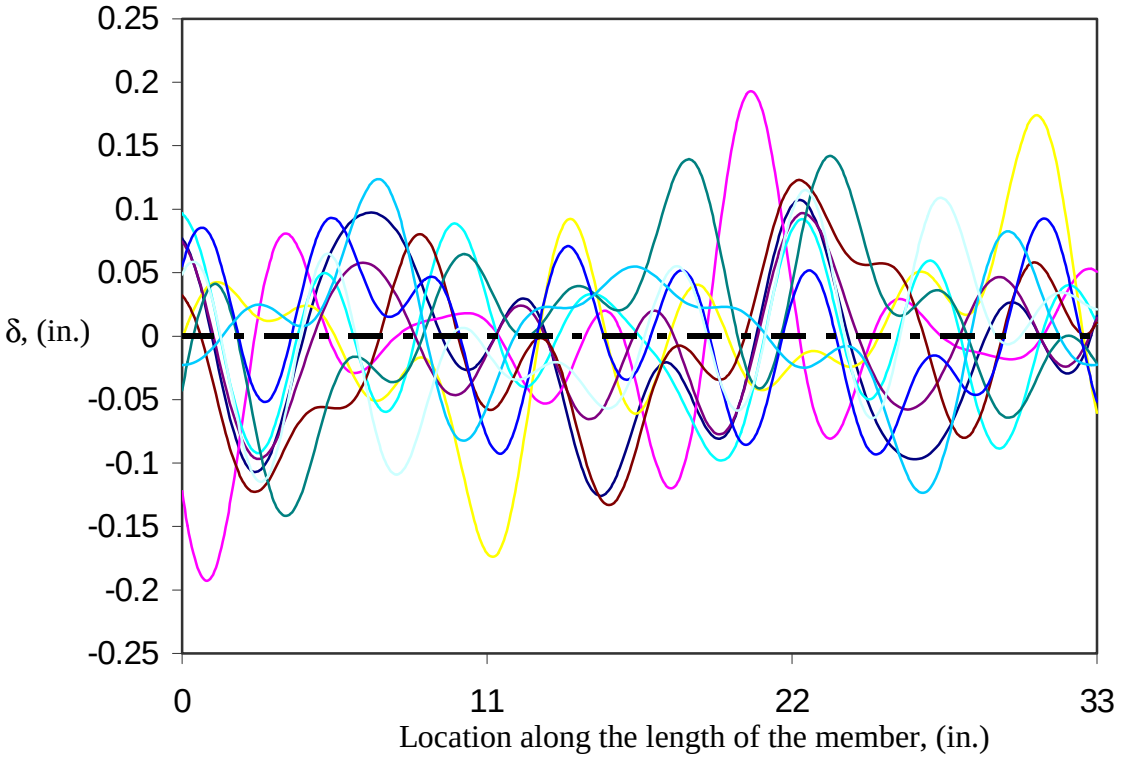


Figure 8.6 Zero mean, $\sigma_i$ =1.0 Stationary Guassian Stochastic Process: 10 Signal

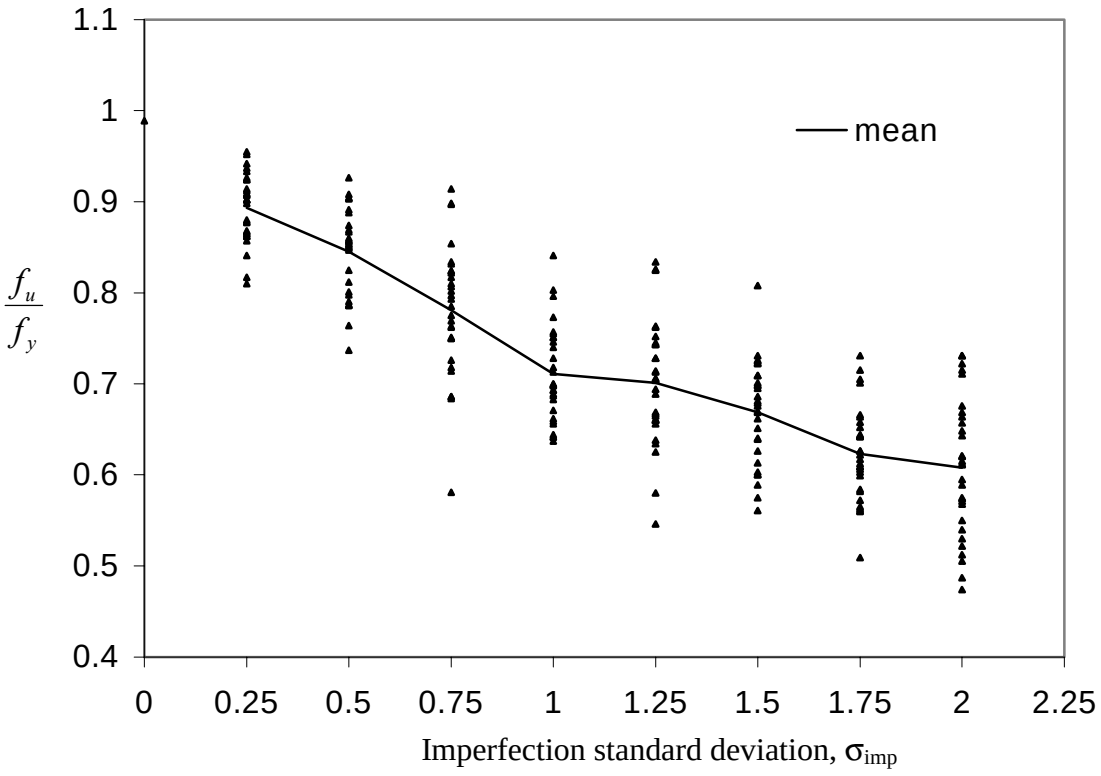


Figure 8.7 Ultimate Compressive Strength vs. Standard Deviation of the Imperfection Signal

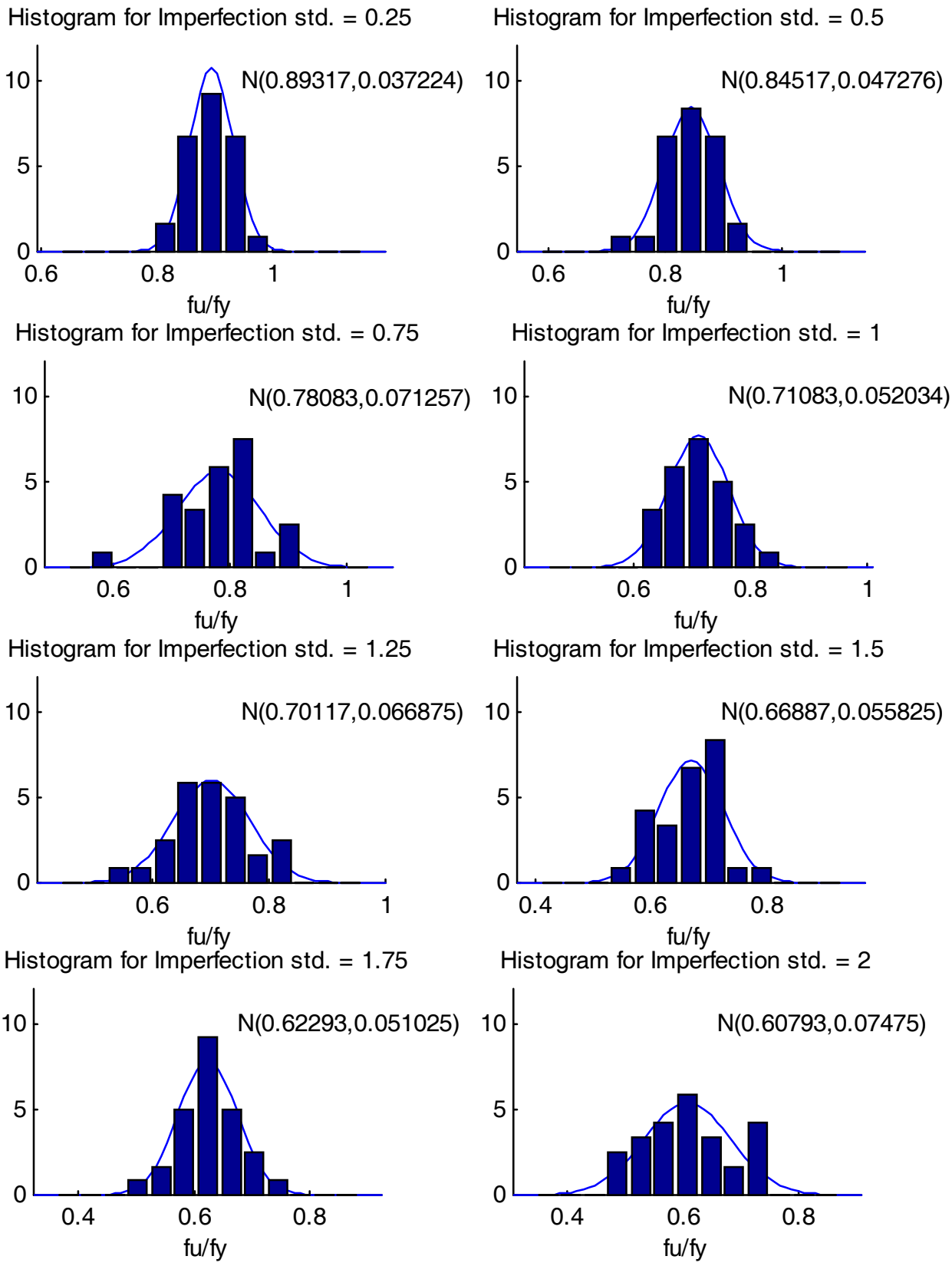


Figure 8.8 Histograms and Normal Distributions Density Function for each $\sigma_{imp,i}$

### 8.3 Initial Geometric Imperfection by Eigenmodes

The same model as in Figure 8.1 is used again to compare the results of the two approaches initial geometric imperfection by eigenmodes and by stochastic process. The initial geometric imperfection is introduced by superimposing the eigenmodes for the local and distortional buckling in different combinations of their magnitudes. The imperfection shapes are shown in Figure 8.9. Magnitudes of the imperfection are selected equal to the imperfections used in the stochastic process. FEM results are shown in Table 8.1 and Figure 8.10.

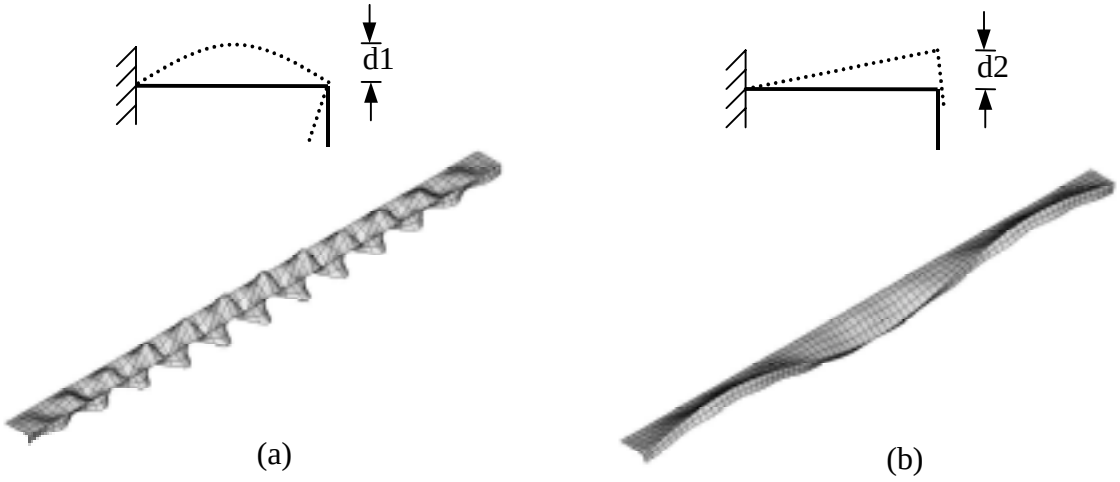


Figure 8.9 Eigenmodes (a) Local Buckling Imperfection Type 1, d1 (b) Distortional Buckling Imperfection Type 2, d2

Table 8.1 FEM Results Ultimate Compressive Strength vs. Imperfection Type 1 vs. Type 2

| | | d2, $f_u/f_y$ | | | | |
|---|---|---|---|---|---|---|
| | | 0 | 0.5t | t | 1.5t | 2t |
| d1, $f_u/f_y$ | 0 | 0.989 | 0.812 | 0.679 | 0.624 | 0.581 |
| | 0.5t | 0.967 | 0.811 | 0.693 | 0.625 | 0.58 |
| | t | 0.921 | 0.793 | 0.685 | 0.623 | 0.574 |
| | 1.5t | 0.881 | 0.773 | 0.681 | 0.621 | 0.578 |
| | 2t | 0.846 | 0.766 | 0.674 | 0.614 | 0.575 |

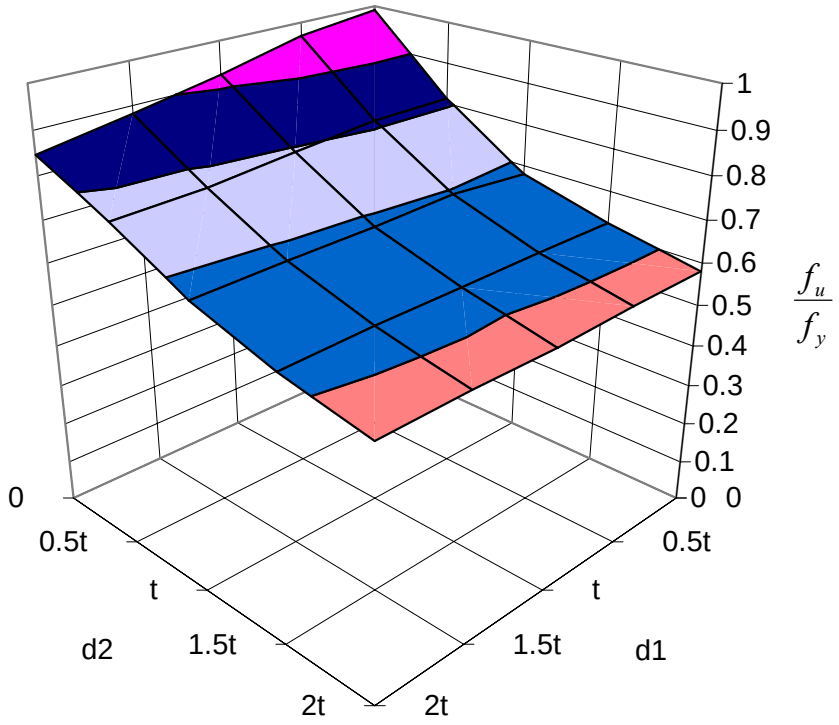


Figure 8.10 Ultimate Compressive Strength vs. Imperfection Type 1 vs. Type 2

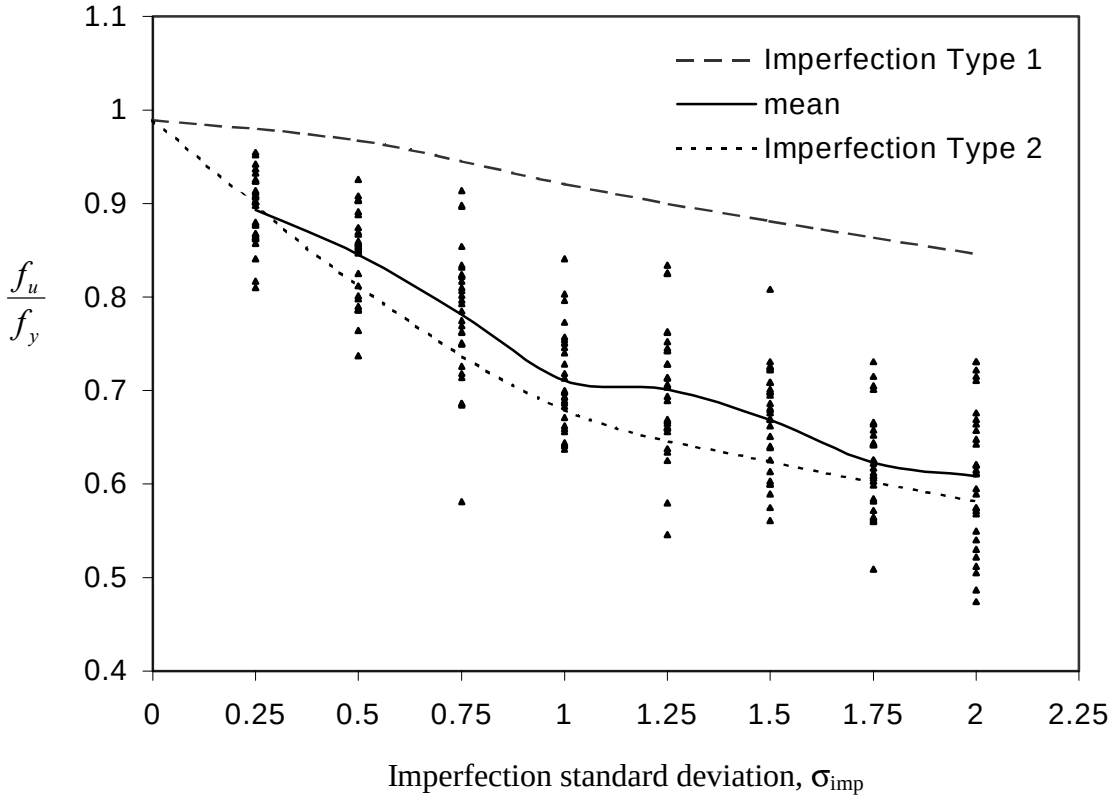


Figure 8.11 Initial Geometric Imperfection by Stochastic Process vs. Eigenmodes

### 8.4 Conclusion

Results from both approaches initial geometric imperfection by stochastic process and by eigenmodes are compared in Figure 8.11. The imperfection type 1 and imperfection type 2 lines are the results from introducing only their own imperfection type which is the results from the first column and first row in Table 8.1 where theirs no superimposing between the two modes. Results from the stochastic process and imperfection type 2 line is surprisingly close and both have significant impact on the strength reduction then the imperfection type 1. This shows that the section studied here is more sensitive to fail in the distortional buckling then local buckling. Although there were some assumptions made for the stochastic process but once some actual measurement of the section in study is available developing a better mathematical model is possible. The stochastic process used in this study is a 1 - dimensional stochastic process. Further study in using a 2 - dimensional stochastic process that could simulate a more realistic geometric imperfection plane is also of interest.

## 9 Summary and Conclusions

The approach formulated by Schafer (1997) also discussed in Schafer and Peköz (1999) for simple lip stiffeners is also satisfactory for complex stiffeners. This conclusion is based on finite element method studies. Finite element modeling agrees well with the Australian test results but improvement in the experimental arrangement should be done to avoid localize failure. Results from the cross section optimization study shows that it is more efficient to have inside angled stiffener then simple lip or outside angled stiffener.

**References**

American Iron and Steel Institute, (1996). AISI Specification for the Design of Cold-Formed Steel Structural Members. *American Iron and Steel Institute* Washington, D.C.

Bernard, E.S., Bridge, R.S. and Hancock, G.J., (1996) "Design Methods for Profiled Steel Decks with Intermediate Stiffeners," *Journal of Constructional Steel Research,* Vol.38, No.1, 1996, pp.61-88.

Hancock, G.J. and Kwon, Y.B., (1992). "Tests of Cold-Formed Channels with Local and Distortional Buckling," *Journal of Structural Engineering,* ASCE, Vol.117, No.7 July, 1992, pp. 1786-1803

H.O. Madsen, S. Krensky and N.C. Lind, (1986), *Methods of Structural Safety*, Prentice Hall, Englewood Cliffs, NJ.

Jay L. Devore, (1991), *Probability and Statistics for Engineering and the Science Third Edition*, Brooks/Cole Publishing Company, Pacific Grove, California.

J.R.Benjamin and C.A. Cornell, (1970), *Probability, Statistics and Decision for Civil Engineers*, McGraw-Hill Hook Co., NY.

Mircea Grigoriu, (1995), *Applied Non-Gaussian Processes, Examples, Theory, Simulation, Linear Random Vibration, and MATLAB Solutions*, PTR Prentice Hall, Englewood Cliffs, NJ

Peköz, T., (1987). *Development of a Unified Approach to the Design of Cold-Formed Steel Members*. American Iron and Steel Institute Research Report CF 87-1.

Rinchen, (1998). "Bending Section Strength of New Generation Cold-Formed Purlin Shape" Bachelor of Engineering Thesis, School of Civil and Mining Engineering, The University of Sydney

Schafer, B.W., (1997). “Cold-Formed Steel Behavior and Design: Analytical and Numerical Modeling of Elements and Members with Longitudinal Stiffeners.” Ph.D. Dissertation, Cornell University, Ithaca, New York

Schafer, B.W., Peköz, T.P., (1999). “Laterally Braced Cold-Formed Steel Flexural Members with Edge Stiffened Flanges.” *Journal of Structural Engineering,* 125(2)

Standards Association of Australia, “Cold formed Steel Structures,” AS/NZS 4600-1996.

Schafer, B.W., “CUFSM, Cornell University Finite Strip Method User’s Manual v1.0d” Cornell University, Ithaca, New York

T.T. Soong, Mircea Grigoriu, (1993), *Random Vibration of Mechanical and Structural Systems*, PTR Prentice Hall, Englewood Cliffs, NJ.

**American Iron and Steel Institute**

1140 Connecticut Avenue, NW
Suite 705
Washington, DC 20036

www.steel.org


Research Report RP-00-3